INFORMATION TO USERS

This manuscript has been reproduced from the microfilm master. UMI films the text directly from the original or copy submitted. Thus, some thesis and dissertation copies are in typewriter face, while others may be from any type of computer printer.

The quality of this reproduction is dependent upon the quality of the copy submitted. Broken or indistinct print, colored or poor quality illustrations and photographs, print bleedthrough, substandard margins, and improper alignment can adversely affect reproduction.

In the unlikely event that the author did not send UMI a complete manuscript and there are missing pages, these will be noted. Also, if unauthorized copyright material had to be removed, a note will indicate the deletion.

Oversize materials (e.g., maps, drawings, charts) are reproduced by sectioning the original, beginning at the upper left-hand corner and continuing from left to right in equal sections with small overlaps. Each original is also photographed in one exposure and is included in reduced form at the back of the book.

Photographs included in the original manuscript have been reproduced xerographically in this copy. Higher quality 6" x 9" black and white photographic prints are available for any photographs or illustrations appearing in this copy for an additional charge. Contact UMI directly to order.

UMI

A Bell & Howell Information Company
300 North Zeeb Road, Ann Arbor MI 48106-1346 USA
313/761-4700 800/521-0600

A

A study of 1/f noise in Aluminum, Al alloys and Copper films

By

Satoshi Hayakawa

A dissertation submitted to the Graduate Faculty in Physics in partial fulfillment of the requirement for the degree of Doctor of Philosophy, The City University of New York.

1999

This manuscript has been read and accepted for the Graduate Faculty in Physics in satisfaction of the dissertation requirement for the degree of Doctor of Philosophy.

April 22, 1999
Date

Leonard O. Roellig
Chair of Examining Comittee

4/22/99
Date

Louis Celenza
Executive Officer

Kelvin G. Lynn

Martin Kramer

C. Rutherford Fischer

Marten denBoer

Frederick Smith

The City University of New York

Abstract

A study of 1/f noise in Aluminum, Al alloy and Copper films

By

Satoshi Hayakawa

Advisor: Dr Kelvin G. Lynn, Leonard O. Roellig and Martin Kramer

The 1/f noise measurement reveals information on dynamical atomic kinetics in solids. Based on a successful development of a highly sensitive noise measurement system, we have studied the 1/f noise in Al, Al alloys and Cu films at the temperature from 11 to 450 K. In Al films, single crystal and bamboo grained films exhibited substantially smaller noise than polycrystalline films at room temperature. This is clear evidence that grain boundaries are responsible for the 1/f noise generation in polycrystalline films. Despite the difference of the noise magnitude, the temperature dependence of all Al samples showed a quite similar behavior at the temperature from 150 to 294 K. The normalized noise magnitude (Hooge Parameter α_H) began to increase about 200 K. This temperature corresponds to an activation energy about 0.5 eV. It is related to a vacancy migration process. In polycrystalline films, this can be specified as grain boundary electromigration. It is known that adding Cu atoms to Al reduces electromigration. Such an effect was observed in Cu doped polycrystalline Al films. For temperatures < 150K, α_H showed no particular structure in polycrystalline Al.

However, in single crystal films, it was found that α_H increased with decreasing temperature. A peak around 35K was found in single crystal, bamboo structure, and polycrystalline Al with 2% wt. Cu (Al-Cu(2%)) samples. The peak temperature is nearly equal in all the samples. This indicates the origin of peaks may be identical. The peak height reveals the cleaner samples showed the higher noise peaks. This counter intuitive result may indicate that the α_H peaks are not attributable to simple thermally activated kinetics. Such a peak was also found in Cu films at about 70 K. Two types of explanation may be plausible. First, this may be due to the complicated dislocation dynamics. The low activation energy removes most of migration species in metals. Only, some dislocation kinetics can be activated. Second, a quantum interference effect, universal conductance fluctuation (UCF), was considered. A small metallic sample can be extremely sensitive to the repositioning of an impurity atom or a defect.

Preface

This research has been conducted at Physics department in Brookhaven National Laboratory and Physics department in Washington State University. The thesis consists of 4 chapters. Chapter 1 introduces a brief history of 1/f noise. It may be realized that 1/f noise, a slow fluctuation phenomenon, is ubiquitous. From pure nature to man-made highways, 1/f noise has been observed. Our primary concern was aluminum and copper thin films, which are utilized in commercialized integrated circuit (IC) chips. They exhibited very small resistance fluctuations and the spectrum showed 1/f noise. How is the 1/f noise created in thin metal films? We tried to answer in Chapter 2. Simple but powerful models are introduced with detail explanations. Based on such arguments, it will be seen that many atomic dynamics may be the fluctuation source in solid. In chapter 3, our successful development of the noise measurement system will be described. The maximum resolution of voltage fluctuation 30 pV has been achieved. How can such an extremely sensitive measurement be performed? This will be explained with technical details. In chapter 4, experimental results and discussion will be shown. We obtained a surprising result for the low temperature noise measurements. The attempt was made to explain this interesting result.

Acknowledgements

I would like to express my deep appreciation to Professor K. G. Lynn, L. O. Roellig and M. Kramer for encouragement and invaluable advice. This work could not have been completed without materials support by Dr. K. P. Rodbell (IBM Research division) and Professor A. H. Verbruggen (Delft University of Technology). In addition to material supports, I deeply appreciate them for numerous discussions of noise physics. I had a wonderful experience in Brookhaven National Laboratory. While I was struggling to develop the experimental setup, H. Hackard and G. Lovehoiden helped me with important technical advice. I am indebted to Dr. Finn Jacobsen for his deep insight. During my dissertation work, one of the unforgettable memories was the traveling across the United States by a car with full of equipment. I like to thank Dr. Y. Y. Shan for dedicated help to reconstruct a part of the research facility. I enjoyed having a discussion during the progress of research with A. Hunt. Dr. M. Petkov, Dr. S. Szpala and I have been working together for 6 years. We are not only just colleagues but also sincere friends. I have been influenced a hard work philosophy by Dr. M. Weber. Dr. T. Gessmann gave me a numerous comments for my presentation. I enjoyed working with all of my colleagues, R. Tjossem, N. Krismanovic, C. Fracassi, S, Rassiga, S. Kelath and M. Seki. Finally I wish to thank my parents for a long time support.

Contents

List of Tables

List of Figures

Chapter 1

Introduction

In a history of physical science, the noise study had been always on a side role compared with a main stream of physics. Rather, noise is unwanted and an annoying nuisance for most of scientists and engineers. However, it has been pondered by many people that the noise might contain a profound information of nature. One type of noise has a fluctuation spectrum inversely proportional to frequency f: this is called a 1/f noise or sometimes a flicker noise. This type of noise has been found frequently in nature. For examples [1], the rate of flow of Nile river over two thousand years, the light intensity of the quasar 3C273 over eighty years or the undersea ocean currents at a depth of 3100 meters in the central Pacific. The phenomena of a 1/f noise can be found not only in nature but also in our civilizations. Musha and Higuchi found a 1/f noise fluctuation in highway traffic in Japan [2]. Voss and Clarke investigated the power spectrum of radio programs for four different radio stations, respectively classic music, jazz-and-blues, rock, news-and-talk. Surprisingly, they found all of the programs showed the 1/f noise power spectrum [1]. Electronics devices are of no exception. Semiconductors have been known to exhibit a 1/f noise for a long time. Since this 1/f noise deteriorates seriously the audio frequency performance, a large effort has been paid to reduce the 1/f noise. This effort has triggered to the entire 1/f noise studies in condensed matter.

In semiconductors, now it is well understood how such a noise is generated and how to control this [3]. In semiconductors, electrons are trapped and detrapped in defects or semiconductor-oxide states in a band gap. This creates a fluctuation of the number of conduction electrons. This is an origin of this 1/f noise. This type of generation mechanism is sometimes called McWhorter type. On the other hand, metals also have been known to exhibit a 1/f noise. However, it was not seriously considered until late 1960's. In 1969, Hooge investigated a vast amount of thin metal films. Then he formulated the phenomenological equation (Hooge formula) [4]. This study had ignited a variety of 1/f noise studies in thin metal films and the entire condensed matters. Due to technological advancements in the 1980s, many types of noise experiment were demonstrated, such as electron irradiation [5], hydrogen diffusion [6], mechanical stress [7], grain size [8] and texture [9] dependence. Those studies disclosed that thermally activated kinetics and mobile defects are a major source of 1/f noise fluctuation [10]. In 1973, Vossen measured the noise in Al films and concluded that the noise index measurements can be used as sensitive indications of potentially open metal film due to electromigration damage [11]. Later, Koch et al. have pointed out a relation between 1/f noise and grain boundary electromigration in pure Al and Al-Cu films [12]. Further, Verbruggen et al. found that a single crystal gold film showed remarkably little noise compared to polycrystalline ones [13]. A similar result was obtained with Al film [14]. This is clear evidence that a grain boundary creates noise. Electromigration is a field-assisted mass transport [15] which results in the formation of metallic accumulation (hillocks) and depletion (voids). Modern

semiconductor devices contain many metal interconnects between individual transistors. As the size of the device decreases, the reliability of such interconnects becomes very important. Several physical processes degrade the reliability of devices, such as electromigration, thermal hillocks, grain collapse, and void-caused stress. This opened a new question. Can the noise study provide a useful information of metallization in IC chips? Chen et al. demonstrated a relation between $1/f^2$ noise and electromigration [16]. This idea has been widely adapted and the technique helps to evaluate the activation energy of electromigration.

A 1/f noise in thin metal films not only provides the information of classical thermal kinetics but also a quantum interference effect. In 1986, Feng, Lee and Stone have pointed out a relation between a 1/f noise and universal conductance fluctuation (UCF) [17]. Under UCF regime, a sample conductance can be extremely sensitive to the position of scatterers. When a single scatterer moves a distance more than a few inverse of Fermi wave vectors, the conductance will change by the order $\sim e^2/h$ in one and two dimensional systems. Subsequently Garfunkel et al. observed such UCF 1/f noise in C-Cu and Si-Au samples from 4.2K to 150K [18].

The 1/f noise in normal metal films is extremely difficult to measure because of its small fluctuation. Many novel techniques have been developed to increase the limit of sensitivity, however, their success has been limited due to the sensitivity of noise measurement system. To date, the low temperature dependence of the 1/f noise power in single crystal films has not been fully studied. Such a study, however, is needed to fundamentally understand the nature of 1/f noise. We

have developed and utilized a new technique (AC cross-correlation technique) to probe this phenomenon in thin metal films.

This is a significant step toward the understanding of the noise mechanism. Due to the existence of unwanted noise, the detection of 0.1 nV level of the signal is relatively difficult. Furthermore, reaching the 0.03 nV level of the spectrum is extremely challenging. To evaluate this signal detection limit, the noise bottom of our system is $\sim 20 pV/\sqrt{Hz}$.

Utilizing this high resolution noise measurement system, we observed for the first time the temperature dependence of the 1/f noise in an aluminum single crystal film down to 11K. This has never been done due to the difficulty of single crystal fabrication and the need for a sophisticated measurement system requiring the detection of a minuscule voltage power fluctuations of 10^{-20} V^2 or less. Temperature dependence of the normalized resistance fluctuation quantity showed a sudden increase at 220 K. This result was somewhat similar to our polycrystalline Al data. A novel result appears at less than 150K. The resistance fluctuation increased with decreasing temperature and reached a peak near 35K. This peak was observed in most of samples investigated. Surprisingly the peak temperatures were quite similar, although the peak maximums were different from each other. The details will be explained later chapter. A further finding is that it seems the cleaner the sample, the higher the noise. Attempt was made to explain these mysterious noise peaks. A complicated dislocation dynamics or a quantum interference effect may be involved in our results.

Needless to say, a better understanding of electron transport and mechanical processes in the micron or submicron scale of metallization is critically important for condensed matter physics and IC technologies. Our new measurement system may be able to reveal new information of physics through the atomic motion in thin film.

Chapter 2

Noise generation mechanism and the fluctuation source

2.1 Overview

Although the existence of noise is everywhere, we may feel unfamiliar with an in-depth argument of noise. One reason is the complexity of noise generation system. Probably, the best language to describe such fluctuations is statistical mechanics. Among a huge field of statistical mechanics, what we need to understand is a part of stochastic process. It is noteworthy to point out a few important points of the stationary stochastic process [19]. This formal treatment provides a basic framework of any kind of noise. First, white noise is explained in detail. This mathematical treatment is fundamental for entire stationary stochastic noise processes, which include a 1/f noise or a shot noise. Second, a local interference model will be introduced. The direct link between a defect repositioning and a resistance deviation will be discussed. It has been known 1/f noise and electromigration have a direct correlation. Indeed, the 1/f noise in metal film at room temperature is shown to be due to electromigration. Third, as an equal importance to the noise description, the fluctuation dissipation theorem (FD theorem) is explained. Further, as an extension of FD theorem, 1/f noise generation due to internal friction will be explained.

What kind of atomic kinetics or defect dynamics could create such a low frequency fluctuation? We will try to answer this question in 2.4. The atomic and

impurity diffusion is scrutinized and dislocation dynamics is suspected. Particularly kinks and jogs may be able to create a 1/f noise at low temperatures. The quantum effects will be considered later. A basic idea is discussed and a primitive quantitative analysis is attempted.

2.2 White noise

White noise is the one of the most well known equilibrium noise phenomena. This gives statistical information of noise generated in media. As a starting point, a following equation may be written.

$$\frac{dX}{dt} = -\frac{X}{\tau} \qquad (2.1)$$

This is a general equation for any noise processes. X may be an electric potential, i.e. an electric dipole potential of the atom due to a phonon scattering. Of course, this gives a thermal noise (white noise) later. However, not only an electric potential (voltage) fluctuation but also X may be the velocity of a molecule in a gas or of a car in traffic. In a particular concern to 1/f noise in metal system, X may be an atomic motion in a certain potential or a dislocation motion, which is treated as a vibrating string. If the process is random and dissipative to the system, any processes can be written by Eq.(2.1). τ is a dragging or dissipation constant. Now we restrict our argument for the white noise generation, especially a thermal

noise. In Fig.(2.1), a schematic of the simple resistance is shown. Eq. (2.1) is easily solved as,

$$X = X_0 \exp(-t/\tau) \qquad (2.2)$$

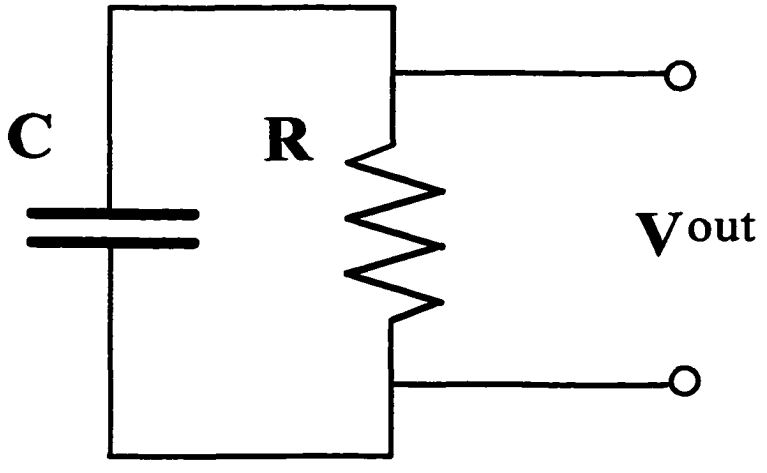

Fig.2. 1: A schematic of parallel coupling of a capacitor and a resistor.

This physical quantity X(t) simply shows time decay function. It looks like just one event is described after t=0. This may be true in short period of time, however it is not for a long period of time in stationary stochastic process. For example a gas molecule may lose a velocity due to the multiple scattering, then it may again receive a new momentum from a collision, this is true for electrons in metals. Stationary stochastic process is assumed multiple events happen in a long period of time. Quite often X_0 is not known originally. To determine X_0, the equipartition theorem is used. Since voltage fluctuation is our concern, X is replaced to V. Then

$$V = V_0 \exp(-t/\tau) \qquad (2.3)$$

An auto correlation function is defined as,

$$\psi(\lambda) = < V(t) \cdot V(t+\lambda) > \qquad (2.4)$$

In convenience, choose t=0.

$$\psi(\lambda) = V_0^{\,2} \exp(-\lambda/\tau) \qquad (2.5)$$

Employing the Wiener-Khinchin theorem (See Appendix A),

$$\psi(\nu) = 2\int_0^{\infty} d\lambda \;\; \psi(\lambda)\cos(2\pi\nu\lambda) \qquad (2.6)$$

Hamiltonian may be described as,

$$H = R\dot{q}^2 + \frac{q^2}{2C} \qquad (2.7)$$

where, q is charge. The equipartition theorem gives,

$$< \frac{q^2}{2C} > = < \frac{1}{2} C V_0^{\,2} > = \frac{1}{2} kT \qquad (2.8)$$

Then $\psi(\nu)$ becomes,

$$\psi(\nu) = \frac{2kTR}{1 + (2\pi\nu CR)^2} \qquad (2.9)$$

τ is replaced by CR. The total voltage fluctuation is computed by resistance and capacitance contribution. Therefore, the total voltage fluctuation is following:

$$V_{thermal}(\nu) = 2\psi(\nu) = \frac{4kTR}{1+(2\pi\nu CR)^2} \qquad \textbf{(2. 10)}$$

In general, a cut off frequency is quite high ~M Hz. Then the spectrum looks flat up to MHz. In scientific literature, often thermal noise is described 4kTR. This is the reason it is so-called white noise. First, we find out an autocorrelation function then apply the Wiener-Khinchin theorem. This approach is quite powerful to determine a fluctuation process and fully utilized following sections to compute 1/f noise.

2.3 1/f noise

1/f noise is usually described as the quantity of power increases with decreasing the frequency in Fig. 2.2.

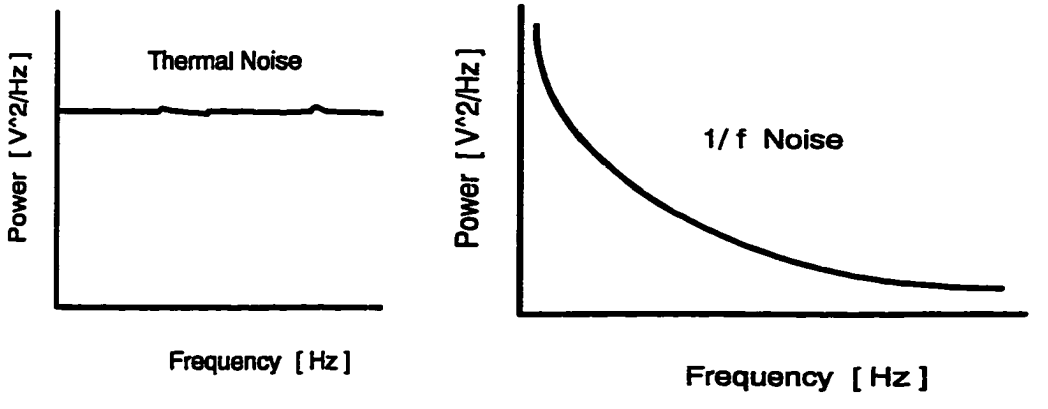

Fig.2. 2: A thermal noise and a 1/f noise spectra.

Now we show how 1/f noise is created. There are many different types of theories about noise generation. However, some of them may not follow the experimental

evidence or other may contain some parameters, which are hard to estimate in real case. Although many materials show 1/f noise, we discuss the noise kinetics particularly in thin metal films. In the previous section, it was shown that the Lorentzian spectrum is obtained if autocorrelation function is described as the function whose time decay is exponential, ~ $e^{-t/c}$. It is easily seen a superposition of Lorentzian spectrum gives 1/f noise spectra in Fig. 2.3.

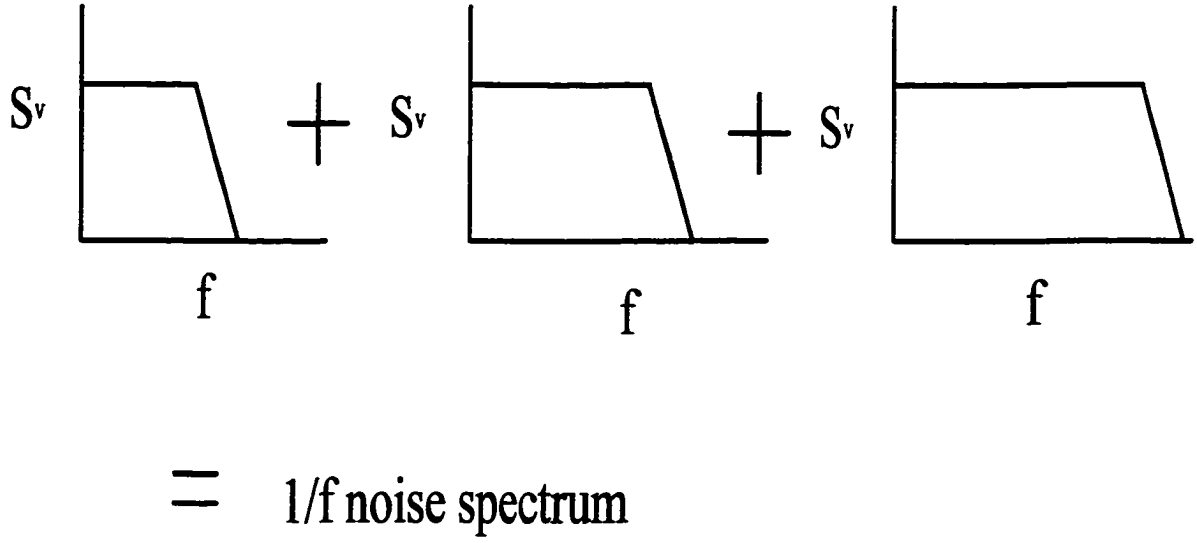

Fig.2. 3: 1/f noise spectra as a superposition of Lorentzian spectrum.

The idea was first demonstrated by McWhoter in a semiconductor-oxide interface [20]. It has been known charge trappings occur in semiconductor-oxide interface. This charge trapping and detrapping process can be described as Eq. (2.1). Therefore each process contributes single Lorentzian with a specific corner frequency. Unlike white noise case, the corner frequency should be quite low, less than kHz. Since trapping and detrapping rate is broadly distributed, 1/f noise spectra is obtained. This is believed to be a dominant 1/f noise generation in semiconductors. On the other hand, this process is called a number fluctuation of

charge carrier. Not only semiconductors but also thin metal films are known to exhibit 1/f noise. In case of thin metal films, the situation is quite different. No large carrier number fluctuation is expected. Rather mobility fluctuation is a key process by thermally activated defects.

2.3.1 Thermally activated defects.

In metal films, even if it is well prepared, normally it contains substantial amount of defects, e.g. interstitial or vacancy clusters, void, impurity atoms and dislocations. And, in most cases, metal films are not single crystals but polycrystalline structure. These defects certainly affect the mobility of electrons. In other word, it contributes an additional resistance. Not only they behave as static scatterers, but also some defects may have an activated motion. Consequently such defects dynamically fluctuate a part of the mobility. This causes 1/f noise. In general, "Noise in most metals is believed to be a mobility fluctuation arising from defect motion" [21]. The question is what kind of defect kinetics contributes a 1/f noise generation or how they create a fluctuation. In Fig.2.4, the schematic of defect jumping is shown. It has been known the hydrogen hopping creates a 1/f noise in metals. This is a simple example that atomic jumping can create a fluctuation. In ordinary thin metal films, it is well established that the source of 1/f noise is grain boundary electromigration at room temperature.

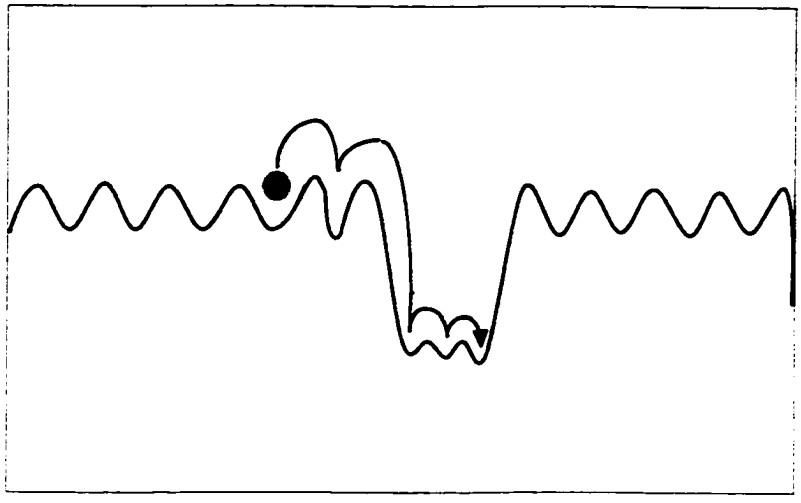

Fig.2. 4: A defect jump inside a metal.

2.3.2 Two Level System (TLS).

When autocorrelation function has a time decay expression and this expression has a wide distribution which correlated any decay constants, 1/f noise is depicted. Based on this idea, Dutta, Dimon and Horn introduced an elegant way to show 1/f noise spectrum [22]. To simplify this jump kinetics, they proposed a two level system (TLS) in Fig.2.5. The two level system consists of two potential wells, which a defect atom switches to another well. This is a thermally activated process. One side of double well is called well A and another B. The life time in well A may be written as, $\tau_A = \tau_0 e^{(E_0 - \frac{\Delta E}{2})/kT}$. And $\tau_B = \tau_0 e^{(E_0 + \frac{\Delta E}{2})/kT}$ in B. Then autocorrelation function A(τ) is decribed as, (See Appendex B),

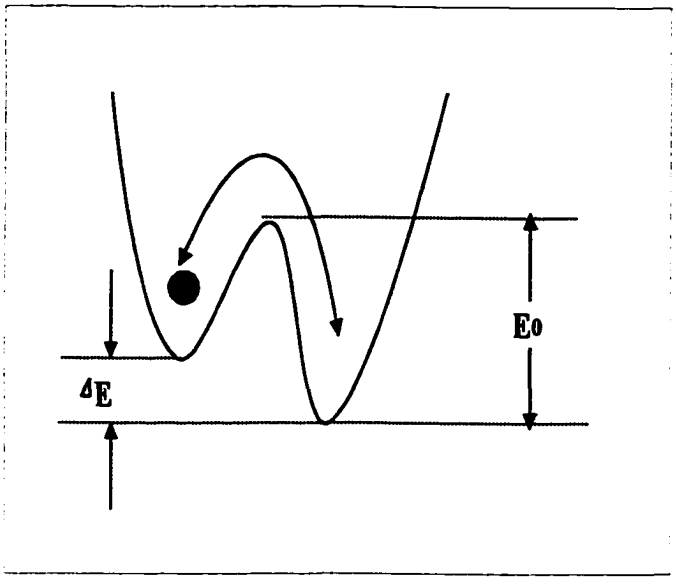

Fig.2. 5: A two level system (TLS).

$$A(\tau) = \frac{1}{4} sech\left(\frac{\Delta E}{2kT}\right) e^{-\frac{\tau}{T_0}} + Const \quad . \qquad (2.11)$$

where, t_0 is

$$t_0 = \tau_0 \frac{e^{\frac{E_0}{kT}}}{e^{\frac{\Delta E}{2kT}} + e^{-\frac{\Delta E}{2kT}}} \qquad (2.12)$$

When E_0 is larger than ΔE, t_0 is,

$$t_0 = \tau_0 e^{\frac{E_0}{kT}} \qquad (2.13)$$

Like white noise case, we obtained the time decaying autocorrelation function. A normalized state value was used, i.e. A=1 and B=0 in Appendix B. Applying the Wiener-Khinchin theorem, the spectrum density S(f,T) is obtained.

$$S(f,T) = \frac{1}{2}\sec h^2(\frac{\Delta E}{2kT})\frac{t_0}{1+(2\pi f t_0)^2} \qquad \textbf{(2. 14)}$$

Constant factor of the autocorrelation function simply gives constant in power spectrum. Single Lorentzian can be obtained. If the activation energy or switching time constant τ_0 has a broad distribution, 1/f noise spectrum can be obtained. In many literatures, $\frac{1}{2}\sec h^2(\frac{\Delta E}{2kT})$ is assumed to be 1, which means the depth of potential wells is nearly same. However, a care has to be taken if $\frac{\Delta E}{2kT}>1$. It should be mentioned that Eq.(2.14) is decribed only for one TLS. If the total number of TLS, N_{TLS} is estimated, this has to be multiplied to obtain a total fluctuation spectra. Since a 1/f noise generation is assumed a broad distribution of activation energies, a normalised distribution function D(E) is multiplied in Eq. (2.14). Then integration by energies gives a final spectrum.

$$S(f,T) \propto N_{TLS}\int D(E)\frac{\tau_0 e^{\frac{E}{kT}}}{1+(2\pi f \tau_0 e^{\frac{E}{kT}})^2}dE \qquad \textbf{(2. 15)}$$

2.3.3 Dutta-Dimon-Horn relation (DDH relation).

In previous section, it has been shown how the noise spectrum is generated through a simple TLS model. Dutta, Dimon and Horn explained more than just a spectrum power. They showed a relation between the noise power S(f,T) and frequency exponent γ. A few assumptions were made; (1) $\Delta E \sim 0$. An

energy difference of each site within a double well is very small. In case where a diffusion process is involved, all quasi-stable sites have similar potentials. (2) The distribution of the activation energies D(E) is smooth. If D(E) can be expressed the expansion form near the maximum energy $\tilde{E}$, a following condition should be met,

$$D(\tilde{E}) >> \sum_{n=1}^{\infty} \frac{\varepsilon_n}{(2n)!} \left(\frac{\pi kT}{2}\right)^2 \frac{d^{2n}}{dE^{2n}} D(E)_{E=\tilde{E}} \qquad \textbf{(2. 16)}$$

where, ε_n is the nth Euler number. If such conditions are satisfied, the following relation is derived,

$$\gamma = 1 - \frac{1}{\ln(\omega\tau_0)} \left[\frac{\partial \ln S_v(\omega, T)}{\partial \ln T} - 1 \right] \qquad \textbf{(2. 17)}$$

Dutta , Dimon and Horn demonstrated this relation by Cu and Ag thin film noise measurement. In Fig.2.6, DDH relation in Cu film is shown. This relation was rigorously tested by several authors, e.g. [23-25]. The detail comparison has made in chapter 4. One of the important features in DDH relation is that the distribution of energies D(E) can be estimated as, in Eq.(2.18). This allows to estimate the energy distribution from the temperature dependence of S_v. Also, Eq. (2.19) is used to estimate the energy.

$$D(E) \propto \frac{\omega}{kT} S_v(\omega, T) \qquad \textbf{(2. 18)}$$

$$E = -kT \ln(2\pi f \tau_0) \qquad \textbf{(2. 19)}$$

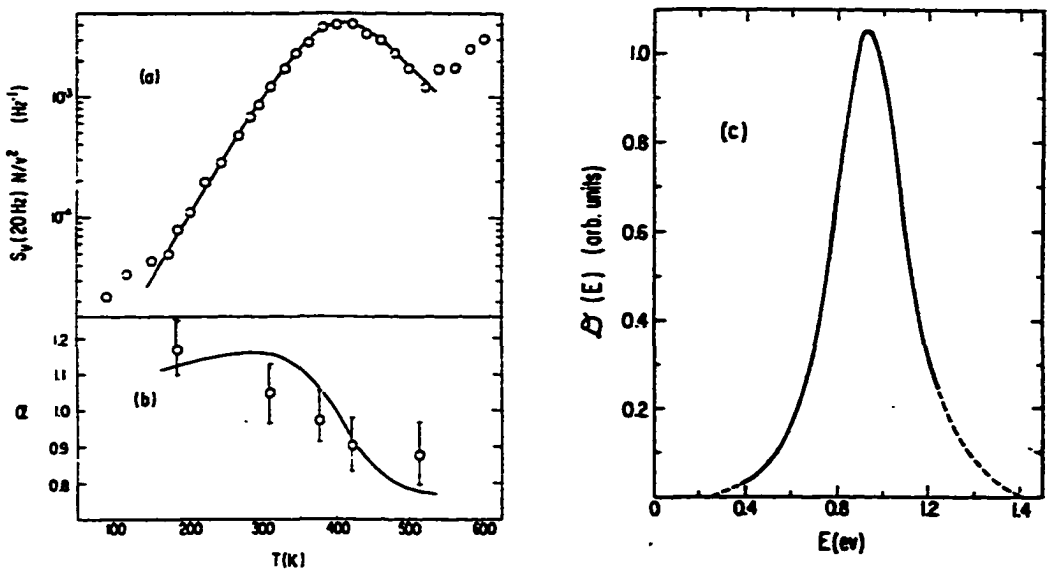

Fig. 2.6 : (a) Noise magnitude at 20 Hz vs. temperature for 800 Å Ag film. The solid line is a smooth fit to the noise peak. (b) Frequency exponent vs. temperature. The solid line is predicted by Eq.(2.17). (c) Energy distribution calculated by Eq.(2.18). Ref. [22]

Above two equations should be complemental. In other words, unless experimentally Eq.(2.17) is proven, the estimation of D(E) may not be reliable.

2.3.4 Local interference model (LI model)

What kind of defects is actually activated? How much resistance fluctuation do they create? Pelz and Clarke calculated such resistance fluctuations by deviations of defect repositioning in metal films [26]. They utilized the static resistivity tensor due to particular defect position calculated by Martin [27]. If two defects are separated more than $R \cdot k_F \gg 7$, the created resistance change is rather independent. This is why this model is called local interference model. This model allows us to estimate the number of defects which contribute the resistance

fluctuation. The resistivity tensor components for several defects are shown in Table 2.1. A normalized anisotropy parameter β is defined as,

$$\beta^2 = \langle(\delta\rho)^2\rangle / \langle\rho\rangle^2 = \langle(\delta\sigma)^2\rangle / \langle\sigma\rangle^2 \qquad \textbf{(2. 20)}$$

The 1/f noise measurement was performed by Clarke and Pelz in electron irradiated Cu films [5,28]. The irradiation dose dependence and annealing behavior strongly supported local interference (LI) model. A similar experiment was achieved by Brigmann et al. in Al films [29]. An interesting point is that none of the defects, shown in Table2.1 seems to be applicable if we consider the 1/f noise at room temperature. In pure metal films, not many point defects, interstitials or vacancies, are available at room temperature. Since their formation energies are rather high and migration energies are low, then most of point defects are either recombined or migrated to the surface even if point defects are created in any means. In some cases, interstitials or vacancies may be trapped by another defects, e.g. dislocation. Such an effect of defect-defect interaction has not been fully studied. Further, a vacancy has a rotational symmetry in perfect crystal which means β=0. No matter how a vacancy repositioned, a net resistance deviation is zero. In short, it seems that LI model is not responsible for 1/f noise in an ordinary case. This model provides an important implication to understand the 1/f noise at room temperature. It is known atomic migration occurs even at room temperature with a relatively high current density due to electromigration. A brief introduction of electromigration and its implication for 1/f noise is discussed in next section.

Defect type	ρ_{xx}	ρ_{yy}	ρ_{zz}	ρ_1,ρ_2	ρ_3	β
Monovacancy	1.00	1.00	1.00	1.00	1.00	0.00
(relaxation)	0.92	0.92	0.92	0.92	0.92	0.00
First neighbor divacancy	1.80	1.80	2.27	2.27	1.33	0.14
(relaxation)	1.65	1.65	2.13	2.13	1.17	0.16
Second neighbor divacancy	2.04	1.85	2.04	2.04	1.85	0.03
(relaxation)	1.73	1.70	1.73	1.73	1.70	0.01
180° trivacancy	3.54	2.58	2.58	3.54	1.62	0.20
(relaxation)	3.35	2.48	2.45	3.35	1.58	0.19
<100> split interstitial	1.08	1.08	2.33	1.08	2.33	0.25
(relaxation)	2.19	2.17	3.63	2.18	3.63	0.16
<110> split interstitial	1.70	1.70	1.07	1.07	2.33	0.25
(relaxation)	3.48	3.47	2.44	2.44	4.51	0.20

Table 2. 1 : Resistivity tensor components and anisotropy parameter β for six types of defects. The components ρ_{xx}, ρ_{yy} and ρ_{zz} are from Ref.[27]; ρ_1, ρ_2 and ρ_3 are the corresponding principal moments. For each defect type, the upper row lists values for the bare defect, while the lower row includes effects from surrounding lattice relaxation. All resistivities are normalized to that of the bare monovacancy. Ref [26].

2.3.5 Electromigration and 1/f noise.

Electromigration is observed in primary thin metal films because a high current density is easily achieved. This is atomic diffusion assisted by electron current. When current density increases, metal atoms can receive enough momentum from electrons to cause a biased self-diffusion even at room

temperature [15]. Blech [30] demonstrated the direct experiment of electromigration in Fig.2.7.

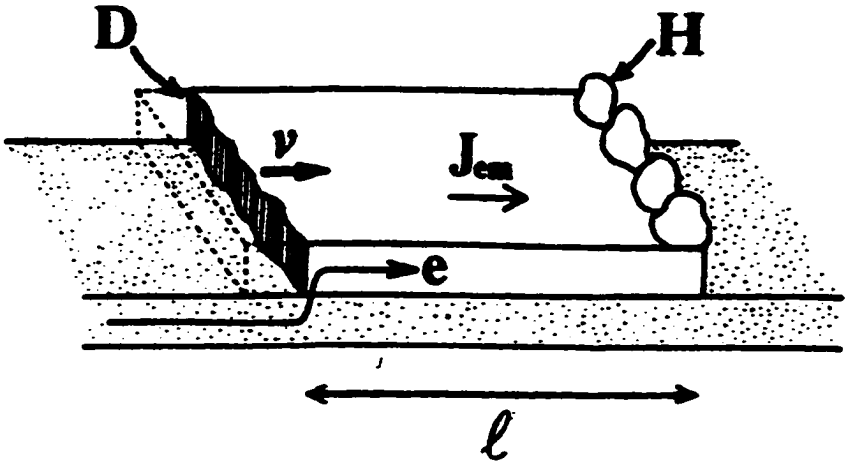

Fig. 2.7 : Blech's drift experiment. Ref. [30]. D: depletion. H: hillocks.

In Fig.2.7, the substrate layer has a relatively high resistance so a dominant component of electron current runs through aluminum strip. Following a direction of "electron wind", one side of Al strip was depleted and another side showed an accumulation of atoms. This is a direct evidence of mass flow. It is known that the majority of mass flow is carried out through grain boundaries, i.e. called grain boundary electromigration (GB electromigration). The activation energies of 0.5-0.8 eV are known in Al. In a single crystal, atomic diffusion is allowed only through a perfect crystal, which is called bulk electromigration. The activation energy 1.47 eV in Al has been obtained by d'Heurle and Ames [31]. This energy is explained as a combination of formation and migration energy of a vacancy. Surface may be an another path for atomic diffusion, which is called surface electromigration. However, this may not play an important role since oxide

metal surface like Al and Cu give a strong resistance against atomic migration. Presumably, GB electromigration may be the primary source of 1/f noise in thin metal films. GB electromigration has a broad distribution of activation energies and the number of participated atoms and vacancies can be substantially high at even room temperature. The following explanations pictorially explained this argument. Let's take a look for a microscopic picture of grain boundary electromigration. When an atom jumps through a grain boundary region, it is equivalent to say that a vacancy moves toward an opposite direction. This jump kinetics may contribute a resistance fluctuation. In previous section, it has been shown the atomic repositioning creates a resistance fluctuation (LI model). On the other hand, it was concluded that vacancies could not create a fluctuation because of a rotational symmetry. However, in case of GB electromigration, the situation should be quite different from diffusion in a perfect crystal. The surrounding environment around grain boundaries no longer holds symmetry like a perfect crystal. Rather it behaves as an anisotropic, which gives for any defects repositioning $\beta \neq 0$. Therefore, even vacancies can create a resistance fluctuation. The relation between electromigration and 1/f noise has been rigorously demonstrated by many authors [32,33]. Koch, Lloyd and Cronin compared with the temperature dependence of the 1/f noise and mean time to failure (MTF) study in Al and Al alloys films [12]. They found a good agreement between two studies. Schwarz et al performed grain size dependence of 1/f noise in Al-Cu thin films, which confirmed the normalized noise magnitude is inversely proportional to the size of a grain [8]. On the other hand, a single crystal Au film exhibited a

substantially low noise by Verbruggen et al [13]. A similar study has been done in single crystal Al films by Homberg et al [14].

2.3.6 Fluctuation dissipation (FD) theorem

Fluctuation dissipation theorem states if a system absorbs some amounts of energy from external environment, the dissipation process generates fluctuation of a physical quantity. For example, an electric resonance circuit which consists of L, C and R has always the width of resonance frequency due to energy dissipation. FD theorem can successfully describe many general fluctuation phenomenon. See Landau and Lifshitz for a detailed explanation [34]. Among a broad field of applications, it is known FD theorem is applicable to the anelastic relaxation. In solid, a stored mechanical energy may dissipate through a specific kinetics. Particularly, the dissipation of internal friction accompanied by thermally activated strain fluctuations. Internal friction in solid has been extensively studied more than a half century. This anelastic behavior reveals many relaxation processes caused by point defects (Snoek effect or Zener effect) or dislocations [35]. Hinted by internal friction peak, Kogan and Nagaev proposed a conductance fluctuation (1/f noise) based on Snoek relaxation [36]. The normalized noise power S_v/V^2 is described as,

$$\frac{S_v(f)}{V^2} \propto \frac{2kTl^2\sigma_s(E_\omega)Q^{-1}}{\pi B(E_\omega)} \frac{l}{Vf} \qquad (2.21)$$

where, l is a mean free path, σ_s is the corresponding cross section by the defect, Q is the quality factor and B(E) is the characteristic value of the elastic modulus multiplied by the square of the atomic volume. The inverse of quality factor Q^{-1} can be directly obtained from the temperature dependence of internal friction experiment. In general, such experiments provide log decrement δ. This can be expressed in terms of the ratio of imaginary and real parts of general modulus, M_I and M_R respectively. And Q^{-1} is directly proportional to δ. Attempts have been made to consider the connection between internal friction and 1/f noise. This has not been so successful since activation energies from both sides of experiments showed both results were not comparable. For example, the temperature dependence of 1/f noise was obtained in Al [29], Cu and Au films [37]. Compared with a majority of internal friction data [35], no strong correlation was found. Noise results showed an order of 1eV at peak temperature in those literatures while a dominant internal friction data showed an order of 0.1 eV at decrement peaks. In addition, no indication has been made for noise study in other metals. Alers et al. demonstrated a direct relation between hydrogen concentration and 1/f noise power while measuring a strain of the substrate by anelastic piezoresistance measurement [38]. This might reveal Snoek effect is a source of 1/f noise. However, they concluded that the hydrogen hopping was a dominant factor rather than the Snoek effect and the correlation between the mechanical anelasticity and the resistance noise was weak.

2.4 Other dynamical kinetics in metals

In previous sections, we discussed how 1/f noise could be generated by different processes or origins. Besides the argument of LI model and an application to electromigration in 2.3.4 and 2.4.5, there is no reason not to consider other defect diffusion may create 1/f noise. This section devotes primary this issue. What LI model described 1/f noise generation was a thermally activated defect switched a position under the asymmetrical potential environment. In a real atomic diffusion, further consideration is necessary. The simple Lorentzian spectrum suggests an observable 1/f noise may arise when the characteristic time $\tau \geq 1$ s in thin metal films. If an attempt time is assumed $\tau_0 \sim 10^{-13}$ s, then E/kT should be ~30 at $\tau = 1$ s. This gives a quick test, whether the assumed kinetics is appropriate to argue the noise creation. Figure 2.8 showed the temperature dependence of the activation energy at a corner frequency 0.1 Hz.

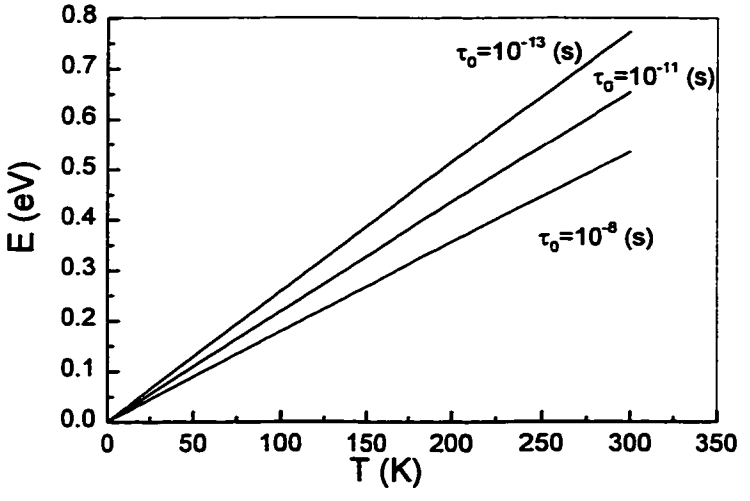

Fig. 2.8: The temperature dependence of the activation energy with different attempt time.

The corner frequency 0.1 Hz was chosen based on our experimental consideration since our real spectrum data suggest it is hard to obtain a good spectrum more than 1 Hz at low temperature. However, this frequency difference is insignificant since one decade of frequency difference only generates an energy difference less than 3%. When the energy is higher than plotted line at a temperature, the fluctuation is rather DC, $f_c \ll 1$. On the other hand when the energy is lower, then the spectra is flatten, $f_c \gg 1$. Another consideration is geometrical asymmetry in metal thin films. This assumption of asymmetry is quite plausible. Since no matter how thin films are fabricated, the thin films are far from a highly symmetrical crystal. For example, the thermal mismatch between metal, substrate and buffer materials creates thin metal films highly stressed. Then a large amount of dislocation may be created. Or most of thin films have polycrystalline structure and the grains have a tilt angle distribution. Such asymmetrical factors can provide that any diffusion species may be able to contribute a 1/f noise. Now let's examine each defect and kinetics.

2.4.1 Point defects

In 2.3.4, it was shown interstitials and vacancies can create 1/f noise. This argument should be able to apply other defects. If any defect species are available to diffuse or move under some restrictions, e.g. dislocations, it is certainly worth to investigate as a potential suspect for the 1/f noise generation. One of the obvious candidates is the metal atom itself. The metal atom itself can diffuse; it is called self-diffusion. For brevity of argument, an assumption was made that a particular

defect is located in a perfect crystal, although defect-defect interaction is unavoidable in a real metal. The dominant self-diffusion process is the vacancy mechanism. Other self-diffusion processes, like interchange or ring mechanism, are less likely important [39].

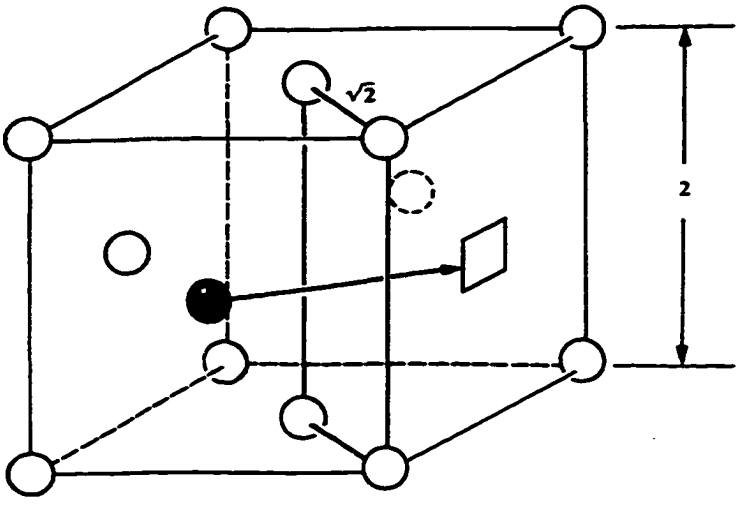

Fig. 2.9: Atomic jump by a vacancy mechanism in FCC.

Self-diffusion by the vacancy mechanism requires the activation energy E_{sd}, which is the sum of the vacancy formation energy E_{vf} and its migration energy E_{vm} in Eq.(2.22).

$$E_{sd} = E_{vf} + E_{vm} \qquad \textbf{(2. 22)}$$

Element	Esd(eV) {Monovacancy}	Esd (eV) {Divacancy}
Aluminum	1.28	1.59
Copper	2.07	2.59
Gold	1.76	2.37
Lithium	0.521	0.69
Nickel	2.88	3.70
Niobium	3.62	4.54
Silver	1.76	2.19
Sodium	0.365	0.46
Tantalum	4.07	5.35
β-Titanium	1.35	2.60
Vanadium	2.93	3.72
β-Zirconium	1.20	2.83

Table 2. 2: The list of activation energies for self-diffusion in different metals.

Table 2.2 shows the list of activation energies in different metals. The listed energies are based on a single vacancy mechanism. When the self-diffusion due to divacancy mechanism is involved, all of the energies are higher than the energies by the single vacancy mechanism. Because of high energies, self-diffusion can not contribute at less than room temperature. In 2.3.5, a strong correlation between a 1/f noise and electromigration was pointed out. The energy of bulk electromigration is nearly as same as the energy of self-diffusion in metals. Employing Eq. (2.19), a peak temperature of 528 K was estimated in Al self diffusion. If an observed spectrum contains a fraction of self-diffusion, then the energy distribution must extend ~0.55 eV. Since no such a broad distribution has been recognized in a thermal diffusion experiments. It is less likely that a 1/f noise is created by self-diffusion at room temperature. How about impurity atoms? We used 99.999 % pure metal to study. However, still 10 ppm of impurities is inside

Host metals	Impurit	Activation energy (eV)	Referen
Cu	Ag	0.97-0.98	[40]
Cu	Al	1.06-1.17	[40]
Cu	Ga	1.02-1.10	[40]
Cu	Ge	0.94-1.13	[40]
Cu	Zr	1.04-1.12	[40]
Cu	Be	1.10-1.12	[40]
Cu	Mn	1.19	[40]
Ag	Sn	0.57-0.86	[40]
Al	Mo	2.72	[41]
Al	Cr	2.72	[41]
Al	Zn	0.343-0.614	[42]
Al	Cu	0.814-0.890	[42]

Table 2. 3: The list of activation energies of impurity atoms in different host atoms. Ref. [40-42].

metal. No matter how we prepared thin metal films, some level of contamination is unavoidable. Although the total amount is a quite small, it may be able to create a 1/f noise. Impurity atoms can be dissolved in solvent metals substitutionally or interstitially. As same as self-diffusion, the vacancy mechanism is dominant in some host metals. Table 2.3 lists activation energies for impurity diffusion in Cu and Al. All data is experimental results.

Theoretical study showed the impurity of transition metals, Zr, Cr, Mn, Fe, Co and Ni have diffusion energies ranging from 1.5 to 2.7 eV [43]. Table 2.3 indicates that most of impurity atoms are not good candidates to the fluctuation generation at less than room temperatures due to high activation energies. The diffusion process is also an important factor for a fluctuation generation. The total diffusion is a sum of interstitial diffusion and substitutional diffusion. However, often either interstitial or substitutional diffusion process dominates. The size of an

impurity atom relative to the host atom exhibits a profound effect for diffusion process. According to Hägg's empirical rule, a fraction of interstitial diffusion is dominated if the ratio of atom sizes λ_i/λ_h of the impurity to the host is less than 0.85 [44]. In other word, larger atoms tend to diffuse substitutionally. Since substitutional diffusion holds exactly the same symmetry for entire diffusion in BCC and FCC crystals, no resistivity tensor can create deviation. Therefore no 1/f noise can be generated unless the asymmetrical environment, e.g. dislocations or grain boundaries are involved. Conversely, smaller atoms tend to diffuse interstitially. Then the impurity atom can take a position either the octahedral or the tetrahedral sites in BCC or FCC crystals. They can be the source of resistance fluctuation even at low temperature.

Host metal	Activation energy (eV)
Pd	0.217-0.270
Ni	0.373-0.469
α-Fe	0.432-0.486
Ta	0.11-0.16
V	0.039-0.059
Ag	0.326
Al	0.42-0.52
Au	0.245
Co	0.52-0.55
Cu	0.40-0.49
Mo	0.40-0.64
Pt	0.26-0.42
W	0.39-0.86
α-Zr	0.31-0.53

Table 2.4: The activation energies of H diffusion in different host metal and alloys. Ref [45].

Hydrogen has been received high attention for diffusion experiments in many years. Indeed, not just diffusion but also many hydrogen diffusion noise measurements were demonstrated by Alers et al. [46], Zimmerman et al. [47] and Scofield et al. [6]. Table 2.4 lists the representative activation energies. 0.1-0.5 eV was found in BCC metals. In all experiments, host metals and alloys which have negative enthalpies of solution were chosen. On the other hand, Au, Cu and Ag have positive enthalpies. Compared with the solubility in Nb at room temperature, Au or Cu should have nearly 13 orders of magnitude less solubility. And Ag has even much less solubility. Alers et al. achieved hydrogen diffusion noise measurement, which hydrogen was charged into Nb up to 3 % by a standard technique [45]. If the same charging technique is applied to a standard micron size Cu thin film, no hydrogen atom can diffuse into such a sample. Therefore a hydrogen diffusion noise is rather realistic in host metals which have negative enthalpies of solution, like Nb, Zr, Ta and Pd. It is less likely hydrogen diffuse into FCC metals. It can be concluded that no hydrogen diffusion noise can be expected in most FCC metals. Next consider other light atom diffusion in metal. Not so many data are available for other light atoms C, N, and O, see Table 2.5.

Again it was shown a majority of diffusion energies are relatively high to take into account for the 1/f noise at room temperature. Although not many data are available, it is less likely that such light atom diffusion is not responsible to a 1/f noise generation in a perfect crystal. However, atomic diffusion process in real metal is far from ideal diffusion in a perfect crystal unlike above mentioned. Defect- defect interactions play an important role quite commonly. Among them,

Host metal	Impurity	Activation energy (eV)
Ag	O	0.48
Co	C	1.65
Cu	O	0.70
γ-Fe	C	1.65
γ-Fe	N	1.76
γ-Fe	O	1.76
Ni	C	1.52
Ni	O	3.13
Pt	O	3.39
α-Th	C	1.65
α-Th	N	0.98
α-Th	O	2.13
V	C	1.02
V	N	1.57
V	O	1.30
Nb	C	1.48
Nb	N	1.58
Nb	O	1.14
Ta	C	1.68
Ta	N	1.65
Ta	O	1.15
Cr	C	1.15
Cr	N	1.20
Cr	O	1.61
Mo	C	1.79
Mo	N	1.13
Mo	O	1.35
W	C	1.96
W	N	1.24
W	O	1.04

Table 2.5 : The activation energies of C,N and O in different host metals.

Ref [48].

grain boundary plays a large role for the diffusion process. It is known the diffusion proceeds more rapidly along grain boundaries than through the lattice. Often a large variation of the activation energies for such diffusion was observed. And such activation energies have broad distributions. This is because the grain boundary diffusion strongly depends on geometrical conditions in a crystal, which imply many different types of diffusion paths and its activation energies. In the previous argument, the activation energies of impurity diffusion have rather small fraction of energy difference, a few tenths of eV, between impurity and self-diffusion. Therefore, most likely impurity grain boundary diffusion is masked by ordinary grain boundary diffusion unless a specific impurity has an extraordinary high concentration or the diffusion energy is substantially different from each other.

2.4.2 Dislocation dynamics

Dislocations can influence the profound effects in materials. Especially, the fact that material strength can be controlled by dislocations has been long concerned by scientist and engineers. A huge effort has been poured into the understanding dislocations. Dislocation kinetics has been established in general although the detailed understanding and precise control still remained. It is nearly impossible to make dislocation free materials. In other words, if a material has crystal structure, all materials contain dislocations. How does a 1/f noise incorporate with dislocations? Two distinctions can be made for a potential noise generation. One is the static dislocation may contribute a 1/f noise generation. For

example, a dislocation can be an easy path for defect transport. This type of diffusion is called pipe diffusion. A vacancy can transport near dislocation core in relatively low activation energy than lattice. This may induce a mass transport and 1/f noise generation. Oches et al. performed temperature dependence of 1/f noise in single crystal Al films in a wide range of temperatures [49]. They concluded the noise generation is due to the pipe diffusion and its peak activation energy ~0.9eV. For another example, Bruner has proposed a different type of relaxation mechanism to explain Bordoni peak in FCC metal. When a dislocation dissociates into partials and a trapped defect resides near partials, the dislocation may switch one stable configuration to another. This may induce a resistance fluctuation. On the other hand, the dynamic dislocation will directly influence a local environment. This will make the local resistivity fluctuate. This dynamic dislocation is caused by mainly two reasons. The one is the existence of stress. Another is thermally activated dynamics. Or both cases may be involved each other. Scofield and Giordano applied mechanical strain to thin Pt and Au films [7]. This revealed a direct information of the 1/f noise through the mechanical relaxation. Just after bending these film substrates, the 1/f noise power immediately jumped a factor of 2-4. Then within an hour, the noise diminished and only 20-30 % stationary increase was remained. Those substrates were released from bending then similar time dependence of noise power was observed. This is a clear example that the mechanical relaxation can create the 1/f noise. When a stress level is high, a dislocation glide can occur. Scofield and Giordano used mica as substrates, which made it plausible to apply a large strain. As a result, it is likely that a dislocation

climb or a jog movement occurred and subsequently point defects were generated. This might be responsible for the 1/f noise generation. In ordinary noise measurements, no external force is applied to metal films and substrate materials. Sometimes internal stress can not be ignored. However, in most cases, samples are kept at room temperature for a while after fabrication, the mechanical relaxation has been done. Although the flow stress remained, no dynamical relaxation, e.g. kink diffusion, can be expected. No such process should contribute the 1/f noise at room temperature.

How about thermally activated dislocation dynamics with or without stress? A variety of dislocation kinetics may belong to this type of dynamics. Followings are candidates of the thermally activated dislocations [50].

(1) Thermal jog

When segments of dislocation lines intrude or extrude from its original glide plane, they are called jogs. Jogs can be formed by the stress or the thermal energy. Dislocation climb process is a famous example of jog formation. If a jog is created from an original dislocation line, a pair of jogs should be formed. The formation energy of a pair of jogs is described as,

$$E_{jog} = \frac{\mu b^2 a}{2\pi(1-\nu)} - \frac{\mu b^2 a^2}{8\pi L(1-\nu)} \qquad \textbf{(2. 23)}$$

where μ is shear modulus, b is a Berger vector, a is the separation length between the original dislocation line and jog dislocation line, ν is a Poisson's ratio and L is the separation length between a jog pair. The formation energy of jogs is much higher than that of a double-kinks formation. Thermal jogs may be considerable

only if the temperature is much higher than room temperature or is highly stressed environment.

(2) Thermal kink

When a segment of a dislocation lies across the original Peierls valley to another, a short segment of dislocation line bridges two dislocation lines which lie in different Peierls valleys. This configuration is called kink. No matter how kinks are formed, they still lie in the original glide plane. This makes it relatively easier to move dislocation lines on a glide plane than the jog does. If one end of dislocation lies a different Peierls valley than the another end, a minimum number of kinks are required due to the geometrical necessity. This type of kinks is called geometrical kinks [51]. If kinks are created from straight dislocation line, a pair of kinks, a double-kinks, should be formed. Compared with a pair of jogs formation, double kinks formation requires a much lower energy. Therefore applied stress may easily create double kinks. Not only the stress, the thermal energy may be enough to create double kinks. This is called thermal kink. The formation energy of a double-kinks is described as,

$$E_{kinks} = \frac{\mu b^2 a}{4\pi(1-\nu)}\left[\ln\frac{a}{e\rho} - (1-\nu)\right] - \frac{\mu b^2 a^2}{8\pi L}\frac{1+\nu}{1-\nu} \qquad \textbf{(2. 24)}$$

Figure 2.10 (A) and (B) show formation energies of a pair of jogs and a double-kinks without any stress. The computation is specifically for Al. The general trend of this figure does not change in most metals. The negative formation energy implies such short double kinks may be created even at 0 K. Since this

theory is based on a continuum model, only crude estimation may be appropriate. Still it is more likely double kinks could be formed at low temperatures.

Our primary concerns of dynamical activation kinetics are in metal thin films. In general, metal thin films are highly stressed and defected. It is quite reasonable to involve stress as a factor into formation energies. Additional formation energy by a stress is written as, $\Delta E_{stress} = -\sigma blx$, where, σ is stress, b is Berger vector, l and x are described as follows. For a double kinks formation, l is a separation length between dislocation lines which lie on Peierls valleys and x is a separation length between two kinks. For a pair of jog formation, l is a segment length of jogs and x is a separation length between the segment of jogs and the original glide plane. For example, σ in Al thin film can exceeds 10 M Pa, b~2Å, l ~10 μm and x ~1000 Å. Then estimated ΔE_{stress} ~1 eV is obtained. This is a considerably large energy and this reduces the energy barriers of thermally activated kinetics, which could take place only at high temperatures without stress. At low temperatures, the thermal formations of any defects are less likely, however the existence of stress may drastically change this situation. Dislocation dynamics is basically multi-atom process and it is more likely that the surrounding environment shows anisotropy. In short, these dynamics may be a potential source of 1/f noise, especially when a mechanical relaxation is involved. Such a noise generation should be either the time dependence or not. Indeed, Scofield and Giordano observed a time dependent effect.

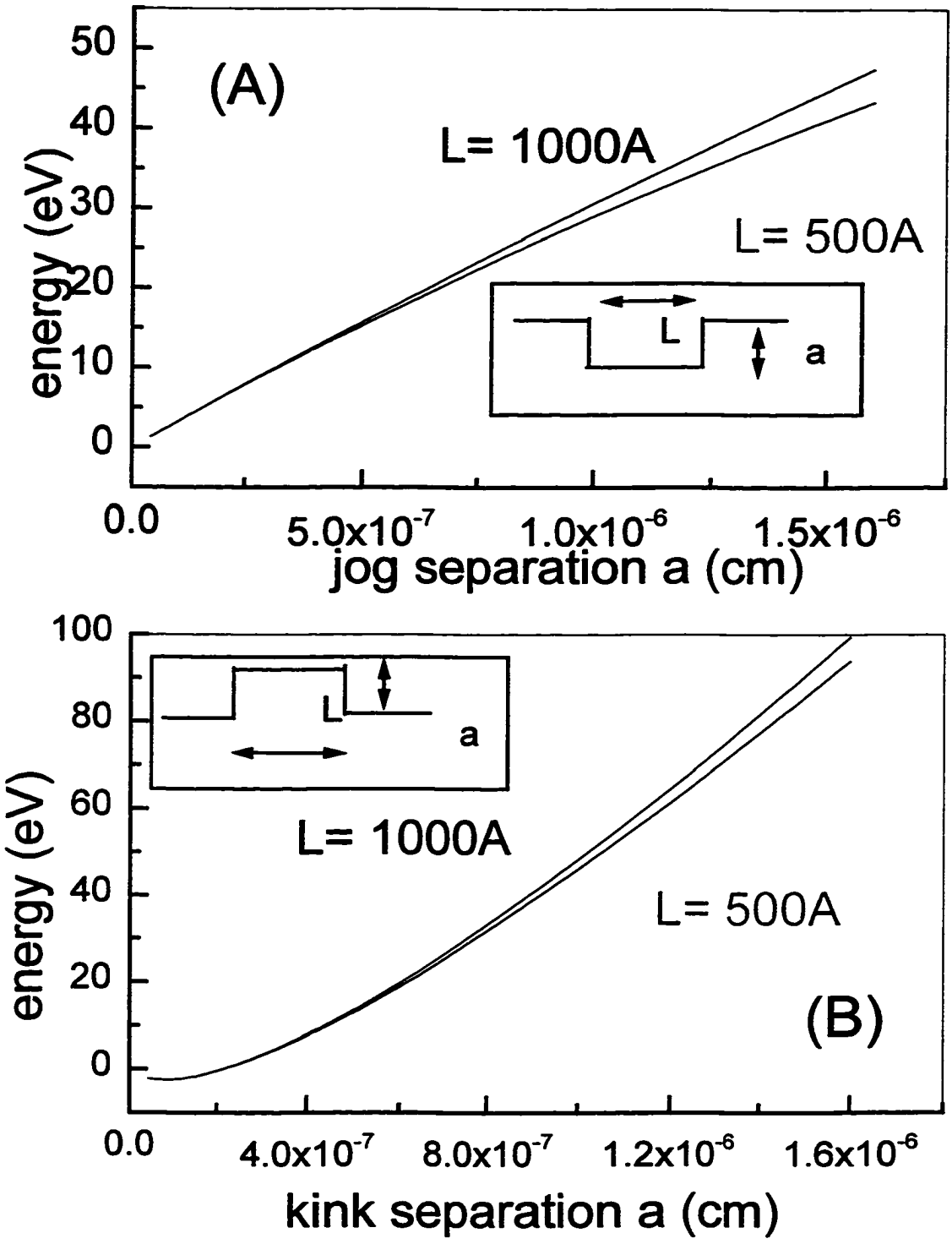

Fig. 2.10: The formation energies of (A) a double kink and (B) a pair of jogs.

2.5 Quantum interference effects

It has been established that the Bloch-Boltzman quassiclassical theory of electron transport can successfully described most of charge carrying phenomenon. The weak scattering theory of conductivity, called Drude model, is described as, $\sigma_0 = \frac{ne^2\tau}{m}$, where n is the electron density, τ is the relaxation time and m is the electron mass [52]. In metals, as the temperature decreases, τ increases so as the conductivity. However, when a metal sample is small and is placed into a low temperature environment, the situation is quite different. In such a condition, injected electrons no longer collide with phonons and can reach one end to another without losing a phase coherent. This transport regime is no longer classical but quantum. Al'tshuler and Lee et al. have exhibited the ensemble averaged conductance value could be universal quantity ~(e^2/h) [53, 54]. this is called a Universal Conductance Fluctuation (UCF). Umbach et al. have found the random magetconductance curves had a unique conductance pattern by changing a magnetic field [55]. Further this conductance fluctuation curve was magnified as the temperature decreased. The fluctuation pattern did not change but simply it was amplified. This startling phenomenon is called magnet fingerprint. Since then a number of experiments were performed. A majority of experiments were either performed by the changing a magnetic field [56] or the changing Fermi energy [57]. Complete calculations of quantum corrections to the conductivity have been achieved by quantum field theory. However, the conceptual understanding is quite easy. One of the best ways is to take a look Aharonov-Bohm (AB) effect with two

simple electron paths. Figure 2.11 shows a noninteracting electron moves from point A to B. The electron is assumed to be spinless.

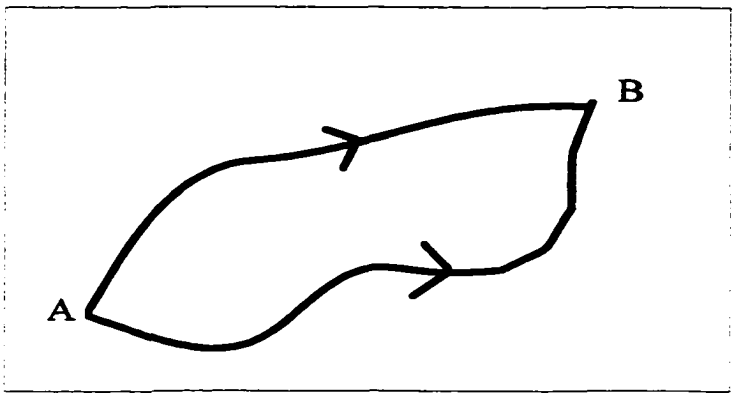

Fig. 2.11: Two trajectories of a electron transport.

The path can be taken a numerous different paths. The total probability of an electron moves from A to B is described as the square of the modulus of the sum of all amplitudes. Each amplitude from A to B is Am_i where i indicates an index.

$$Total\ Probability = \left|\sum_i Am_i\right|^2 = \sum_i |Am_i|^2 + \sum_{i \neq j} Am_i\ Am_j^* \qquad (2.25)$$

The second term in Eq.(2.25) is the interference term. In case of the number of trajectories is infinitely large, this term is insignificantly small since a summing up all phase terms from different lengths of trajectories gives no contribution. However, if the number of trajectories is finite, the interference term may not be small. If the magnetic field can modify an electron phase, the total probability may periodically change. This is AB effect. In a diagram, each point is

given as the input of electrons and output in Fig.2.11 In ordinary thin metal film samples, many electron paths have to be considered in Fig.2.12.

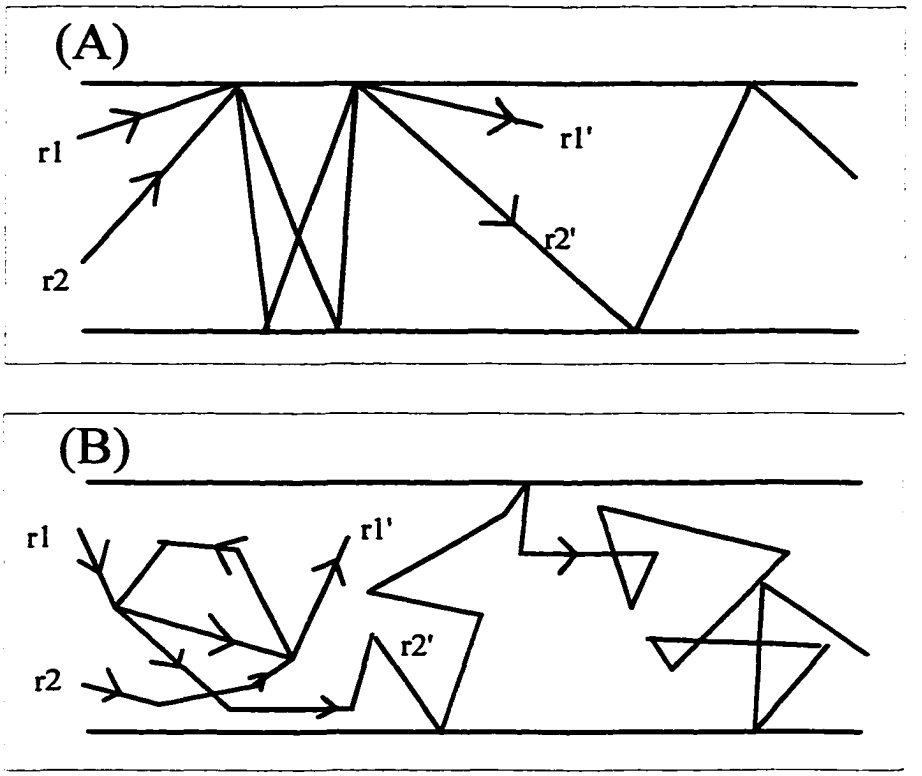

Fig. 2.12: The multiple electron scattering. (A) Forward scattering is dominated and (B) Back scattering is enhanced.

In a clean and small meal sample at low temperatures, the electron scattering process is dominated by diffusive forward scattering in Fig.2.12 (A). In such a multiple scattering regime, the long range correlation has been calculated by Feng et al. and Kane et al. [58,59]. They obtained the conductance fluctuation an order of e^2/h. On the other hand, when the metal films are fabricated by physical

vaporized deposition (PVD) at low substrate temperatures, the deposited metal atoms can not be crystallized well. As a result, the crystal structure is more like amorphous, i.e. sometimes called "a glassy metal". Such metals show a weakly localization (WL) at low temperatures. The generated localized potentials behave strong electron scatterers. Thus, the electrons are scattered much short distance than those in clean metals. Then some amounts of injected electrons are backscattered in Fig.2.12 (B). In such a short elastic scattering regime, Lee et al estimated the conductance fluctuation an order of e^2/h [54]. To introduce the magnetic field effect, the simplified four probe electron paths are shown in Fig.2.12 (A) and (B). In (A), the two paths form a closed loop. And electrons travel along the upper path and the lower in the same sense. The correlation of two conductivity $\sigma_{r1r1'}\sigma_{r2r2'}$ is calculated by the product of the transmission probability, $P(r_1, r_1') * P(r_2, r_2')$. This type of transmission channel is called diffuson channel. When the magnetic field (B field) is applied on the paths, the additional relative phase $\frac{e}{\hbar}\int \vec{A}\cdot d\vec{l}$ is introduced. Since both arms of the closed loop have a same sense of electron paths, the B field effect is canceled out. On the other hand, the loop in (B) has the opposite sense of the path along the upper path and the lower. When a B field is applied, the contribution of the relative phase $\frac{e}{\hbar}\int \vec{A}\cdot d\vec{l}$ is not canceled out. This is the broken of time revearsal symmetry. This type of transmission channel is called cooperon channel. The same effect is arised if a chemical potential changes. Since both channel cases, the estimated conductance fluctuation is an order of e^2/h, which is called the universal conductance

fluctuation (UCF). In WL regime, the number of diffuson channels and cooperon channels are nearly equal. Under the B field, the noise suppression factor two was demonstrated by McConville and Birge [60].

2.5.1 A quantitative analysis of UCF 1/f noise

These UCF phenomena are rather static, i.e. the fluctuation is time independent. Feng et al. proposed the dynamical UCF by impurity scattering. If one impurity moves a distance more than k_F^{-1}, then the conductance of the sample will be changed by the order of e^2/h in one or two dimensional system. If the impurity has a slow motion of switching or diffusing, this may create a low frequency conductance (resistance) fluctuation. This is a basic mechanism of UCF 1/f noise generation. A most of thermally activated defects or impurities are stable at low temperatures. However, if the activation energy of some kinetics is quite small, it may be possible that the slow kinetics could be a source of UCF 1/f noise.

Next we will attempt a quantitative argument of UCF noise. The conductance phenomena by correlated electrons is well explained by the Landauer formulation in Eq.(2.26), where $t_{m,n}$ is the transmission amplitude.

$$G = \frac{e^2}{h}\sum_{m,n}\left|t_{m,n}\right|^2 \qquad \textbf{(2. 26)}$$

The transmission matrix can be calculated by the perturbation expansions in $1/(k_F l_{el})$. The following arguments have been done by several authors, Feng et al. [17], Stone [61] and Garfunkel [62]. One disordered metallic cube of the volume L^3 is considered. Elastic scattering length l_{el} is much shorter than L and

inelastic scattering length L_{in} is longer than the sample size L, i.e. $l_{el} \ll L < L_{in}$. If one strong scatterer is activated, then the conductance fluctuation $(\delta G_1)^2$ is described as,

$$(\delta G_1)^2 = \left\langle \{G(\vec{r}_1) - G(\vec{r}_1 + \delta\vec{r}_1)\}^2 \right\rangle \qquad \textbf{(2. 27)}$$

$$\cong (\frac{e^2}{h})^2 \qquad (1 \textit{ and } 2\,\text{dim})$$

$$\cong (\frac{e^2}{h})^2 (\frac{1}{k_F l_{el}})^{d-1} (\frac{L}{l_{el}})^{2-d} \alpha'(k_F \delta r_1) \qquad (3\,\text{dim}) \qquad \textbf{(2. 28)}$$

$$\alpha'(x) = 1 - \left(\frac{\sin(\frac{x}{2})}{\frac{x}{2}} \right)^2 \qquad \textbf{(2.29)}$$

where δr_1 is the displacement length of the activated specie. $\alpha'(x)$ describes a phase shift sensitivity factor for $k_F \delta r_1$. The assumption $K_F \cdot l_{el} \gg 1$ is used.

At finite temperature, the correlation energy range E_c has to be considered. In Fig.2.12 (A) and (B), it was shown that two electron paths are correlated and this creates the fluctuation. Unless the temperature is not zero, the energy of conduction electrons is spread near the Fermi energy. Two electrons may not have exactly same energies. When such correlated paths are considered, how much energy difference is allowed to correlate electrons? This will be answered by a following argument. When an electron moves one point to another, the classical action may be introduced S(P,E).

$$S(P,E) = S_p - Et \qquad \textbf{(2.30)}$$

Now assume that another electron moves on a same path but it carries a slightly different energy E+ΔE.

$$S'(P,E) = S_p - (E + \Delta E)t \qquad \textbf{(2. 31)}$$

We set a moving distance L_T, which is $L_T = \sqrt{D\tau}$. Then the change of phase Δφ is written,

$$\Delta\varphi = \frac{1}{\hbar}(S' - S) = \frac{\Delta E}{\hbar}t = \frac{\Delta E}{\hbar}\frac{L_T^{\,2}}{D} \qquad \textbf{(2. 32)}$$

If the phase change is 2π, then $E_c = \Delta E = \frac{hD}{L_T^2}$. This energy is called correlation energy. At finite temperature, the energy spread is ~kT. Therfore the thermal length L_T is defined as $L_T = \sqrt{\frac{hD}{kT}}$, the length to create the phase diffrence 2π when two electrons move on the same path but the energy is different ΔE~kT.

When a sample size L is smaller than L_T, ΔE > kT, no diminish of the conductance fluctuation $(\delta G)^2$ is taken place. When the sample size is larger than the thermal length $L > L_T$ or $kT > \Delta E$, then the energy averaging effect has to be considered. The reduction factor is $\frac{\Delta E}{kT} = \left(\frac{L_T}{L_{in}}\right)^2$ in 1 and 2 dimension. In 3 dimension, the correlation factor $\langle \delta G(E)\delta G(E + \Delta E)\rangle$ does not decay so rapidly as 1 and 2 dimensional cases [53]. Rather $(\delta G)^2$ diminish only $\left(\frac{L_T}{L_{in}}\right)$.

All $(\delta G)^2$ is effective up to e^2/h. In other words, the universal conductance fluctuation has a saturation regime. In a non-saturation regime, if the number of scatterers is increased by N, the expected conductance fluctuation is written as,

$$(\delta G_N) = N(\delta G_1) \qquad (2.33)$$

Here, the number of scatterers linearly increased the total fluctuation $(\delta G_N)^2$. Feng et al. pointed out that this may not be the case in low dimension. For example, in 1 dimensional case, a random walk electron can pass through the scatterer over and over again. This easily reaches a saturation regime. However in 3 dimensional case, the number of possible paths is substantially large. Thus the saturation regime is effective. In Eq.(2.27), (l_{el}/L) is multiplied in 3 dimension in the limit $K_F \cdot l_{el} \sim 1$. Since the cross sectional area of a scatterer is l_{el}^2, the simplest expression of the probability which electron is influenced by the scatterer is l_{el}^2/L^2. However, the back-scattered electron may revisit to the scatterer by a factor L/l_{el}. This gives (l_{el}/L) in Eq.(2.27). When $K_F \cdot l_{el} \gg 1$, the reduction factor is $\frac{(\delta r)^2}{A}$, where A is a cross sectional area normal to the net current direction. Since the forward scattering is rather dominant, it is not necessary to count a revisit factor. At finite temperature in real samples, inelastic scattering length is much shorter than the real sample length, $L_{in} < L$. Each coherent regions are independent and the classical averaging should be considered, i.e. the coherent volume divided by the total volume $(L_{in})^3/ L^3$. In WL regime, the fraction of the conductance fluctuation, $(\delta G)^2/G^2$, is written as,

$$\left(\frac{\delta G}{G}\right)^2 = \left(\frac{L_{in}}{L}\right)^d \left(\frac{\delta G}{G_{L_{in}}}\right)^2 \qquad in\ L >> l_{el} \qquad (2.34)$$

The classical averaging relation of G_{Lin} and G is

$$G = \left(\frac{L}{L_{in}}\right)^2 \left(\frac{L_{in}}{L}\right) G_{Lin} = \left(\frac{L}{L_{in}}\right) G_{Lin} \qquad (2.35)$$

Then $(\delta G)^2$ is written as,

$$(\delta G)^2 = \left(\frac{Lin}{L}\right)(\delta G_{NLin})^2 \qquad (2.36)$$

In a clean rectangular sample in 3 dim, the fraction is written,

$$\left(\frac{\delta G}{G}\right) = \left(\frac{AL_{in}}{AL}\right)\left(\frac{\delta G_N}{G_{Lin}}\right) \qquad (in\ clean\ metal) \qquad (2.37)$$

where A is a cross sectional area. The classical averaging relation of G_{Lin} and G is

$$G = \left(\frac{L_{in}}{L}\right) G_{Lin} \qquad (in\ clean\ metal) \qquad (2.38)$$

This is a clear difference between WL and Clean metal regimes. Then $(\delta G)^2$ is written as,

$$(\delta G)^2 = \left(\frac{L_{in}}{L}\right)^2 (\delta G_{NLin})^2 \quad (in\ clean\ mtal) \qquad (2.39)$$

After the whole consideration is included, the total fluctuation may be written as,

$$(\delta G)^2 = N(\delta G_1)^2 \cdot \{\textit{Thermal length factor } E_c > kT \textit{ or } E_c < kT\} \times \{\textit{Averaging factor by phase coherent volume}\} \times \{\textit{Classical averaging factor between } G \textit{ and } G_{Lin}\} \quad \textbf{(2. 40)}$$

In dirty or WL regime in 3 dimension, the following assumptions are made, Ec < kT. Our primary concerned temperature range is from 10K to room temperature. Of course, this is not the case at less than 1K, $K_F l_{el} \sim 1$. In other words the elastic scattering length is quite short ~Å, $l_{el} \ll L_T$, $L_{in} \ll L$. The conductance and the fractional fluctuation, $(\delta G)^2$ and $(\delta G)^2 /(G)^2$ are,

$$(\delta G)^2 = \left(\frac{e^2}{h}\right)^2 n L_{in} L_{\min}^2 \left(\frac{l_{el}}{L}\right)(k_F)^{-2} \alpha'(k_F \cdot \delta r) \quad \textbf{(2. 41)}$$

$$\left(\frac{\delta G}{G}\right)^2 = R^2\left(\frac{e^2}{h}\right)^2 n L_{in} L_{\min}^2 \left(\frac{l_{el}}{L}\right)(k_F)^{-2} \alpha'(k_F \cdot \delta r) \quad \textbf{(2. 42)}$$

L_{min} describes the shorter length either L_{in} or L_T.

In a clean rectangular metal in 3 dimension, Ec < kT and $K_F l_{el} > 1$.

$$(\delta G)^2 = \left(\frac{e^2}{h}\right)^2 n L_{in}^4 L_T \frac{(\delta r)^2}{(l_{el} L)^2 A}(k_F)^{-2} \alpha'(k_F \cdot \delta r) \quad \textbf{(2.43)}$$

$$\left(\frac{\delta G}{G}\right)^2 = R^2\left(\frac{e^2}{h}\right)^2 n L_{in}^4 L_T \frac{(\delta r)^2}{(l_{el} L)^2 A}(k_F)^{-2} \alpha'(k_F \cdot \delta r) \quad \textbf{(2.44)}$$

One fluctuator creates the fractional fluctuation $\frac{1}{n}\left(\frac{\delta G}{G}\right)^2$, which is called the coupling factor per fluctuator. In 2.3.2, the noise power was estimated in Eq.(2.14). The dimensionless noise parameter α_H, called Hooge parameter, is introduced to describe the noise power,

$$S_v = \alpha_H \frac{V^2}{N_0 f^\gamma} \qquad \textbf{(2. 45)}$$

where, f is frequency, N_0 is the number of atoms and V is the voltage across the sample. Sorting the one fluctuator fraction, Eq.(2.15) and Eq.(2.45) can be combined as,

$$\frac{S_v(\omega,T)}{V^2} = \frac{S_G(\omega,T)}{G^2} = \left(\frac{\delta G}{G}\right)^2 \int D(E) \frac{\tau_0 e^{\frac{E}{kT}}}{1+(\omega\tau_0 e^{\frac{E}{kT}})^2} dE = \frac{\alpha_H}{N_a f^\gamma} \qquad \textbf{(2. 46)}$$

Since unit volume was assumed, N_a is the number of atoms per unit volume. Now α_H may be expressed in LI and UCF regime.

In LI regime,

$$\alpha_{HLI} = n_s N_a (\beta\sigma l_{net}) \int D(E) \frac{\tau_0 e^{\frac{E}{kT}}}{1+(\omega\tau_0 e^{\frac{E}{kT}})^2} dE \qquad \textbf{(2.47)}$$

In UCF regime in disordered metals,

$$\alpha_{HUCF} = n_s N_a R^2 \left(\frac{e^2}{h}\right)^2 L_{in} L_{\perp}^2 \left(\frac{l_{el}}{L}\right) (k_F)^{-2} \alpha'(k_F \delta r) \int D(E) \frac{\tau_0 e^{\frac{E}{kT}}}{1 + (\omega \tau_0 e^{\frac{E}{kT}})^2} dE$$

(2.48)

In UCF regime in clean metals,

$$\alpha_{HUCF} = n_s N_a R^2 \left(\frac{e^2}{h}\right)^2 L_{in}^4 L_T \left(\frac{(\delta r)^2}{(l_{el} L)^2 A}\right) (k_F)^{-2} \alpha'(k_F \delta r) \int D(E) \frac{\tau_0 e^{\frac{E}{kT}}}{1 + (\omega \tau_0 e^{\frac{E}{kT}})^2} dE$$

(2.49)

Chapter 3

The noise measurement system

3.1. Noise measurement technique

In this chapter, we introduce the basic idea of noise measurement and explain the technical detail of our noise measurement system. To measure a targeted noise, it is extremely important not to measure other noises. This means that a noise measurement is all time competition between a target noise and other unwanted noise. Another important concept of noise measurement is to identify what noise we are measuring. Currently our noise measurement system can detect as low as $20pV/\sqrt{Hz}$ fluctuation from a low resistance sample, less than 10Ω. The measurement temperature can be changed from 11K to Room temperature for low temperature setup and can reach up to 450K for high temperature setup. Before we go further detail of our noise measurement system, let's look back at a history of noise measurement systems. This gives more comprehensive understanding of noise measurements.

Figure 3.1 shows one of the earliest noise measurement setup. This system consists of a stable constant current source, a measurement sample, DC decoupling capacitors, a transformer and a First Fourier Transformation system (FFT). To obtain a high stability of a current, the current source often employed was a high capacity battery and a current control resistor. The transformer has dual purpose, which one is to amplify a signal and another is to transform the impedance from the source side. This is the simplest system. If an expected voltage fluctuation is

rather high, more than a μV or the spectrum density is well extended to 10Hz or more, then this system can provide enough sensitivity. Although simplicity is an advantage, there are a couple of disadvantages. First, it requires large DC decoupling capacitors to measure the low frequency spectrum, less than 1Hz because the impedance of a capacitor is inversely proportional to the frequency. A higher impedance by capacitor provides a lower voltage input into the primary side of transformer. As a result, a signal to noise ratio is down. And these capacitors must be a low current leakage for high sensitivity. In other words, the standard electrolytic capacitors can not be used although this type of capacitors is commonly applied for most high capacitance requirements. In short, special capacitors are necessary. Second, the effective transformer gain is expected to be low. Since the input impedance of a transformer is proportional to frequency, the input voltage is reduced as the frequency decreases. The DC decoupling capacitors and transformer strictly limit the low voltage measurement at low frequencies.

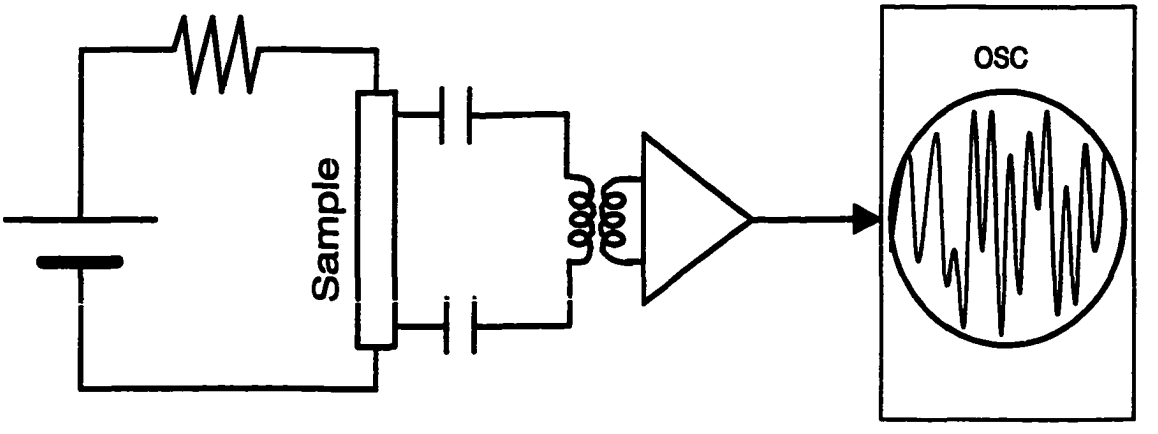

Fig. 3. 1: The simplest setup for noise measurement.

3.2. The single modulation technique.

Instead of applying DC, AC current excitation may remove such disadvantages. In 1987, Scofield proposed an AC bridge excitation method to measure a low frequency fluctuation [64]. We call this AC excitation technique as a single modulation technique. Fig.3.2 shows the schematics. This technique has drastically changed a sensitivity of the noise measurements. And this is a one of the most popular techniques. As matter of fact, many noise experiments have been conducted by this technique. The principle is described as follows. A wheatstone bridge is excited by AC current. This bridge is separated an upper part and a lower part. The upper part of bridge consists of the resistance decade boxes and variable capacitor. The lower part of bridge is a measurement sample which has a five terminal structure.

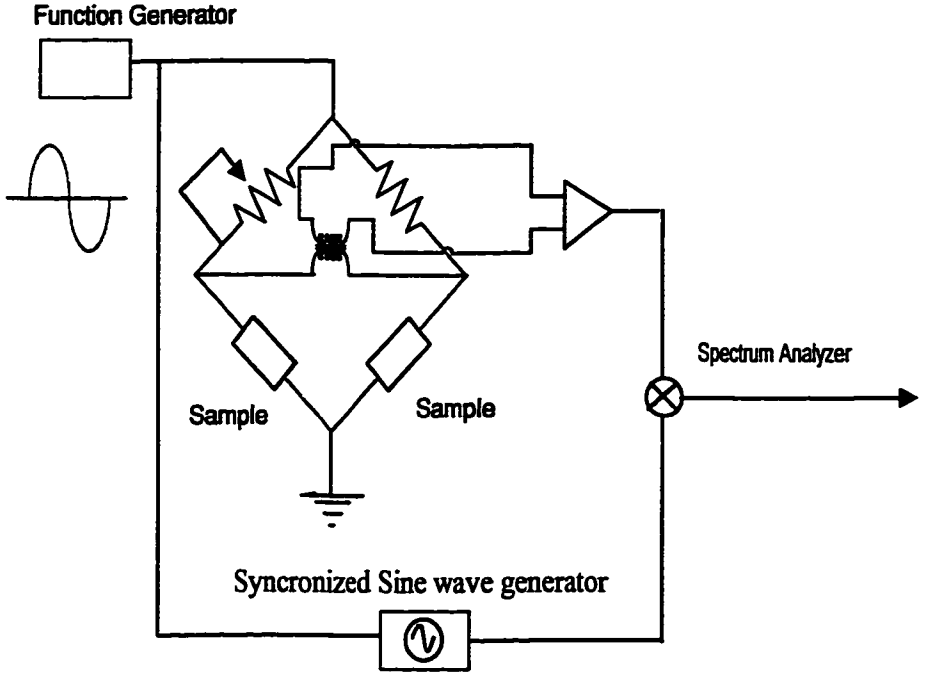

Fig. 3. 2: The single modulation technique.

After the bridge is equilibrated, the error signal is sent to the gain transformer and a preamplifier with band pass filter. Then the amplified error signal is sent to a synchronized demodulator. The demodulator separates the original input signal into two spectrums. One is the fluctuation spectrum we want and another is the spectrum which the dominant spectrum has a doubled carrier frequency component. Such high frequency spectrum is easily filtered out by passing the signal through a low pass filter. Finally only a successfully amplified fluctuation signal is sent to FFT. One of the great advantages of this technique is the Wheatstone bridge excitation by AC. No DC decoupling capacitor is necessary. Since the passing signal through the transformer contains primary a carrier frequency component, no serious problem has to be faced about transformer efficiency. A working frequency of electronic components and equipment can be for standard audio frequencies. This system has removed all DC decoupling problems, which the predecessor could not avoid. However, still one problem has been remained, i.e. a white noise. Any resistive sample must exhibit a white noise. For example, when the sample resistance is 10Ω and the sample temperature is 100K, then the spectrum density of the white noise is 5.5×10^{-20} V^2/Hz. If any expected fluctuation spectrum density is less than that, it is impossible to observe. This obstacle is eliminated by AC cross-correlation technique.

3.3. AC cross-correlation technique

If a fluctuation signal is taken by the single modulation technique, which described a previous section, the unavoidable noise, e.g. a white noise and a

preamplifier noise, has to be taken into account before accurate data can be extracted. To obtain only the fluctuation signal, one solution is to subtract the background noise, which is obtained without any bias current after the standard measurement is taken. The background noise in these two measurements can differ for following reason. The Johnson noise level is higher in a sample when a current is applied to it than when no current is applied because the sample is heated. Verbruggen et al developed a novel technique which can eliminate background noise without a subtraction procedure [64].

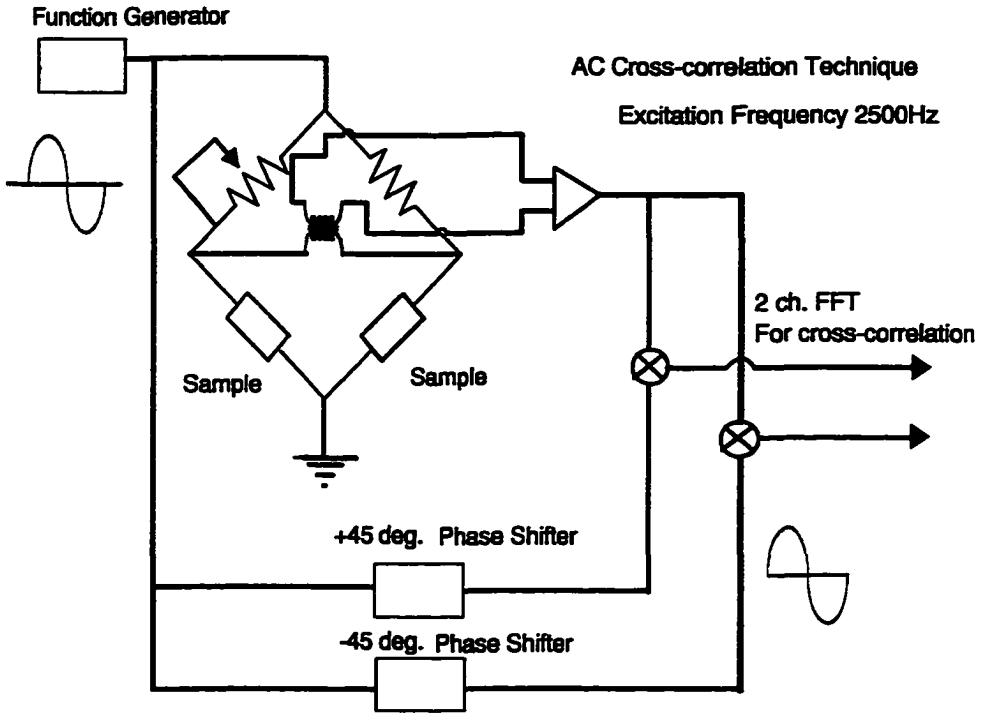

Fig. 3. 3: AC cross-correlation technique.

3.3.1 Principle

Fig.3.3 is a schematic diagram showing, a five-terminal sample and two upper arm resistances, forming a Wheatstone bridge. This bridge is excited by the AC function generator. The output signal is:

$$V_{out} = \Delta R(t) I_0 \sin(\omega_0 t) + V_0 \sin(\omega_0 t) + V_t(t) \qquad \textbf{(3. 1)}$$

The three terms in Eq.(3.1) are as follows; resistance fluctuation, an imbalanced bridge, and a thermal noise term. The second term is zero, it is assumed that if the bridge is perfectly balanced:

$$V_{out} = \Delta R(t) I_0 \sin(\omega_0 t) + V_t(t) \qquad \textbf{(3. 2)}$$

The output signal is amplified by a gain G, and is modulated by $\pm\pi/4$ [rad] phase-shifted sine wave:

$$U(t) = U_0 \sin(\omega_0 t + \frac{\pi}{4}) \qquad \textbf{(3. 3)}$$

The modulated signal S± is:

$$S_{\pm} = U_0 \sin(\omega_0 t \pm \frac{\pi}{4}) \otimes G\{\Delta R(t) I_0 \sin(\omega_0 t) + V_t(t)\} \qquad \textbf{(3. 4)}$$

Passing through a Low Pass filter, the $\Delta R(t) \cos(2\omega_0 t)$ and $\Delta R(t) \sin(2\omega_0 t)$ terms can be eliminated if the corner angular frequency is set $\omega_c \ll \omega_0$. Since $\Delta R(\omega) \propto 1/f$, $\Delta R(2\omega_0) \cong 0$.

After Fourier transforming S±, then the cross-correlation of S_+ and S_- is obtained. Using the following relations, the power spectrum S_v is obtained. White noise is not frequency-dependent. Further if the frequency is shifted, the spectrum does not change. This is shown as Eq.(3.5):

$$V_t^2(\omega-\omega_0)=V_t^2(\omega+\omega_0) \qquad (3.5)$$

Eq.(3.6) expresses the average of the cross-correlation for the thermal noise spectrum at different frequencies is 0.

$$\langle V_t(\omega-\omega_0)\cdot V_t(\omega+\omega_0)\rangle=0 \qquad (3.6)$$

$$S_v=S_+S_-^*=\frac{(U_0G)^2}{8}[\Delta R(\omega)I_0]^2 \qquad (3.7)$$

The spectrum of the cross-correlation was demonstrated to show the actual reduction of thermal noise. Fig.3.4 shows a comparison of the spectrum power S_v between single modulation technique and AC cross correlation technique. A test sample was a single crystal Al film at room temperature. The spectrum result clearly demonstrated that single modulation technique provide a combination of 1/f noise spectrum and thermal noise. On the other hand, AC cross correlation technique showed its advantage, which is the random noise reduction. The reduction factor is about 10. Two sharp spikes were shown in the spectrum about 15 and 45 Hz. This is due to the modulation of power line harmonics and a bridge

excitation signal. In real measurements, such an artificial noise peak spectrum was removed before the non-linear fitting procedure was performed.

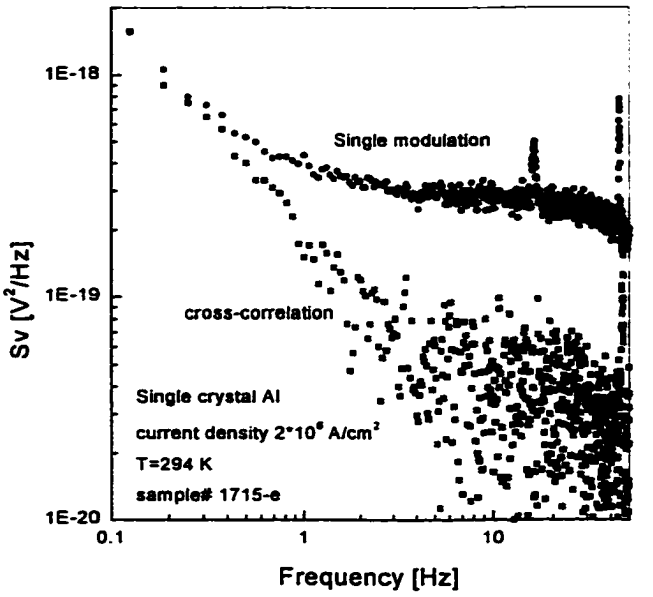

Fig. 3. 4: The noise power comparison with a single modulation technique and a AC cross-correlation technique.

3.3.2 The technical details in the system

Although the principle of the AC crosscorrelation technique has been shown, the detail technical arguments are necessary to accomplish a high performance. Followings are part by part details.

(1) Wheatstone bridge

Let's take a look at the Wheatstone bridge carefully. Since we want to measure a fluctuation only from a test sample, it is preferable the upper bridge parts creates insignificant noise. Although the sample temperature can be a quite

low, the upper parts of the Wheatstone bridge are, of course, at room temperature. The resistance of one upper arm is ~1kΩ. This creates a thermal noise power 1.6×10^{-17} V^2/Hz. From a testing sample, an expected noise power is about less than 1×10^{-21} V^2/Hz at low temperature. It seems impossible to measure such a small spectrum from such noisy upper bridges. Fig.3.5 shows a simplified schematic of the Wheatstone bridge, where the symbol of the voltage source described the thermal noise. The input voltage V_{in} to the transformer is,

$$V_{in} = \frac{Z_{tr}}{2R_{ub} + Z_{tr}} 2\sqrt{4kTR_{ub}} \qquad (3.8)$$

where, Z_{tr} is an input impedance of the transformer, R_{ub} is the arm resistance of upper bridge. Z_{tr} is frequency dependent. Since we chose the excitation frequency ~2500Hz, Z_{tr} ~150Ω is estimated. If a computation is made a straight forward, then, the total contribution of V_{in} from upper bridge arms is ~560 pV.

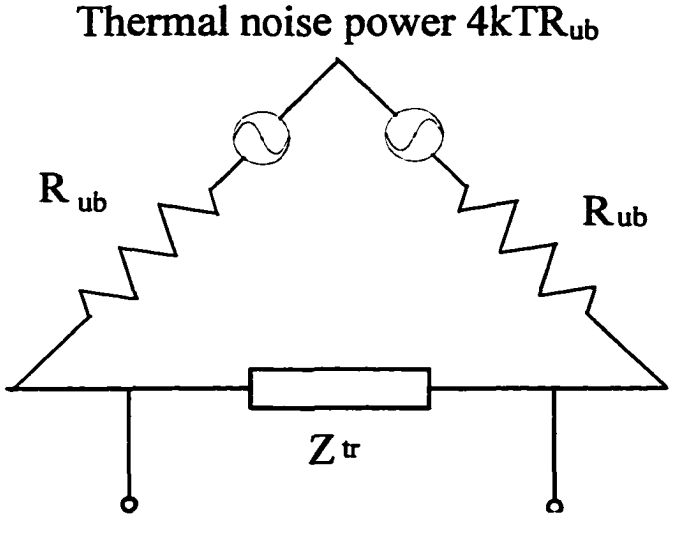

Fig. 3. 5: The thermal noise in Wheatstone bridge.

This is only true if the total impedance of the sample is higher than the transformer input impedance. All of measurement samples at low temperatures show lower impedance. Here, the term "impedance" means nearly the same as resistance because the reactive component of sample impedance is quite small. Therefore Z_{tr} is replaced by the sample impedance of 10Ω. The final V_{in} is ~40 pV. In 3.2.1, the random signal spectrum is reduced a factor 10. The net spectrum contribution is $\sim 2\times10^{-22}\ V^2/Hz$.

To achieve an optimum bridge balance, a four decades resistance box, 0.1 to 100Ω, and the variable resistance box, 10mΩ resolution, was used. Since the measurement samples normally contain the residual capacitance, the capacitance decade box, 1 to 1000pF, is attached in parallel to the resistance decade box. When the sample resistance is very small, less than 5Ω, the bridge is extremely sensitive

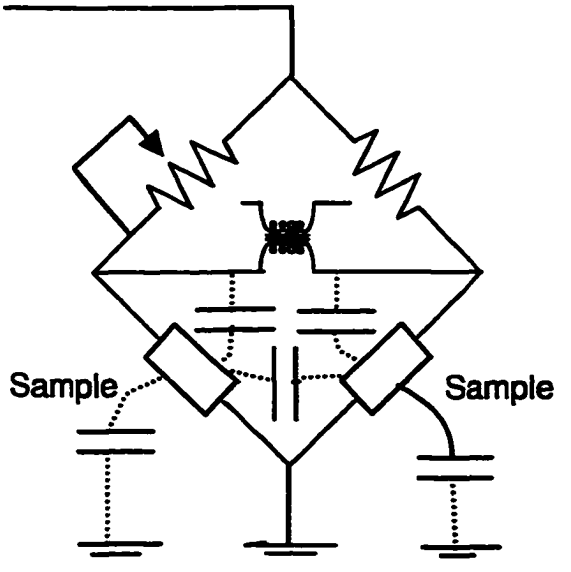

Fig. 3. 6: The stray capacitance.

to the capacitance. The extra variable capacitance, 100pF maximum, was installed. An existence of the stray capacitance always makes impossible to the perfect bridge balance in Fig.3.6 although all electronic components were common grounded. The last concern is the higher order harmonics. Quite often the current density in a sample can be as high as $4\times10^6 A/cm^2$. The Joule heating creates the additional resistance $\Delta R_{Joule}(t)$ in Fig.3.7. The $\Delta R_{Joule}(t)$ contains spectrum components with the frequency $2\omega_0$. Then the $\Delta R_{Joule}(t)\cdot I_0(t)$ provides higher order harmonics, dominantly the third order harmonics. This is very hard to avoid technically and limits a high gain of the amplifier. The only way to reduce is a passing through the band pass filter equipped with the preamplifier.

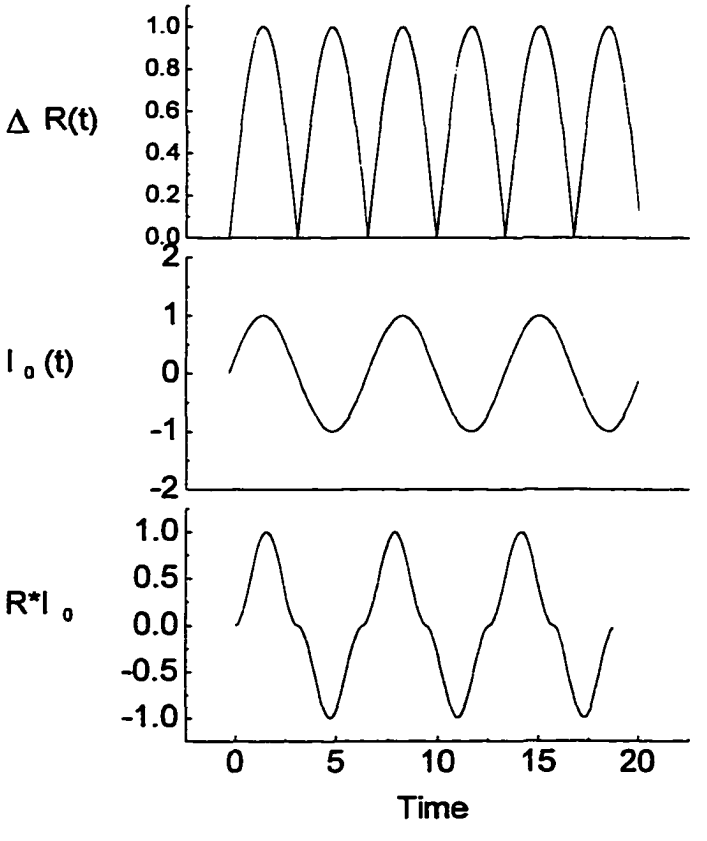

Fig. 3. 7: Higher harmonics generation of $\Delta R_{Joule}(t)\cdot I_0(t)$ by simultaneous sample heating $\Delta R_{Joule}(t)$.

(2) Transformer.

The transformer we used is the Stanford Research SRS554. At the beginning, the Princeton Applied Research Model 1901A (PAR1901) was also used. PAR1901 has a high gain option. However the lowest noise figure contours has rather narrow area than SRS544, i.e. the eye of the noise figure is smaller. The reason is PAR1901 has a much higher secondary resistance ~150kΩ than SRS544, which has ~5kΩ. This restricts the performance range of the source resistance. Since the change of a source resistance is rather large, typically 2 to 30Ω, when the sample temperature changes from 11K to 290K, the transformer has a gain dependence on the source resistance. The following is a test for the source resistance dependence of the transformer gain. Fig.3.8 shows a test setup and the result is shown in Fig. 3.9. The excitation frequency 2500Hz was chosen. This is one of the multiplication factors to compute a real noise power.

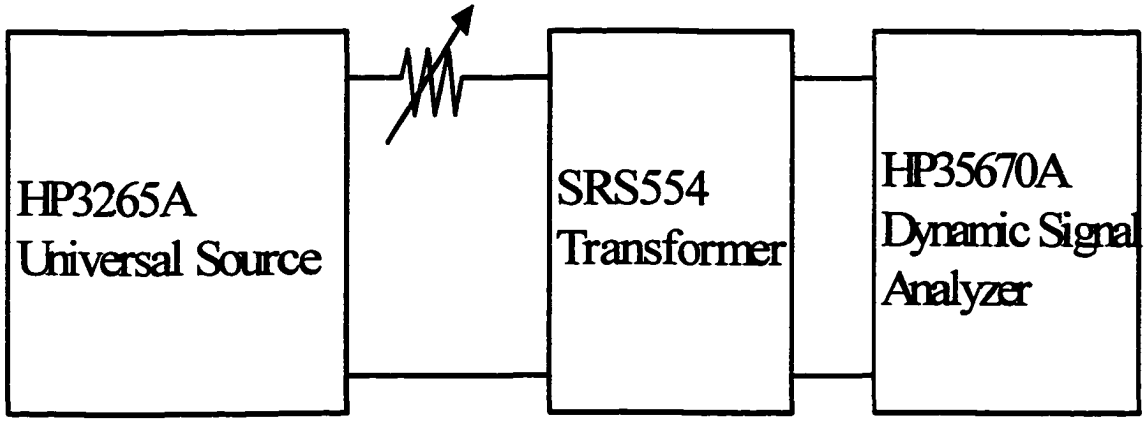

Fig. 3. 8: A test setup for the resistance dependence of a transformer gain.

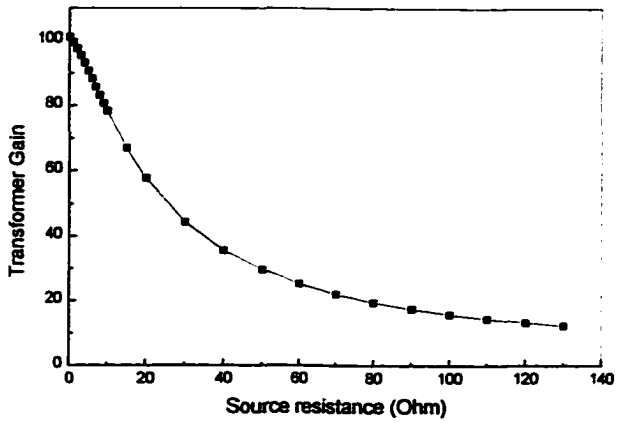

Fig. 3. 9: The resistance dependence of transformer gain.

(3) Preamplifier.

The Stanford Research SRS560 is employed as the preamplifier. The band pass filter is set to the lower corner frequency 1kHz and the higher 3kHz. This band pass filter suppressed the higher harmonics and helped to achieve higher gain. The preamplifier was operated by a battery mode without batteries. Instead, the DC power was supplied from outside the box to avoid a large power transformer noise.

(4) A copper shielding box

The Wheatstone bridge, transformer and preamplifier were installed in a large copper shielding box. This prevents from the noise contamination from outside and provides the center of ground. This ground can be chosen either a power line ground or a floating as virtual ground.

(5) The four channel oscilloscope

The four-channel oscilloscope, Tektronix TKS475, monitors the bridge excitation voltage, a preamplifier output, the ±45° phase adjustment and detection.

(6) Phase Locked Loop (PLL) based the signal demodulation system.

This unit was a home made system which performs the phase detection and the demodulation. The block diagram is shown in Fig.3.10. The PLL detects a phase of the sync signal from the function generator. Respect to the original phase, the purified sine waves, which has a harmonic distortion more than 40dB, are generated and shifted the phase ±45°. The input signal and the two phase shifted sine waves are demodulated and then filtered to remove a higher part of the separated spectrum.

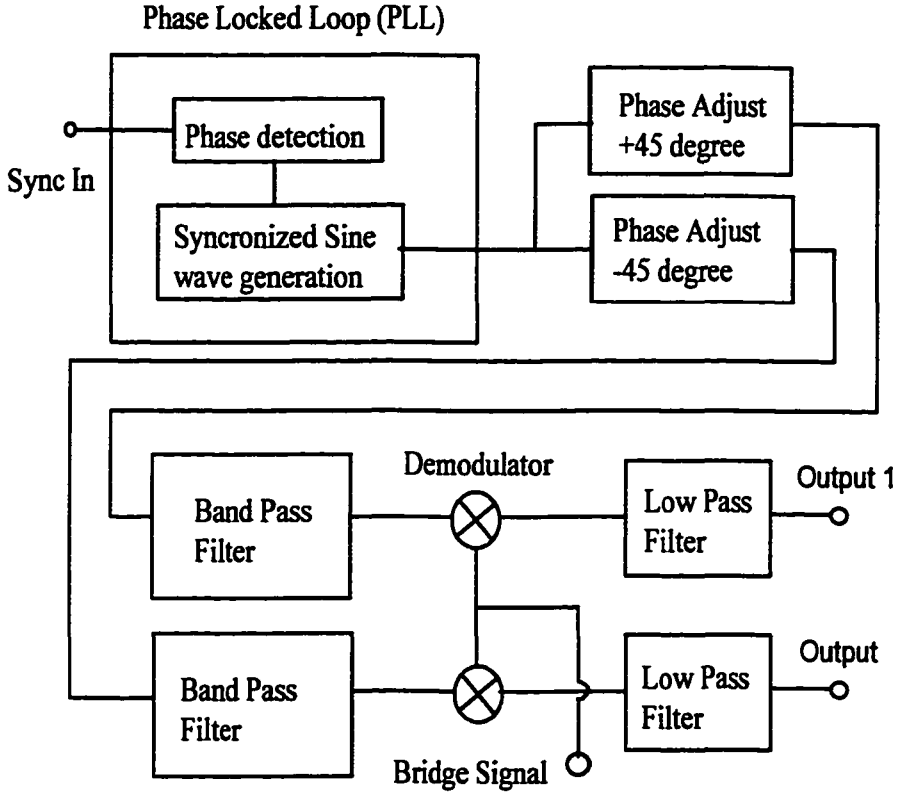

Fig. 3. 10 (A): The block diagram of the signal demodulation system.

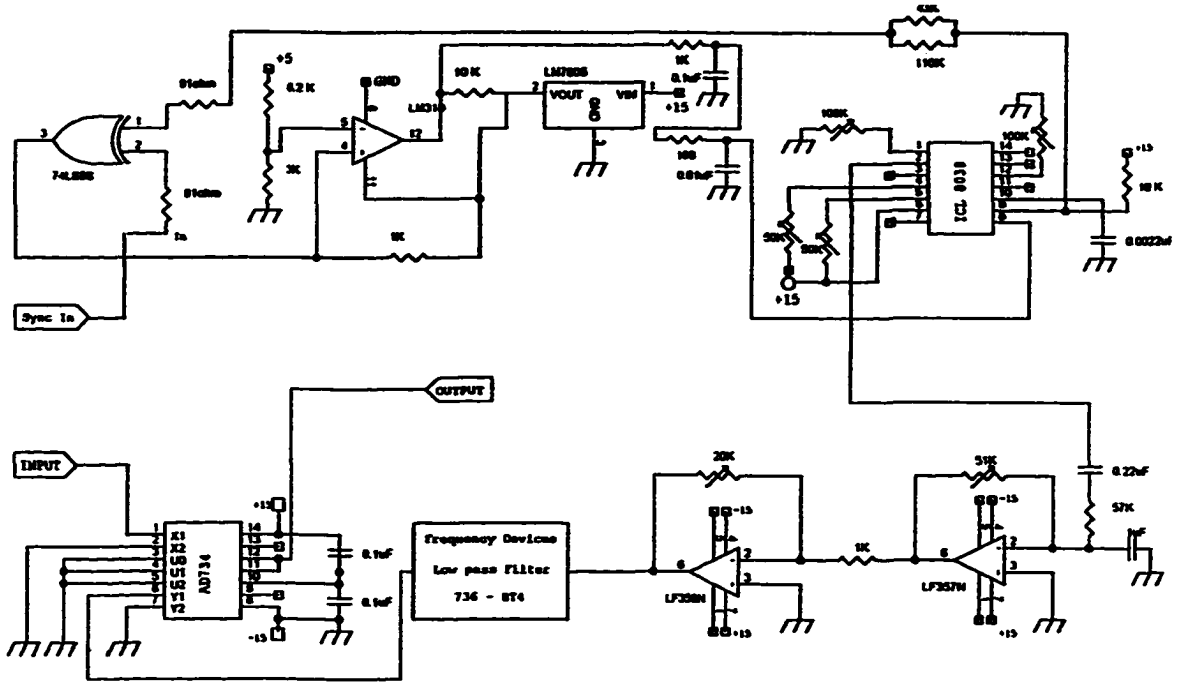

Fig. 3. 10 (B): The electronics schematics of phase sensitive detection and demodulation.

(7) Low pass filter

The two demodulated signals pass another pair of analog low pass filters, which the corner frequency was set 50 Hz: Frequency Devices Model 902.

(8) The spectrum analyzer

To analyze a small signal, a high resolution front end D/A converter is necessary to be equipped in a spectrum analyzer. The spectrum analyzer, HP35670A, satisfies above requirements (16 bits A/D). And two channels real time data acquisition makes it possible to show the spectrum cross-correlation.

(9) The refrigeration system

The sample temperature can be changed from 11K to 290K for low temperature setup. In general, the refrigeration system for the noise measurement has been performed by the open flow helium cryostat. This has a certain advantage compared with a standard closed cycle refrigerator, which is a mechanical vibration. The open flow helium cryostat has technically very few vibration sources, e.g. the bubbling noise. Therefore, to achieve the low noise environment at low temperatures, it seems the best refrigeration system. However, the low temperature noise measurements quite often require a long measurement time since the expected spectrum is very small and many number of data acquisition is required to average out to obtain the cross-correlation spectrum. As a result, a large amount of helium is necessary. This is not cost effective. On the other hand, the closed cycle refrigerator requires no extra helium and an operation is fully continuously. However, this has a constant vibration source, which comes from a displacer motor. This is an unavoidable noise source and the primary displacing frequency ~2Hz was observed. This spectrum peak is too close to our expected spectrum, up to 10Hz. In short, this is unusable. To avoid the displacer vibration, we employed APD DMX-20 low vibration interface. This is originally designed for Mossbauer Spectroscopy. This interface fits over the standard DE202 flat flange refrigerator. The internal cold head and the external cold head are mechanically decoupled. A rubber bellows is used only physically connected part. The heat exchange gas is filled to transfer the cooling from the cold head end to a

sample mount. This removes mechanical vibration problem completely while a continuous operation is performed.

(10) The temperature control system

Once the mechanical vibration is under control, the next obstacle to reduce is the temperature stability. The temperature stability is crucially important to achieve a very low frequency noise measurement at low temperatures. In a pure theoretical argument, this worry is irreverent. Let's consider the cooling down the lower part of a Wheatstone bridge in Fig.3.11.

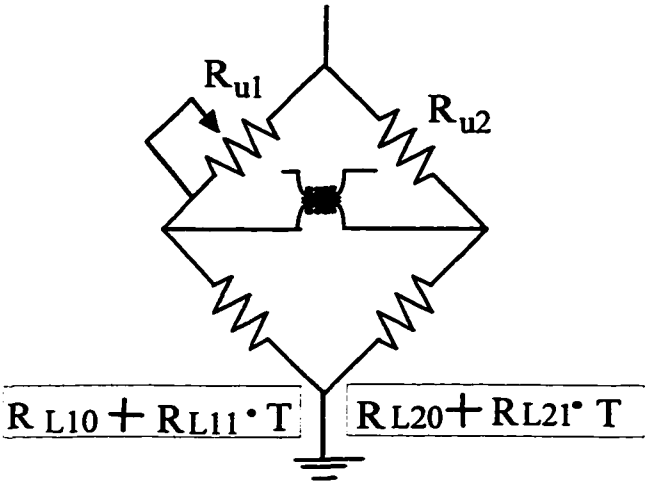

Fig. 3.11: The cooling down the lower part of a Wheatstone bridge

When the bridge is completely balanced, $R_{U1}R_{L2}=R_{U2}R_{L1}$. R_{L1} and R_{L2} can be written as $R_{L1}=R_{L10}+R_{L11}\cdot T$ and $R_{L2}=R_{L20}+R_{L21}\cdot T$. The bridge balance equation does not have any temperature dependence. However, this is not a realistic argument. When the sample temperature decreases or increases 1K, approximately 1μV of error signal is detected. Where does it come from? The primary suspect is the coupling or stray capacitance. A change of the temperature creates a change of

the voltage across the sample. This also induces the change of the coupling and stray capacitance. In other word, if the temperature is not well stabilized, the fluctuation of the sample temperature should be observed. This fluctuation spectrum is varied as $1/f^2$ or even higher exponent. At the beginning, we faced this difficulty. To overcome, the thermal filter was installed in Fig.3.12. The thermal filter consists of two rods, Stainless steel 304 and Copper. The principle of a filtering is a similar to a CR passive filter. Fig.3.12 shows the temperature fluctuation before the thermal filter was installed and after. An obvious improvement was demonstrated. After the thermal filtering, a temperature fluctuation of 10mK during 20 minutes was observed. A platinum resistor is used to measure the temperature fluctuation. However, a net spectrum component of the temperature fluctuation noise is still unknown. How low is enough? To prove systematic noise was not significant, the noise was measured for an 800 cm long, 50 micron diameter Cu wire. Since the volume of Cu wire is much larger than the thin films, only temperature fluctuations due to the system can be detected. Under similar conditions, the generated noise power, S_v, in the Cu wire was always significantly less than the background white noise, therefore showing that all of the measured noise spectra were generated by the sample films.

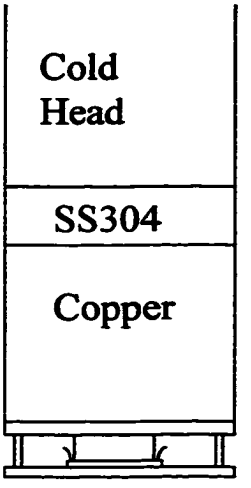

Fig. 3. 12: Thermal Filter.

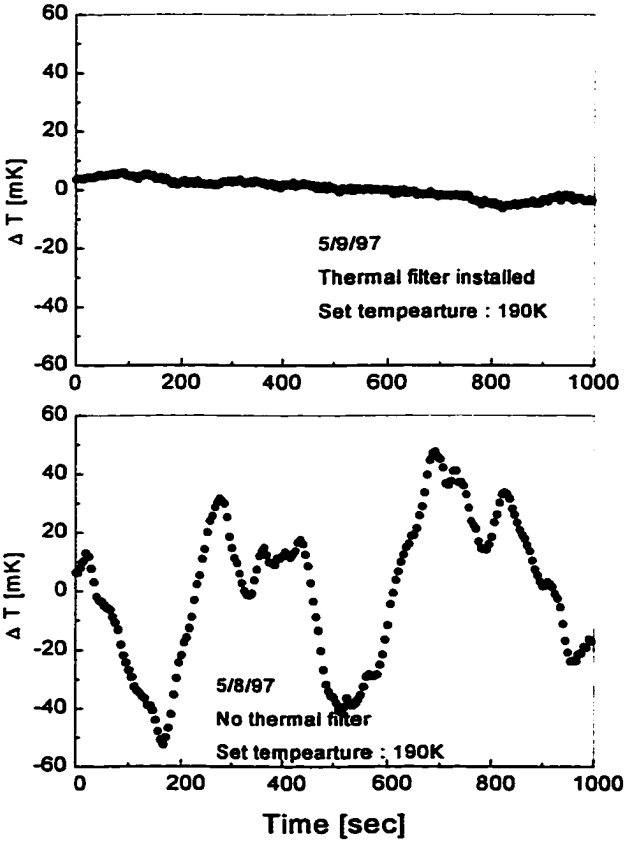

Fig. 3. 13: Thermal Filter Performance.

Chapter 4

Results and Discussion

4.1 Overview

In this chapter, we show the experimental results and related discussions. A total of 18 samples, 15 of Aluminum (Al) and 3 of Copper (Cu), were investigated. First, the details of sample fabrication are explained. When the sample impurity is desired, the fabrication process is crucially important. Besides an original material purity, the fabrication process could result in a primary material contamination. If the samples contain high level of impurities, the identification of the noise source would be a difficult task. Second, in 4.3, the basic noise spectrum results and several aspects of the real measurements will be explained. For example, under a high current density, the sample can create some amount of joule heat. It will be shown how much the final spectrum can be influenced. Third, the noise results under the specific physical conditions are discussed.

Before the detail results are analyzed, the experimental conditions were followings. All of the noise data was obtained by AC cross-correlation technique, which was performed with the excitation frequency of 2500-2516Hz, and a sample current density of $(2\text{-}4)\times10^6$ A/cm^2. Due to the high current density, heating of the sample was expected. The observed frequency span was 50Hz, with a resolution of 0.0625 Hz (Resolution line 800). Two hundred cross-correlated spectra were averaged out to obtain one spectrum. A Hanning FFT input signal window was

used. Due to the two stage of DC blocking capacitance through the signal demodulation, the lowest frequency data contains ~30% error from direct spectrum reading. Based on our measurement setting, this frequency corresponds 0.0625 Hz. Additionally, it is known that the real dynamic signal analyzer shows an error at a frequency bin right next to DC when a DC is applied. This is due to the discrete signal acquisition. Although most of the 1/f noise spectrum showed no inconsistency to the entire spectrum because the lowest frequency spectrum data is increased by rather an order but not by a factor, still the lowest frequency spectrum data was eliminated through the entire measurements for high precision measurements.

In the low temperature measurements, the additional procedures were taken into account. All low temperature noise results demonstrated that no temperature hysteresis was found in any samples. Therefore, a setting temperature can be quite arbitrary. However, a sudden increase of setting temperature creates a high heat load to the heater and this reduces the life of heater due to a loosening contact between the heater and a cold head. Because of this reason, most of the low temperature measurements were taken from near the room temperature down to 11K. In typical measurements, the decrement of a temperature was chosen 10-30 K. It has been taken about an hour to reach the temperature equilibrium from one temperature to another. The cross-correlation spectrums were inconsistent just after the excitation within a few minutes. This might be simply explained by a Joule heating of the sample.

To express the noise magnitude, quite often the noise power spectrum at 1Hz is taken to compare with spectra from different temperatures or bias currents. The most of the 1/f noise spectrum show the frequency exponent is not exactly 1. However, if the spectrum quantity at 1 Hz is chosen, it can avoid the complication of quantitative analysis. If the overall fluctuation is so critical, it has to be evaluated by the integrated quantity. This case arises, when the total fluctuation is relatively small but also the frequency exponent changes relatively high amount. This will be discussed later.

4.2 The details of samples

4.2.1 Al samples

All polycrystalline Al samples were fabricated at IBM T.J.Watson Laboratory, York Town Heights. The Al purity 99.999% was used. Al and Al-Cu metallization was e-beam evaporated onto an oxidized Silicon substrate. Al-Cu metallization consisted of 0.7-2.0 wt.% Cu. During deposition, the substrate was not heat-treated. In some case, the samples were annealed 450C for an hour under the forming gas. The samples were mounted on 24 pins dual in line packages (SD-5008-324 Kyocera). Electrical contacts were made by an ultrasonic wire bonder. The samples were patterned by a standard lift-off process. The total arm length which consisted of part of the Wheatstone bridge is 450 μm. The width is 1-4 μm and the thickness is 1000-1300 Å. A sample schematics is shown in Fig.4.1 (A).

The single and bamboo grained samples were fabricated at Delft University of Technology, DIMES, The Netherlands. The combination technique

of zone melting recrystallization and graphoepitaxy was used [64]. Grooves were made in the substrate by electron beam lithography and reactive ion etching. A blanket of Al was deposited on the groove by sputtering. The thermal annealing let Al metal flow onto the grooves. The Al purity 99.9995% was used. Scanning electron microscope (SEM), Atomic force microscope (AFM) and Transmission electron microscope (TEM) were used to characterize these samples. The local crystallographic orientation was also measured using Electron Backscatter Kikuchi Pattern (EBKP) analysis. The crystal structure in these samples was distorted from a perfect single crystal. These samples had a gradual crystallographic rotation of approximately 0.05 °/μm about the axis perpendicular to their sidewalls. The total arm length is 400 μm and the groove width is 0.6 μm in single and bamboo grained samples, see in Fig.4.1 (B). The thickness 3500-5000 Å was estimated by the resistivity coefficient measurement. The mounting and wirebondings are the same procedure as polycrystalline Al samples.

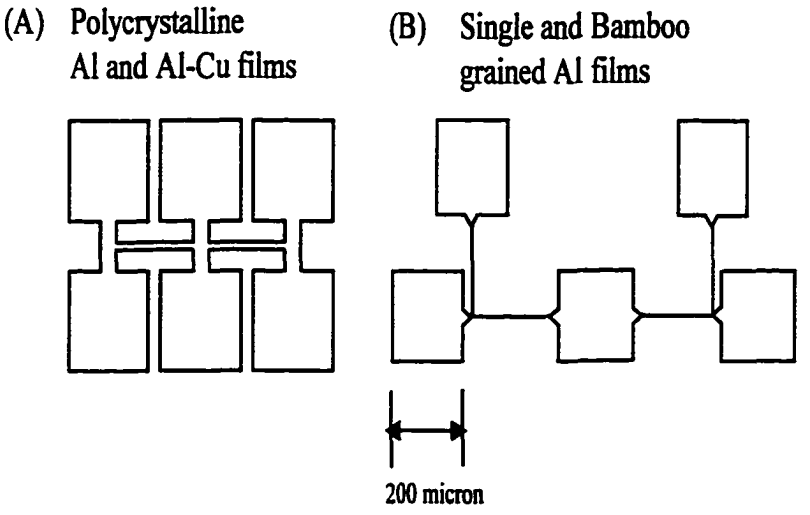

Fig. 4. 1: Sample schematics. (A) Polycrystalline Al and Cu samples. (B) Single and bamboo grained samples.

ample name	Structure and Composite Poly : Polycrystalline	imensions μm × μm × Å)	esistivity (μΩ-cm) at 294 K	Annealing
D E-Al	Poly , Pure Al	450 × 4 × 1000	3.42	No
-Al wl	Poly, Pure Al	450 × 1.3 × 1000	3.6	No
AD l-0.7Cu	Poly, Al-Cu(0.7%)	450 × 4 × 1300	3.57	No
-Al w4	Poly, Pure Al	450 × 4 × 1100	3.13	No
450 l-2Cu wl	Poly, Al-Cu(2%)	450 × 1.5 × 1400	3.19	450C 1 h
450 l-2Cu w4	Poly, Al-Cu(2%)	450 × 4 × 1300	2.93	450 C 1 h
l-2Cu	Poly, Al-Cu(2%)	450 × 4 × 1400	3.13	No
714-b	Single	400 × 0.6 × 3550	2.85	No
715-a	Single	400 × 0.6 × 4400	2.86	No
715-b	Single	400 × 0.6 × 4040	2.86	No
715-e	Single	400 × 0.6 × 3800	2.95	No
26-7-d	Bamboo grained	400 × 0.6 × 4770	2.76	No
26-7-f	Bamboo grained	400 × 0.6 × 4900	2.77	No
26-12-a	Bamboo grained	400 × 0.6 × 5570	2.80	No

Table 4. 1: The summary of Al samples

4.2.2 Cu samples

The thermal oxide S_iO_2/p-type Si(100) substrates were patterned by a standard liftoff technique. The liftoff pattern were the same as polycrystalline Al samples in Fig.4.1 (A). All of the depositions were made at room temperature. An initial adhesion layer of Cr was used to promote adhesion of the Cu onto the Si. The Cr was electron beam evaporated. Subsequently, Cu was electron beam evaporated without breaking vacuum [65]. The summary table of all samples is listed below.

ample name	Structure and Composite Poly: Polycrystalline	Dimensions (μm × μm × Å)	Resistivity (μΩ-cm) at 294 K	Annealing
ACP1	Poly , Pure Cu	450 × 4 × 1200	2.37	No
ACP2	Poly, Pure Cu	450 × 4 × 1260	2.37	No
ACP3	Poly, Pure Cu	450 × 4 × 1170	2.43	No

Table 4.2: The summary of the Cu samples.

In a few samples, we were not able to measure the noise successfully. In most of the case, the samples had been disconnected by the electrostatic damage. In a few cases, the samples were disconnected by a sudden voltage application of resistance measurement, because the full compliance voltage was applied from a multi-meter at the beginning of resistance measurement mode. To avoid such a damage, the current bypassing circuit was inserted.

4.3 Basic power spectrum and several other aspects

Figure 4.2 shows the typical noise power spectrum in Al-2%Cu film; the background noise (Johnson and preamplifier noise) were clearly suppressed more than one decade, and the 1/f noise spectrum is readily distinguishable.

The Hooge formula explains the noise power is linear to the applied voltage square in Eq.(2.45). This has to be confirmed to prove the resistance fluctuation creates the 1/f noise. If the deviation from the Hooge formula is significant, then it is worth to take a look some non-linear effects. In semiconductor 1/f noise, the carrier number

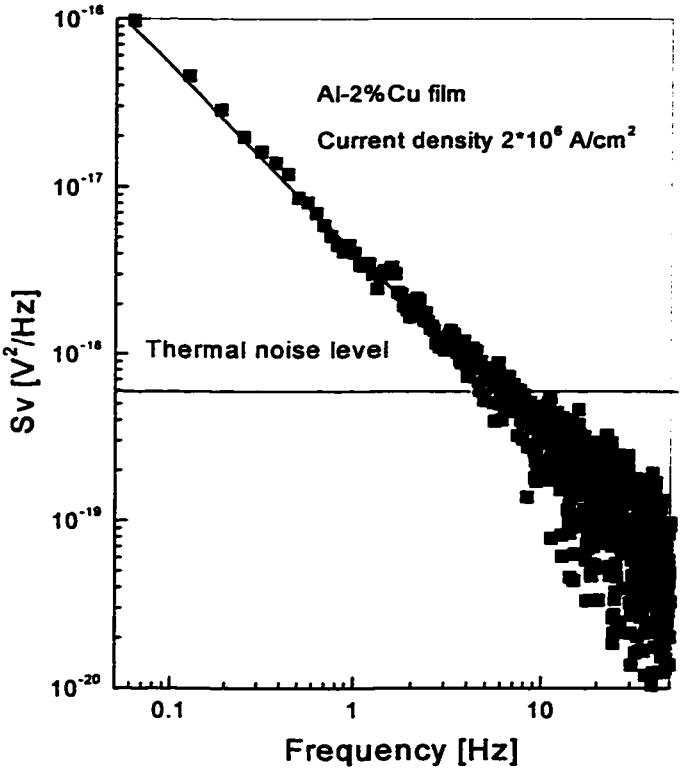

Fig. 4. 2: Typical noise power Spectra in Al-Cu(2%) at 294 K.

fluctuation is believed to be the noise source. Since the number of carrier is a function of applied electric field and this is characterized by the exponential function, this exhibits the non-linearity to the applied current. Figure 4.3 (A) shows an example of the noise power linearity. A solid line indicates a quadratic curve. The sample was 450 °C annealed Al-Cu(2%). It was clearly shown such noise linearity holds up to the current density 4×10^6 A/cm^2. To make sure that the spectrum hold the scale invariance, the frequency exponent is shown in Fig.4.3 (B). The frequency exponent did not change at all. The whole spectrum is linear to the applied voltage. This was observed in all samples within the temperature range from 10 K to room temperature. The additional proof is shown in Fig.4.4. The sample was a single crystal film at room temperature. When the sample temperature was more than 400 K or the applied current density was more than 3-4×10^6 A/cm^2, the linearity was broke down. Beyond such conditions, the atomic instability is substantially increased due to some diffusion processes, e.g. grain boundary electromigration or atomic diffusion by thermal gradient. These instabilities and diffusion effects are especially prominent in polycrystalline samples at high temperatures. However, under the commonly applied conditions, it can be concluded that the all noise power results hold a linear relation to the applied voltage, or current. This guarantees the fluctuation is caused by a resistance fluctuation, in other words a mobility fluctuation. This is an important conclusion that eliminates other possibilities of fluctuation. Another question should be approached whether this fluctuation comes from bulk or surface? This

has been demonstrated by Hooge [4], which the noise was essentially created in bulk. This has been adapted in most of metal noise studies. One of the prominent external noise sources is a contact noise. This effect takes place by a thermomechanical contact instability. Therefore, no strong material dependence should emerge and the weak correlation of the temperature dependence is expected. In a realistic view, this may occurr in the area where a wirebonding was made. Very few samples exhibited such effects. The dominance of the contact noise can be eliminated and the noise was created in bulk.

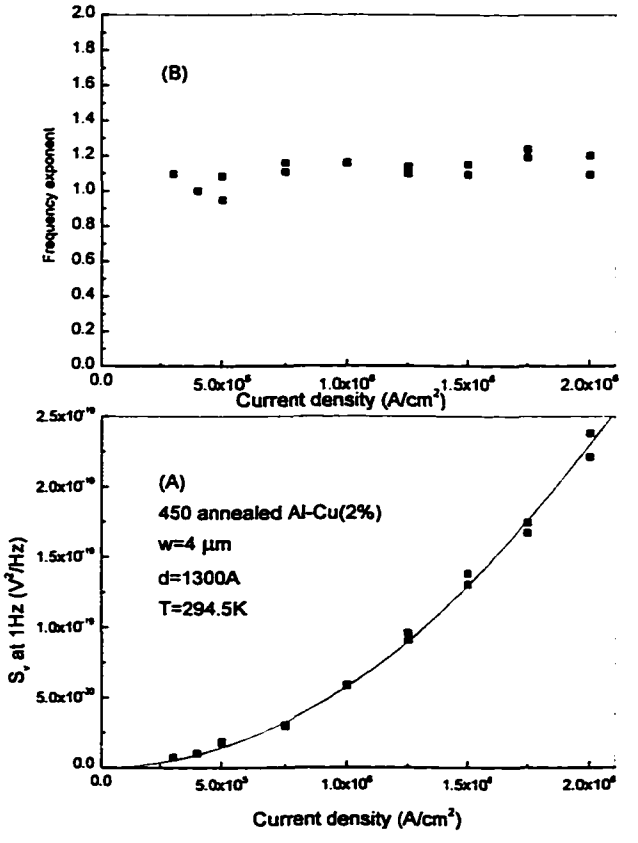

Fig. 4. 3: (A) The linearity of noise in Al-Cu(2%). (B) The frequency exponent.

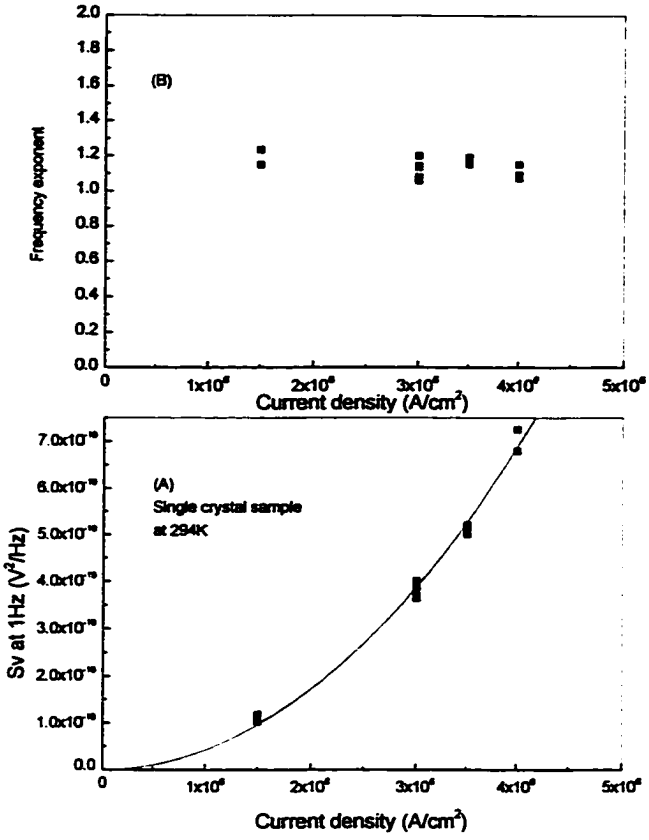

Fig. 4. 4: (A) The linearity of noise in single crystal film. (B) The frequency exponent.

4.3.1 Joule heating effect

Joule heating was observed under the most measurement conditions. The temperature was increased with increasing the current density in Fig.4.5. The temperature increase due to Joule heating is obtained by a following procedure. The low temperature dependence of a sample resistance is obtained. The linear data fitting of this temperature dependence can give a resistance coefficient dR/dT from the data above 100 K to room temperature. Then a several resistance measurements are taken by different current bias. The temperature increase is computed by the additional resistance multiplied by $(dR/dT)^{-1}$. A typical four

probe resistance measurement system, e.g. Keithley model 2000, supplies 1 mA as a current bias. When such a low current is applied, the temperature increase due to Joule heating is negligible. This resistance value was used as a standard. The temperature increase at room temperature was less than 2 K in all Al samples up to the current density 4×10^6 A/cm^2 and less than 2.5 K in all Cu samples up to the current density 3×10^6 A/cm^2. Up to the current density limit, Joule heating did not influence the spectrum results. And this is consistent to the previous linearity argument.

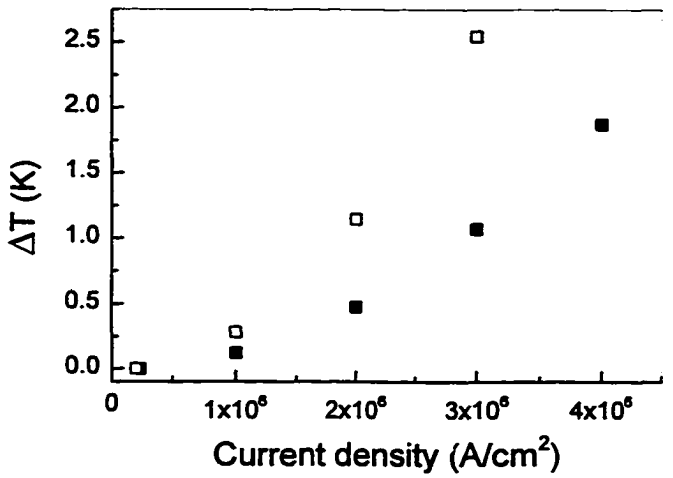

Fig. 4. 5: Temperature increases due to Joule heating.
Black Square: Polycrystalline Al (20 AD E-Al 1000).
Open Square: Polycrystalline Cu (aUACP1)

4.3.2 Thickness determination

Although the thickness of all polycrystalline samples from IBM were previously measured by the deposition rate meter, the thickness was determined by the temperature coefficient technique in all samples. As mentioned by previous

section, dR/dT was obtained. By comparing a thermal coefficient of the material resistivity, in Eq.(4.1), l/A is estimated. This is widely accepted technique to estimate the sample geometry, since a thermal coefficient of resistivity has a weak correlation of the material internal parameters, i.e. grain boundaries or light doping.

$$\frac{dR}{dT} = \frac{d\rho}{dT}\frac{L}{A} \qquad (4.1)$$

4.3.3 Size effect

Size effect can take place when the dominant scattering length of the sample is longer than the sample geometry. At room temperature, no consideration is necessary since electron-phonon scattering length is much shorter than the sample size. However a care should be taken at low temperatures. It will be discussed later.

4.3.4 The fluctuation to thermal noise ratio

In real noise measurements at low temperatures, it is difficulty to obtain the precise spectrum data between 150 K and 200 K in Fig. 4.6. The noise power data showed the largest error within this temperature region. The primary reason may be explained by the fluctuation to thermal noise ratio. Comparing to the thermal noise curve, the ratio is the highest in such temperature region. In other words, 1/f noise is deeply buried by the thermal noise.

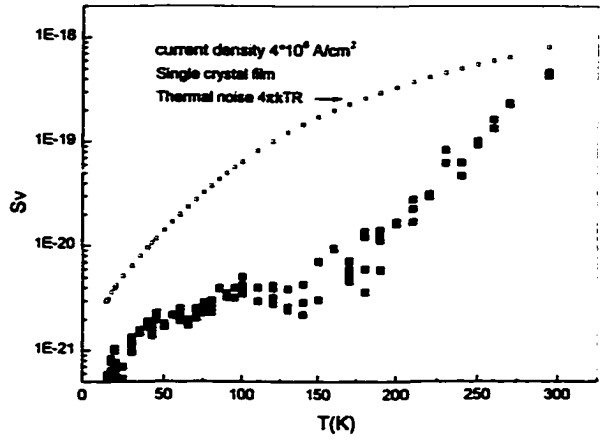

Fig. 4. 6: The temperature dependence of thermal noise: open square, and 1/f noise: Black square. Sample: Single crystal (1715b).

4.4 Polycrystalline Al films

4.4.1 High temperature result

The 1/f noise was investigated in a pure polycrystalline Al sample at high temperatures. Figure 4.7 shows the temperature dependence of the normalized noise power S_v/V^2 and spectrum slope in Al film. The noise increased monotonically up to 390K to a maximum then decreased but again increased at 430 K. The frequency exponent showed a minimum value 1 at the noise power peak then increased rapidly to 2. In Fig.4.7, a peak in noise was observed. There are a several reports [12,16] stating that Al showed a peak in noise magnitude around 330K; however, we observed the noise peak temperature at 390K. This indicates the migration energy of the grain boundary defect is microstructure dependent. Vossen pointed out the potential correlation between the noise and electromigration failure in 1973 [11]. Koch et al demonstrated the peak magnitude

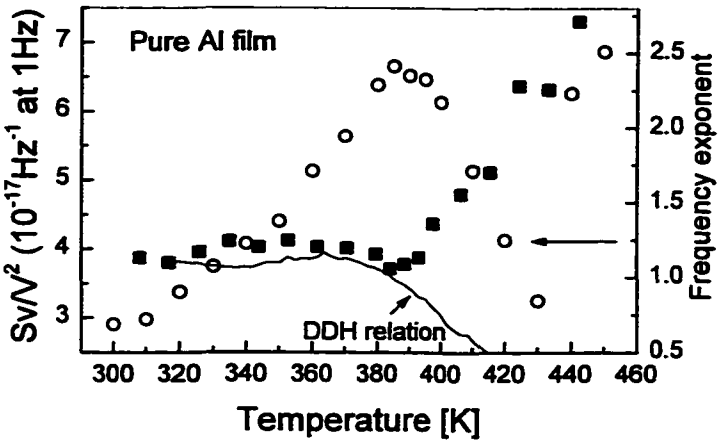

Fig. 4. 7: The temperature dependence of S_v/V^2 and frequency exponent in pure Al film. Open Circle : Sv/V2; Black Square : Frequency exponent ; Solid line : DDH Calculation (Eq.2.17).

in Al and Al alloy film corresponded to the activation energy of GB electromigration [12]. They investigated normalized noise power in Al and Al-Cu(4%). A higher peak temperature was obtained in Al-Cu(4%) film because it is known that such films have higher activation energies than pure Al film in electromigration process. This agrees with a median time to failure study (MTF study) in which the value for activation energies was between 0.48 and 0.8 eV [66] for pure polycrystalline Al. Under accelerated failure mode conditions, i.e. high temperature and high current density, the distribution of time to failure was measured in a large number of test Al films. Once MTF was determined, Black's empirical formula was applied to obtain the activation energy in Eq.(4.2), where A is constant, n is ~2, j is a current density and E is an activation energy.

$$t_{50} = MTF = Aj^{-n} \exp\left(\frac{E}{k_b T}\right) \qquad (4.2)$$

It is known such activation energy has a broad distribution of energies. This is a favorable condition to create a 1/f noise. To estimate activation energy from the 1/f noise study, an attempt time of atomic diffusion on a grain boundary has to be used, however this is not well known. Therefore, most measurements have employed the inverse of the phonon frequency, 10^{-13} sec. This gives the activation energies higher than those reported in the literature by median time to failure accelerated testing. Table 4.3 summarizes previous measurements of peak temperature and activation energies, T_p and E_a. All of the activation energies seem to be higher than those obtained in MTF studies. One possible reason is that a real attempt time of atomic diffusion may be more than an order below the inverse of phonon frequency. If τ_0 increases an order, then the energy difference at near peak temperature is about 0.07 eV. To reach the comparable value of activation energies, $\tau_0 \cong 10^{-9}$ may be appropriate. However, the detail is still not well understood. Figure 4.7 shows the exponent gradually decreasing to the lowest point ~1 at 390K, then rapidly increased to more than 2. Until the noise power peak, the behavior of the frequency exponent may be described by the DDH relation. However, after this peak, the DDH relation can not model the data. This result indicates that after the peak, the process of noise generation is changed from simple thermally activated kinetics to a more complicated system. As the temperature increased at more than 400K, the slope α changed from 1 to 2. In this $1/f^2$ regime, resistance drift was observed. It is established that resistance drifts causes $1/f^2$ noise, and could be a leading process in generating $1/f^2$ noise. On the

Reference number	T_p (K)	E_a(eV) $\tau_0 = 10^{-13}$ (sec)
This thesis	390	0.94
16	325	0.79
67	410	0.99
12	310	0.75
12	323	0.78

Table 4.3: Summary of previous measurements of peak temperature T_p and activation energies

other hand, $1/f^2$ noise could arise from electron scattering by a slow drift of activated Al atoms under an applied electric field. Unlike the DC electromigration study, no noticeable abrupt jump in resistance was observed. Celasco et al. reported the temperature dependence of the $1/f^2$ noise and attributed the $1/f^2$ noise was created by grain boundary movements or the creation and annihilation of vacancies. Cottle and Chen pointed out that the $1/f^2$ noise could be generate by the fluctuation of vacancies around grain boundaries and should be related to the electromigration rate [31]. If so, the $1/f^2$ noise should be directly correlate the MTF studies. They formulated the noise power can be described as follows,

$$S_v(f) = \frac{Aj^3}{Tf^2}\exp(-\frac{E_a}{k_b T}) \qquad (4.3)$$

where, A is a constant, j is a current density, E_a is an activation energy, f is frequency. The denominator T implies the $1/f^2$ noise is very sensitive to a change of sample temperature. It was argued that A can be shown to be inversely proportional to the electron mobility. They also found the Al samples, which exhibited a higher noise, had shorter life time than the samples which showed the normal level of noise. As a result, no strong correlation was established. The $1/f^2$ noise was dominant at their measurement temperatures which are commonly used for MTF studies. Many recent studies support the $1/f^2$ noise is generated by electromigration. Our measurement result also showed a good agreement with their results.

It is worth mentioning that the DDH relation, Eq.(2.17), predicts a spectral slope slightly less than 1 at the temperature of the noise power peak. However, the observed value for the spectral slope was always slightly more than 1 at the peak. This is obviously more than the fitting error, ~0.01, of the slope value. A similar result was obtained with Cu [65].

Although the activation energy of noise peak agreed with that of a MTF study [12], the detailed mechanism of the formation of the peak is not well understood. Especially the complex part is that two different physical phenomena were observed at different temperature regions. However their origin of kinetics was assumed to be the same, i.e. electromigration. An attempt has been made to estimate the number of fluctuators in pure polycrystalline Al sample by applying Eq.(2.47). A peak value of S_v/V^2 is 1.5×10^{-17}. And a number of atoms is 1.08×10^{13}. τ_0 is the attempt time for atoms 10^{-13}. D(E) is assumed the normal

distribution of the activation energy 0.9 eV. The standard deviation 0.05 was chosen to the best fit. β ~0.25. σ is the total scattering cross section, $\sigma \sim 4\pi k_f^2 \sim 4.1\times10^{-16}cm^2$. The electron-phonon scattering length 411 Å was quoted by Reale at room temperature [68]. Since this is inversely proportional to the temperature, 309 Å was obtained at a peak temperature 390 K. The net scattering length l_{net} is dominated by the electron-phonon scattering length above the room temperature. 145 ppm of fluctuator concentration was obtained. This number seems quite reasonable. The largest uncertainty attributes from a β value. Since β ~0.25 describes the deviation value of <100> or <110> which is split interstitial in a perfect crystal. Here we assume diffusion species are rather interstitials or vacancies in grain boundaries. It is not clear that how such anisotropy is incorporated to the β calculation. However, this is always true that no matter what the environment is asymmetry, β value must be less than 1. If such extreme case β ~1, the concentration 9 ppm was obtained. Another extreme case also can be considered in grain boundary diffusion. The vacancy diffusion is supposed to be a primary diffusion in a grain boundary, which is a quite normal assumption. Since computed β value for vacancy migration in perfect crystal is zero, only a possible way that the vacancy diffusion has non-zero β is asymmetrical environmental factor. This is also a reasonable assumption because the grain boundary region has to contain asymmetrical crystal structures. It may be able to assume a non-zero β value in vacancy diffusion. And this β could be a very small, $\beta \ll 1$. This condition should require a substantial amount of fluctuators. The detail study of β value has not been done so far.

4.4.2 Low temperature result

If the noise source has a thermally activated kinetics, the noise spectrum should reduce as the temperature decreases. In Fig.4.8, the cross-correlation spectra at different temperatures are shown. To demonstrate the temperature dependence of the noise power S_V, S_V at 1 Hz was chosen in Fig.4.9, which shows the typical temperature-dependence of S_V at 1Hz in Al-Cu(2%) film at temperature from 11K to 300K. The magnitude of S_V at 1Hz changed nearly three and a half decades. Between 200 K and 260 K, the rate of decreasing S_V was the largest. Such two features have been observed in all Al samples regardless crystal structure and the composite. This suggests the basic kinetics may be identical. Hooge parameters α_H in different samples at room temperature are compared in Table 4.4. This also indicates the primary noise source is grain boundary electromigration.

Sample name	Composite	α_H at 294K
AD E-Al	Pure Al	$9.79 \pm 0.19 \times 10^{-4}$
E-Al w1	Pure Al	$7.93 \pm 0.08 \times 10^{-4}$
2AD Al-0.7Cu	Al-Cu(0.7%)	$6.43 \pm 0.03 \times 10^{-4}$
E-Al w4	Pure Al	$3.60 \pm 0.18 \times 10^{-4}$
A450 Al-2Cu w1	Al-Cu(2%)	$1.94 \pm 0.03 \times 10^{-4}$
A450 Al-2Cu w4	Al-Cu(2%)	$9.77 \pm 0.08 \times 10^{-5}$
Al-2Cu	Al-Cu(2%)	$6.30 \pm 0.10 \times 10^{-5}$

Table.4.4 Hooge parameters α_H at 294 K in polycrystalline samples.

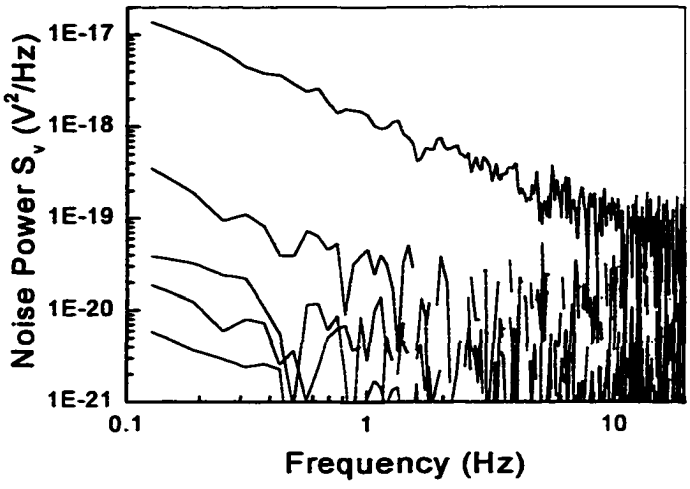

Fig. 4.8: The noise power spectrum at different temperatures. From the highest noise power, 294 K, 240 K, 200 K, 140 K, 100 K and 40 K respectively. (Al-2%Cu film)

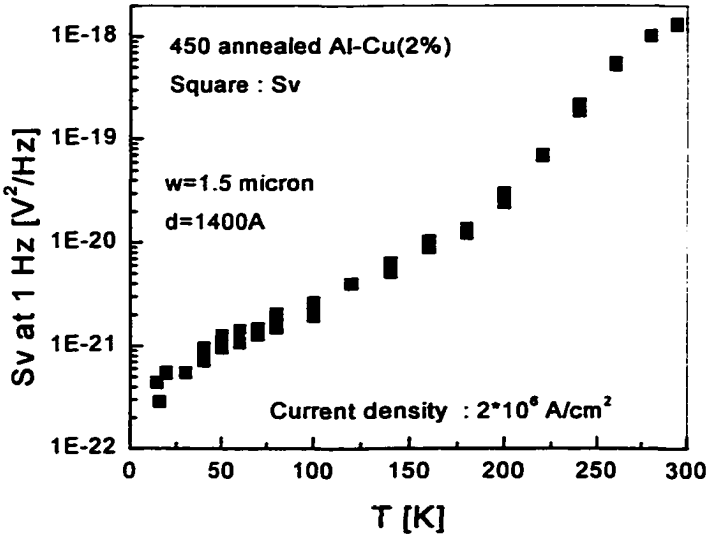

Fig. 4.9: The temperature dependence of Sv at 1 Hz in Al-2%Cu film.

It is known that adding Cu to Al reduces the electromigration process. Cu atoms tend to segregate from inside the grain [12] to the grain boundary then precipitate as $CuAl_2$ in grain boundaries, especially at a tri point. This prevents from the progress of grain boundary electromigration. The noise suppression should be expected by adding Cu atoms. It was observed more than an order of α_H differences. This indicates that adding Cu to Al suppresses the α_H and this is supporting the idea that the noise comes from the grain boundary in Table 4.4. It is obvious that an annealed sample shows less noise because the some intrinsic defects can be annealed out. Although the two Al-Cu(2%) samples were annealed prior to the measurements, there was not much difference from the non-annealed Al-Cu(2%) sample. Probably, all samples had the ample time to age by themselves. Since all samples had been more than several years after the fabrication. Figure 4.10 (A) and (B) compare the temperature dependence of α_H in Al-2%Cu and pure Al films. All of the samples have showed the similar behavior in the temperature dependence of α_H. If a grain boundary diffusion is the main source of noise, then even though the Cu atoms in the grain boundary suppressed defects diffusion, the threshold energy of defects diffusion can not be influenced by the existence of Cu atoms. Indeed, they exhibited nearly same threshold temperatures at 200 K, which was consistent that the lowest activation energy was ~0.5eV for all samples listed above by applying Eq.(2.19).

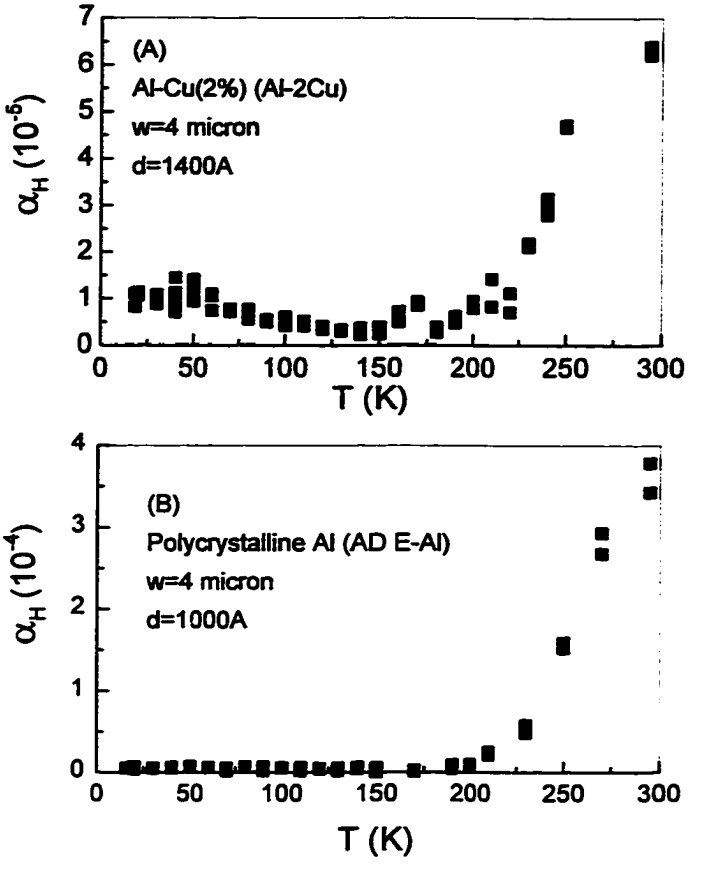

Fig. 4.10: The temperature dependence of α_H in (A) Al-Cu(2%) and (B) Polycrystalline Al films.

The 1/f noise has been observed within the entire temperature range from 11K to 295K. This implies there should be another noise source in addition to the diffusion in a grain boundary. If the noise arises from point defects in the crystal [22], the activation energy can be quite low, 0.1eV, due to interstitial migration. However, such kinetics may be less likely since it requires a substantially high energy to create. Rather thermal kinetics by some impurities or dislocation thermal dynamics may be appropriate to discuss. A further argument is presented in a section of single and bamboo grained samples. The experimental demonstration of the DDH relation at low temperatures has been rigorously performed by many

authors. Only in a noise study of hydrogen diffusion, the DDH relation was well demonstrated in low temperature regime. The DDH relation directly connects a simple Lorentzian kinetics to the total noise formation. In addition, this gives a convenient energy scaling. Therefore, if this model is applicable, the thermally activated kinetics can be quite specified. And identification would be easier. Figures 4.11 (A) and (B) show the temperature dependence of the frequency exponent. It has been found that the all samples exhibited a quite similar behavior. The exponent began to increase slightly as the temperature reduced from 295K to approximately 220 K. Then it reduced down to approximate 180 K. Below 180 K, no particular pattern was emerged and most of the samples just showed the exponent as nearly 1. The computed frequency exponent by Eq.(2.17) was shown as a solid line in Fig.4.11 (A) and (B). The consistency between the theory and the experiment was observed. This implies that the DDH analysis is valid and the energy scaling is reasonable. Homberg et al. studied the noise in single and bamboo grained Al samples from 140 K to 500 K [48]. They found the threshold energy ~0.58 eV in single and bamboo grained and less than 0.6 eV in polycrystalline samples. The threshold energy ~0.3 eV was observed by Briggmann et al. in polycrystalline Al [28]. Our results showed the threshold energy ~0.48 eV. Here, the argument is limited in polycrystalline. In case of single or bamboo grained samples, a different argument is necessary. This is explained in 4.5.

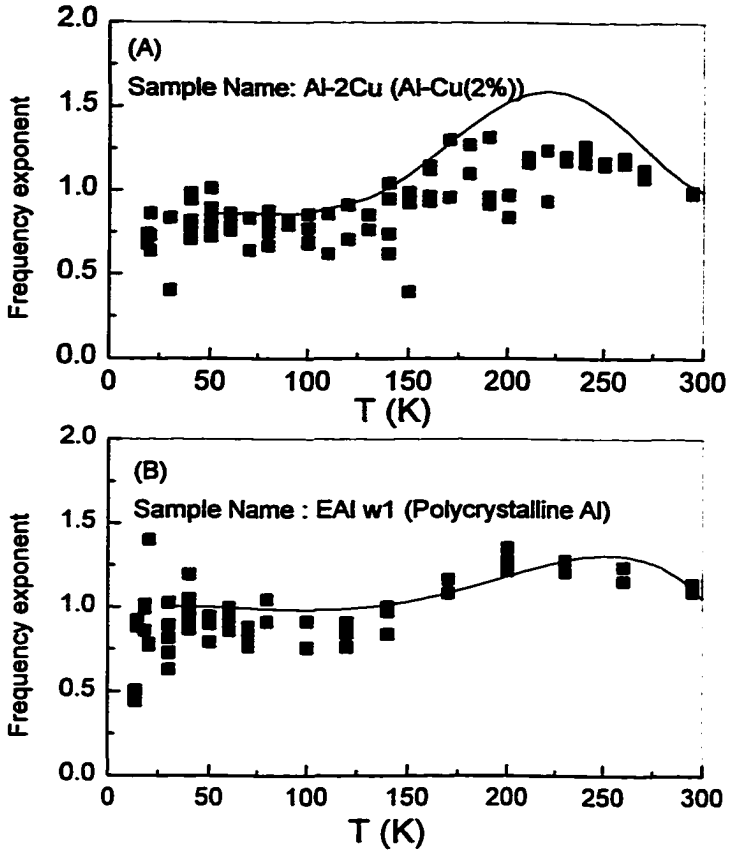

Fig. 4. 11: The temperature dependence of the frequency exponent in (A) Al-Cu(2%) and (B) Polycrystalline Al. The solid line was computed by Eq.(2.17).

The discrepancy of the energies can be explained by grain boundary diffusion. It is well known the grain boundary diffusion is strongly the microstructure dependent, i.e. the composite, grain size and mechanical stress. Not only the peak activation energy but also the energy distribution is depending on the materials. A direct correlation between the 1/f noise and grain boundary diffusion was demonstrated by Scharz et al., who studied grain size dependence of 1/f noise in Al-Cu(2%) films [8]. Sample grain size was carefully controlled by the deposition rate and substrate temperature. $S_V \propto 1/a$ was observed, which a is the

grain size. In our case, since all polycrystalline Al samples were fabricated under similar conditions except Cu doping, the grain size effect was expected to be equally influenced to the final noise results.

4.4.3 Annealing effect

Two samples were annealed at 450 °C in one hour. In metals, annealing proceeds three types of processes: recovery, recrystallization and grain growth. Compared with well-treated bulk, thin metal films are highly defected. In other words, an excess energy is always stored toward to relax. By a heat treatment or annealing, this excess energy can be gradually relaxed, which is called recovery. Our polycrystalline samples have been kept more than several years since the original fabrication. Thus the prominent point defects should have been annealed out, such as interstitials or vacancies by aging. Only the effect , which is expected to be annealed, is a mechanical relaxation by the dislocation glide and climb. It should reduce some amount of residual stress. Although a major stress is relaxed by a heat treatment, still a fraction of the stored strain energy remains and contribute as a driving force to the process: recrystallization. The recrystallization process contributes to enlarge a relatively strain free region and to reduce surrounding highly strained regions inside a grain. Such a strain free region has a very low dislocation density compared with the strained regions. The recrystallization temperature 80 °C (353 K) is given by Guy and Hren [69]. This is defined as the temperature at which the highly cold worked pure metal and alloy completely recrystallize in about one hour. In our case, Al samples are not cold worked but stressed by the adhesion to a substrate or a buffer material.

Nevertheless, this temperature may provide a relative benchmark. When a strain free metal is kept at high enough temperature, a grain boundary can migrate and the grain size increases: grain growth. This type of boundary migration is much slower than the other boundary migration under the recrystallization process. The annealing temperature 450 °C is high enough to grain growth in bulk Al. If the grain growth is apparent in our samples, the noise reduction should be expected. However, such effect was not observed. Two reasons might be pointed out. One is the annealing time one hour was too short to achieve a noticeable amount of a mechanical relaxation. The other is thickness inhibition. When the sample geometry is sheet like, e.g. film, grain growth can be restricted. The growth rate of a grain reduces when the dominant grain size reaches the thickness of the sample. The grain growth finally stops after the size reaches two to three times of the thickness. In thin metal, a driving force associated with cylindrical boundaries is decreased than that with spherically curved. Besides, a two-dimensional grain growth must contain the process that the grain boundary has to migrate on a surface. This requires higher energy than grain boundary migration in bulk. The grain size of our polycrystalline Al samples is estimated a few thousands Å by high resolution scattering electron microscope (SEM). This is consistent with the result of other standard physically vaporized deposition (PVD) under the similar deposition parameter. All above arguments were based on a single phased metal, which the metallic phase is only α. However Al-Cu alloy consists of the two phases, i.e. α and θ within the range of experimental temperatures. Therefore, a grain growth further limited by the dispersed second phase particles [70]. In short,

the grain growth in our samples was less likely occurred. Since no noticeable change was observed in the noise measurements, it can be concluded that the annealing at 450C in an hour did not increase the noise. Indeed, this may be another support that grain boundary diffusion is a primary noise source since this is independent from inside a grain.

4.4.4 Discussion

The 1/f noise may be generated by the grain boundary diffusion process. However, this may not be exactly grain boundary electromigration. If the energy argument is correct in Eq.(2.19). The kinetics may contain the vacancy formation process. Since bulk vacancy formation energy is ≈0.66eV [71], it is less likely that vacancies are formed in bulk at less than room temperature. And a migration energy is slightly less than the formation energy ≈0.66eV [71]. It can be concluded the noise is created outside of crystal. Since surface or interface is not preferable region to diffuse due to the high activation energy, only possible regions where the vacancy can diffuse are a grain boundary or dislocations. Dislocations can act as relatively fast diffusion paths, i.e. pipe diffusion. A pipe-diffusion energy ~0.85 eV was found in Al by Volin et al. [72]. In some cases, dislocations may be a major source of the 1/f noise generation, e.g. in single crystal. However, it is not known how much the pipe diffusion is suppressed by the existence of impurity (Cu) atom. On the other hand, Cu atoms tend to be segregated from Al crystal and precipitate at a tri point in grain boundaries. This suppresses grain boundary diffusion. The noise suppression was observed under the existence of Cu atoms. This may be evidence that grain boundary diffusion is a primary noise source in polycrystalline

Al films. Although this is not directly an equivalent to electromigration which contains mass transport, the obvious correlation of the activation energy between the 1/f noise and electromigration suggests electron assisted vacancy migration may be involved to the 1/f noise process. Particularly, such electron wind may play an important role. If electron wind agitate a vacancy motion, it should reduce the thermal portion of the activation energy. And this induces a vacancy migration. Since no large scale of mass transport can be observed in this regime, the vacancy diffusion should create some levels of concentration gradient. Since no net mass transport is observed, the dynamical equilibrium may be generated by the vacancy migration assisted by electron wind and the concentration gradient. In a special case of electromigration, this type of a dynamical equilibrium has been observed more than 20 years ago [30]. Under a normal accelerated test condition, an Al strip simply shows electromigration. However, when the length of the Al strip is shorter than the critical length, the mass transport is not observed. This striking effect was first observed by Blech [73]. The mechanism is now understood by the atomic back flow. For example, if DC is applied to a short strip of Al, Al atoms can diffuse through grain boundaries toward the anode by assisted electron wind. This creates the internal stress by the atoms or vacancies. Due to the increase of a number of atoms and of the stress, the difference of the free energies can be created one region to the other. This energy difference pushes atoms backward. As a result, the concentration gradient and electron wind force can reach the equilibrium. Of course, if the equivalent energy of internal stress is higher than any

threshold energies to start hillock, dislocation slip or climb, the effect of back flow saturates. The net drift velocity can be written as,

$$V = V_{EM} - V_{BF} \qquad (4.4)$$

where, V_{EM} is electromigration velocity and V_{BF} is back flow velocity. Further V_{EM} and V_{BF} can be described as,

$$V_{EM} = BZ^{*}e\rho j \qquad (4.5)$$

$$V_{BF} = B\Delta F / L \qquad (4.6)$$

where, B is a mobility (=D/kT), Z* is the effective charge, e is an electron charge, ρ is resistivity, j is a current density, ΔF is the difference of free energies and L is a strip length. The critical length L_C can be derived when V=0 in Eq.(4.4).

$$L_C = \frac{\Delta F}{Z^{*}e\rho j} \qquad (4.7)$$

It is interesting to see such a relation in terms of the noise study. If the strip length reaches L_C, does the 1/f or $1/f^2$ noise continuously change or sudden decrease? So far no reports has been made. Above argument was strictly under electromigration regime and primary kinetics is the atomic process. On the other hand, in 1/f noise regime, the primary kinetics may be the same as grain boundary electromigration. However, the low temperature environment does not allow participating many atoms to diffuse and the mobility should be very small.

Therefore the concentration gradient may also be small and may occur locally. This may be a main difference between the effect of no drift by the critical length and a standard 1/f noise kinetics. This clearly indicates that the concept of the critical length is irreverent in 1/f noise regime. Albeit, it behaves the thermal kinetics as electromigration. This similarity of thermally activated kinetics has been observed in 1/f noise measurements. And the drift or migration quantity is proportional to the electron current density in a standard drift experiments. This is also consistent with 1/f noise measurements. The deviation from the quadratic noise power respect to the applied voltage may reveal a detail of diffusion kinetics although most of the noise power results showed a good agreement with a quadratic behavior. And the experimental determination of such deviation is difficult to perform due to the relatively small deviation. Nonetheless, the investigation may be plausible.

Is there any other potential noise source, which can be consistent with full experimental results and with microscopic metal physics? The theory which contains the non-linear dependence of the applied current or voltage may be a less likely. Nagaev and Kogan proposed the 1/f noise be created by internal friction [35]. To incorporate the theory, it is necessary to know the mechanical attenuation factor. However, it is very hard to know this factor in thin metal films. Only crude qualitative argument was attempted. In Eq.(2.21), the most temperature sensitive part is TQ^{-1}. Most of internal friction experiments showed Q^{-1} has a peak structure after a mechanical treatment was performed, i.e. Bordoni peak. This mechanical relaxation is due to a dislocation relaxation. The Q^{-1} tends to show a broad peak

rather than a sharp peak. This implies that the relaxation process has a distribution of energies. Although a similarity of the energy distribution could be pointed out, a poor correlation was found after the comparison between Q^{-1} and the temperature dependence of the 1/f noise. Another approach to correlate Q^{-1} and the 1/f noise spectrum was attempted. The inverse of quality factor Q^{-1}, i.e. log decrement, is known to have a simple relationship between the forced frequency and the peak relaxation temperature T_P.

$$2\pi f = \tau_0^{-1} \exp(-\frac{H}{k_b T_P}) \qquad (4.8)$$

where H is activation enthalpy, f is the forced frequency and τ_0 is an attempt time of atoms. Kê performed the temperature dependent of internal friction in polycrystalline Al by a torsional vibration experiment at 0.8 Hz [74]. The peak temperature 300C (573 K) was observed in several samples and the activation energy 1.48 eV was obtained. If extrapolation was made to estimate the frequency at 390 K, the frequency corresponds ~ 10^{-6} Hz. This frequency is too low to be observed. Compared with other internal friction results in Al [34], it is less likely to see the correlation and obtain a consistent explanation.

4.5 Single and bamboo grained Al films

4.5.1 Overview

Single and bamboo grained samples were investigated in low temperature noise measurement. Four single crystal and three bamboo grained samples were tested. Hooge parameters α_H at 294 K are listed below.

Sample name	Crystal structure	α_H at 294K
1714-b	Single	$2.89 \pm 0.05 \times 10^{-5}$
1715-a	Single	$6.00 \pm 0.35 \times 10^{-5}$
1715-b	Single	$2.83 \pm 0.10 \times 10^{-5}$
1715-e	Single	$2.39 \pm 0.53 \times 10^{-5}$
126-7-d	Bamboo grained	$3.05 \pm 0.15 \times 10^{-5}$
126-7-f	Bamboo grained	$5.26 \pm 0.49 \times 10^{-5}$
126-12-a	Bamboo grained	$2.32 \pm 0.20 \times 10^{-5}$

Table.4.5: Hooge parameters α_H at 294 K in single and bamboo grained samples.

All of the samples showed smaller α_H than polycrystalline samples. And no substantial difference was observed in single and bamboo grained samples. Verbruggen pointed out the 1/f noise was found even in single crystal gold films [13]. This has been confirmed by Homberg in single Al films [14]. Our results

demonstrated previous results well. Although the α_H is nearly an order below in single and bamboo grained samples, some certain amounts of resistance fluctuation were remained at room temperature. Grain boundary diffusion can not occur in single crystal and less likely occur in bamboo grained samples. Since the bamboo structure has grain boundaries perpendicular to the current direction, the net diffusion is quite small. This has been proven by many life time tests [31]. Figure 4.12 shows the temperature dependence of the noise power S_V in single crystal (1714-b). The magnitude of S_V at 1Hz changed nearly three and a half decades. An over all temperature dependence indicates not so much difference from polycrystalline ones.

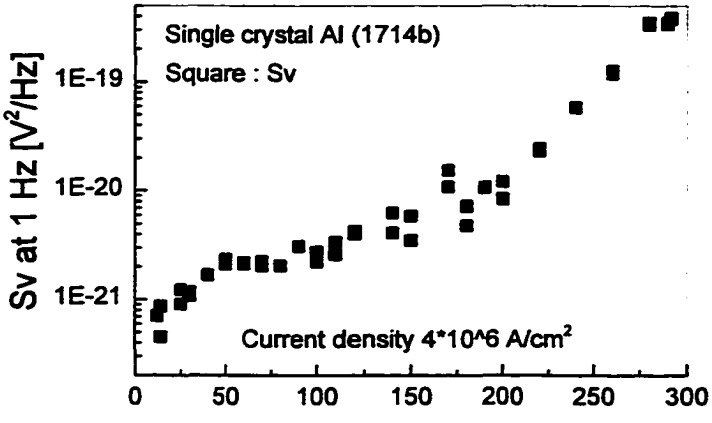

Fig. 4. 12: The temperature dependence of Noise Power Sv in Single crystal film. Sample name ; 1714b.

4.5.2 Low temperature measurement result

Homberg et al. proposed the pipe diffusion along dislocations may be the origin of 1/f noise in single and bamboo grained samples [48]. They observed a wide range of temperatures from 140 K to 500 K and observed a fluctuation peak

at about 340 K in both types of samples. The activation energy ~ 0.8 eV was found. The temperature dependence of Hooge parameter α_H is shown in Fig.4.13. A novel result appears at less than 150K. The α_H increased with decreasing temperature and reached a peak near 35K. All single crystal and bamboo samples showed the peaks. At a peak temperature 35 K, the noise power linearity was tested in Fig.4.14. The quadratic behavior of noise power is obviously remained. And the frequency exponent also showed constant ~0.85. It can be concluded this is a resistance fluctuation.

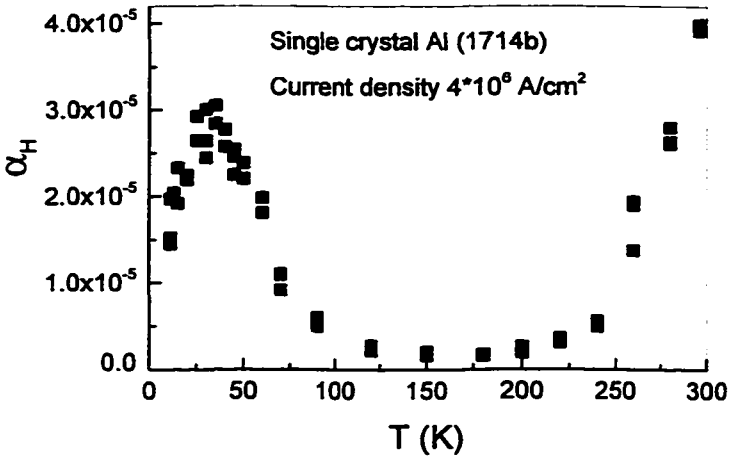

Fig. 4. 13: The temperature dependence of α_H in Single crystal Al film (1714b).

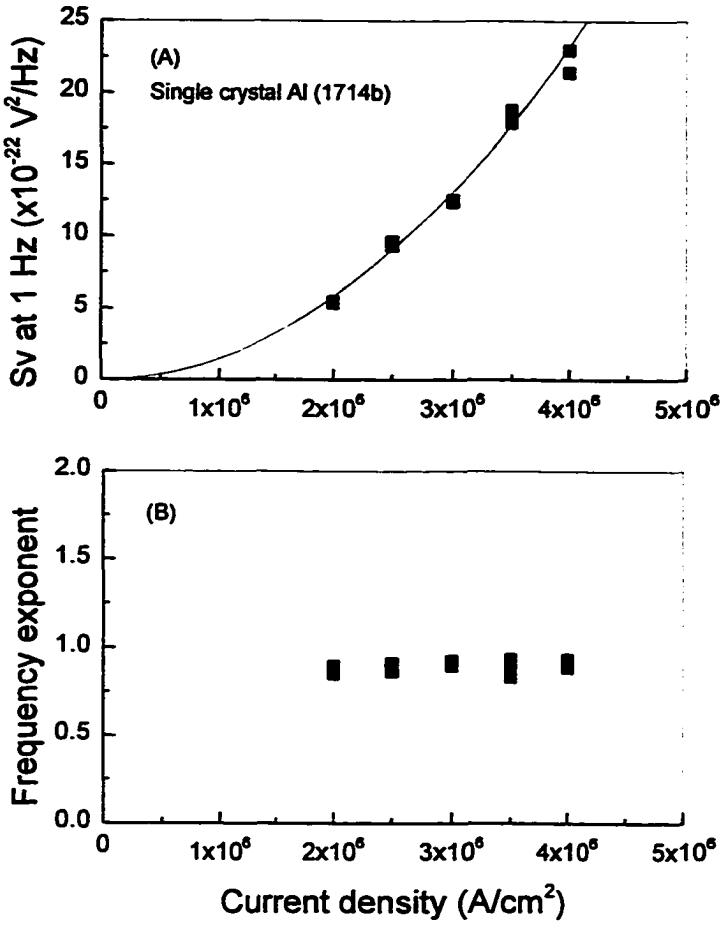

Fig. 4. 14: (A) The noise linearity and (B) Frequency exponent.

4.5.3 Discussion

The detailed examination of all samples revealed that the peak was observed in most of samples investigated. Surprisingly the peak temperatures were quite similar although the peak maximums were different from each other. In single crystal films, the α_H peak varied from $1.2 \cdot 10^{-5}$ to $3.7 \cdot 10^{-5}$. In polycrystalline pure Al and annealed Al-2% wt. Cu films, no peak was seen. In these films, α_H simply decreased with decreasing temperature. The peak values of α_H are listed in Table 4.6.

Sample name	Composite	Peak α_H
E-Al w1	Pure Al	No peak found
2ADAl-0.7Cu	Al-Cu(0.7%)	No peak found
E-Al w4	Pure Al	7.1×10^{-6}
A450Al-2Cu w1	Al-Cu(2%)	9.1×10^{-6}
A450 Al-2Cu w4	Al-Cu(2%)	4.3×10^{-6}
Al-2Cu	Al-Cu(2%)	1.2×10^{-5}
1715-a	Single	3.7×10^{-5}
1714-b	Single	2.7×10^{-5}
1715-b	Single	1.6×10^{-5}
126-12-a	Bamboo	4.9×10^{-5}
126-7-f	Bamboo	3.4×10^{-5}

Table: 4.6 α_H Peaks.

When the current density exceeded $4 \cdot 10^6$ A/cm^2, a steady resistance drift was observed in all samples. The temperature increase was more than 1.5 K in single and bamboo grained and 2.0 K in polycrystalline samples. In the high current density case $1/f^2$ noise due to drift was observed and occasionally sharp resistance jumps were detected. The samples were measured over a period of one year and still showed equivalent temperature dependence and noise power. Occasionally a sample turned out to be permanently noisy after an extremely high current density was applied ($> 4 \cdot 10^6$ A/cm^2), presumably due to electromigration damage. After the first noise measurement was completed, one single crystal

sample was annealed at 310 °C for 72 hours in Ar. No change was observed in either the α_H peak height or the overall temperature dependence.

4.5.3.1 $\alpha_{H(max)}/\alpha_{H(min)}$ versus RRR

Fig. 4.15 shows the relationships between; the ratio of α_H maximum (peak) to α_H minimum, ($\alpha_{H(max)}/\alpha_{H(min)}$), and the residual resistivity ratio, RRR, at 294K and 15K. The α_H minimum was chosen between the peak temperature and room temperature. When the α_H ratio is unity, no peak is found in the temperature dependence of α_H. Surprisingly, a trend appeared where $\alpha_{H(max)}/\alpha_{H(min)}$ increased proportionally to RRR. It is noteworthy that cleaner samples show higher $\alpha_{H(max)}/\alpha_{H(min)}$. This result implies that defects or impurities, which are responsible for the residual resistance, may not contribute to 1/f noise simply through thermally activated kinetics. One can, thereby, postulate that less defects or impurities create higher noise at lower temperatures. Clearly this argument is not intuitive. One would expect more defects, or impurities to create more 1/f noise in this low temperature regime. The volume of all of the samples was similar ~10^{-10}cm^3 (See Table 4.7). The size effect contributes as one component of resistivity at low temperatures because the electron-phonon scattering length and sample lateral dimension are comparable. The resistivity at 15 K is listed below in Table 4.9. If the size effect was dominated in observed resistivities, the single and bamboo grained samples must show higher resistivity because over all dimensions are equal or smaller than polycrystalline samples.

Sample name	Crystal Structure	$\alpha_H(max)/\alpha_H(min)$	RRR (294K/15K)	Symbol
DLT126 #12	Bamboo	10.8	22.8	■
1715-a	Single	13.7	18.1	▼
1714-b	Single 310C 70h annealed	18.3	17.3	●
1715-b	Single	15.7	13.7	▲
Al-Cu(2%)	Polycrystalline 450C 1h annealed	2.93	10.1	□
Al-Cu(2%)	Polycrystalline As deposited	4.0	10.0	◆
Al-Cu(2%)	Polycrystalline 450C 1h annealed	2.04	9.4	O
E-Al 1000	Polycrystalline As deposited	1.392	5.8	×
E-Al 1000	Polycrystalline As deposited	1.0	4.6	Δ
Al-Cu (0.7%)	Polycrystalline As deposited	1.0	4.0	∇

Table 4.7 : The relation between α_H ratio and RRR.

Sample name	ρ at RT (μΩ-cm)	Volume ($10^{-10}cm^3$)
DLT126 #12	2.80	1.336
1715-a	2.86	1.036
1714-b	2.82	0.978
1715-b	2.86	0.972
Al-Cu(2%)	2.93	2.35
Al-Cu(2%)	3.13	2.52
Al-Cu(2%)	3.19	0.925
E-Al 1000	3.13	1.971
E-Al 1000	3.60	0.716
Al-Cu (0.7%)	3.57	1.434

Table 4.8 : A supplemental information of samples.

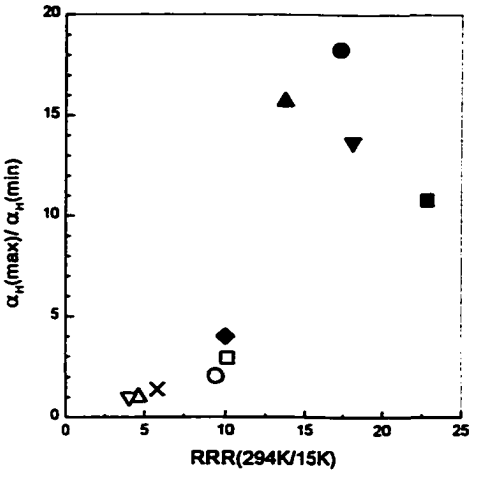

Fig. 4. 15: $\alpha_{H(max)}$ /$\alpha_{H(min)}$ versus RRR (294K/15K).

However, such higher resistivities were not observed. It can be concluded the higher resistivity samples are more defected. Although they should contain the size effect in resistivity, this effect is not dominated. And the size effect should not be responsible for the resistance fluctuation, if local scattering is the fluctuation source.

The attempt has been made to estimate the number of fluctuators by employing Eq.(2.47). In clean metals, electron-phonon scattering processes dominate the total inelastic scattering process, i.e. L_{in}=L_{ep}. The elastic scattering is dominated by diffusive surface scattering. An attempt has been made to estimate the number of fluctuators N_s (T=35K) in a single crystal sample. L_{ep} is estimated to be 1-10 μm by the Fuch-Sondheimer formula [75]. L_{el} was estimated by L_{ep} and geometrical consideration to be a few hundred nm or longer. The concentration of Al atoms is N_a~$6\cdot10^{22}/cm^3$.

Sample Name	Crystal Structure Poly: Polycrystalline	Resistivity at 15K (10^{-7} × Ω-cm)
E-Al w1	Pure Al	7.83
E-Al w4	Pure Al	5.40
2ADAl-0.7Cu	Al-Cu(0.7%)	8.93
A450Al-2Cu w1	Al-Cu(2%)	3.40
A450 Al-2Cu w4	Al-Cu(2%)	2.90
Al-2Cu	Al-Cu(2%)	3.13
1715-a	Single	1.58
1714-b	Single	1.65
1715-b	Single	2.09
126-12-a	Bamboo	1.23

Table 4.9 The resistivity at 15 K.

The last term in Eq.(2.47) represents the temperature dependent term, which consists of the distribution of activation energies D(E) and Lorentzians. The best fit gives Ea~0.08 eV at the distribution center and D(E) was estimated to be a relatively narrow gaussian with the standard deviation ~ 0.001. The last term can be expressed as ~10^{-2} T /f [22]. An activation energy of 0.08eV may suggest that TLS by interstitial switching could be the fluctuation source, therefore β ~0.25 was chosen in Ref. [26]. As a result, N_s (T=35) gives 0.1-10 ppm thermally activated defects in a sample. This seems to be reasonable. However, as mentioned earlier, it is believed that 1/f noise at room temperature is caused by thermally activated defects. The α_H of polycrystalline samples is an order of magnitude higher than

those of single crystal samples, which simply suggests polycrystalline samples have higher defect concentrations. If the LI model is applied for polycrystalline films at low temperatures, it predicts the higher α_H than for single crystal films. Compared to single crystal results, the α_H peaks were rather small or not measurable for polycrystalline samples. Our results can not be explained by the LI model. Other defects, i.e. vacancies, interstitial clusters or impurity atoms, are stable at less than 150K [76].

4.5.3.2 Dislocation kinetics

If direct defect kinetics are the main sources for this fluctuation, the most likely candidates are dislocations. Dislocations have a variety of thermally activated dynamics. Dislocations are intrinsically anisotropic and their dynamics contain multi-atom processes, which are favorable for dynamical resistance fluctuations. The expected activation energy may be quite low. Our fitting result in Eq.(2.19) gave E_a~0.08 eV which corresponds the estimation by Dutta et al. [22]. Among many kinds of dislocation dynamics, this requirement of low activation energy may only allow double kink formation or kink diffusion [49]. A dislocation density of 10^9 cm^{-2} was found in single crystal samples by TEM study [77]. Ho et al. has reported that the stress in thin Al films can exceed several hundred MPa at room temperature [78]. The activation energy for double kink formation or kink diffusion depends on the stress and dislocation characteristics, e.g. the distribution of kink heights and separation lengths. Therefore the distribution of activation energies is expected to vary from sample to sample. However, a variation in activation energy between samples was not observed. Further, a relationship between the effects of dislocations and the RRR dependence

of α_H was not directly observed. In a double-kinks formation process at low temperature, the dominant geometry of thermally formed double kinks should be a small size and this activation energy is very small E « 1. This type of dislocation dynamics is rather close to phonon dynamics except a stress. In other words, this dynamics is a fast process that should be a comparable to a phonon attempt time. Those short life time kinetics only should contribute a white noise, at least high corner frequency spectrum, rather than 1/f noise. Only the way to create a slow fluctuation is some types of demodulation process, e.g. a beat. LI model explains the defect-defect dipole interaction is considerable when $kF \cdot R < 7$. Even if it is considered a moderately dislocated sample, a dislocation density $\sim 10^{11}$ cm^{-2}, still the thermally activated dislocation dynamics which contains a double kinks formation should be sparse, i.e. $kF \cdot R \gg 1$. Basically LI model was formulated for the point defect noise. It is not known how much this argument is valid.

The kink diffusion process for the noise generation may also reach a same conclusion. If a kink diffuses slowly in a sample, this can be a certain candidate of slow fluctuation. If the resistivity of a kink is estimated from the theoretical calculation of dislocation resistivity, e.g. Brown [79], this gives a reasonable value to create a resistance fluctuation. Verbruggen et al pointed out the annealing effect of the Aharonov-Bohm oscillations in Au rings was observed when the ring temperature increased at 20 K [56]. They attributed that the thermally activated dislocation motion, kink diffusion, changed the electron conduction paths. At low temperature, the stress should increase due to thermal mismatch between a substrate and a metal. It is known the kink diffusion velocity is finite even the

temperature down to absolute zero when the activation energy is comparable to kT. However, their experiment indicated the diffusion of the kinks was fast and completed prior to the oscillation measurements. It is a reasonable to apply this idea that the velocity of the kink may be fast enough. If so, no time dependence of 1/f noise spectrum can be expected. And indeed, it was not observed. Albeit, it is conceivable but unlikely that stress influences our results.

4.5.3.3 Quantum effects

It is known that quantum interference in small metallic samples is very sensitive to the distribution of defects and impurities. Theoretical [53] and experimental [80] studies confirmed the deviation of the conductance is of the order of $(e^2/h)^2$ within a phase coherent volume, which is called the universal conductance fluctuation (UCF). Feng, Lee and Stone [17] estimated that one impurity, which moves a few Fermi lengths, creates an observable time-dependent fluctuation i.e. UCF 1/f noise. Indeed, UCF 1/f noise has been observed by several groups [18, 59, 81]. However, in metal UCF noise studies, all of the measurements were performed in either weakly or strongly disordered strips or films. On the other hand, no report has been made for dynamical UCF 1/f noise in clean or ordered 3 dimensional metals. This UCF regime requires the elastic scattering length L_{el} to be much shorter than the inelastic scattering length L_{in}. In normal bulk metals, it is impossible to satisfy such a condition because $L_{el} > L_{in}$. However, in clean metals, this condition could be met if L_{el} could be reduced due to small sample geometry. In the study of single crystal Al foils [82], it has been reported that a single crystal Al exhibits a substantially long L_{in}, e.g. 1000 μm at

10K and varies as $T^{-3.0}$ to $T^{-3.5}$, which depends on crystallographic orientation. In a typical thin film, it is hard to expect such long L_{in}, however, it is still reasonable to expect that L_{in} could be long enough to satisfy $L_{in} > L_{el}$. Under this transport mechanism, dominant elastic scattering should be surface or interface diffusive scattering i.e. like an electron guide cavity. Since the specularity of the surface scattering is small in metals, high elastic scattering rates may be expected. One more important length scale is the thermal diffusion length, L_T, which is described by $L_T = \sqrt{\hbar D / kT}$, where D is the diffusivity. This is another dephasing length due to thermal broadening. If $L_{el} > L_T$, the electron is out of phase even before single scattering. A crude estimation was made for L_T at 35K; hundreds of nm was obtained, which is somewhat close to L_{el}. According to the RRR dependence of α_H ratio shown in Fig.4.15, if the concentration of material defects and impurities could influence L_{in}, it may be understandable that our result is due to the enhancement of UCF 1/f noise. Defects can contribute to inelastic scattering, e.g. it is known that dislocations have long range strain fields which affect inelastic scattering. The similarity of peak temperature for all samples suggests that the origin of this UCF 1/f noise may be identical. Low activation energy may suggest a specific type of TLSs, e.g. bistable defects formed by a partial dislocation [83], may be the source of UCF 1/f noise.

Stone suggested that UCF noise was reduced under the presence of a magnetic field because it reduces the cooperon channel contribution in disordered metals [84]. The noise reduction factor 2 has been estimated. A magnetic field 0.2±0.01T has been applied to single crystal samples. No reduction was observed

at any temperature. Feng et al. [57] and Hershfield [85] described a particular case, in which UCF noise does not depend on the magnetic field. Clean metals have significantly less back scattering components than metallic glasses, therefore the diffuson channels are dominated. Detailed studies with a stronger magnetic field would be useful in illuminating this point.

A crude estimation of the number of defects was made by employing Eq.(2.49). Most of the parameters have been chosen from the previous calculation for LI model. (e^2/h) is $(25.8\ k\Omega)^{-1}$. Lorentzian integral part which consists of the energy integration of a density function D(E) and a Lorentzian is approximately ~ 10^{-2} at 1 Hz. Fermi wave length $k_F^{-1} \sim 0.57$ Å in Al. $\alpha(k_F\ \delta r) \sim 1$. δr is a distance for impurity or defect switching. This is one of the largest uncertain factors, which is estimated somewhat close to lattice spacing ~ 4 Å. This may be reasonable if the dislocation dynamics is assumed. After all parameters were considered, the number of activation defects ~ 10^2 was estimated in a single crystal sample.

4.6 Polycrystalline Cu films

4.6.1 Results

Three polycrystalline Cu samples were studied in noise measurement. The current density 3×10^6 A/cm^2 was applied. This current density created temperature increase ~ 0.2 K. Due to higher electromigration resistivity, no instability was observed. The temperature dependence of α_H was quite similar to Al results in Fig.4.16 (A). Surprisingly, peaks were found in all samples. No substantial change was observed in a frequency exponent in Fig.4.16 (B). When T > 150 K, the increase of α_H may be due to GB electromigration.

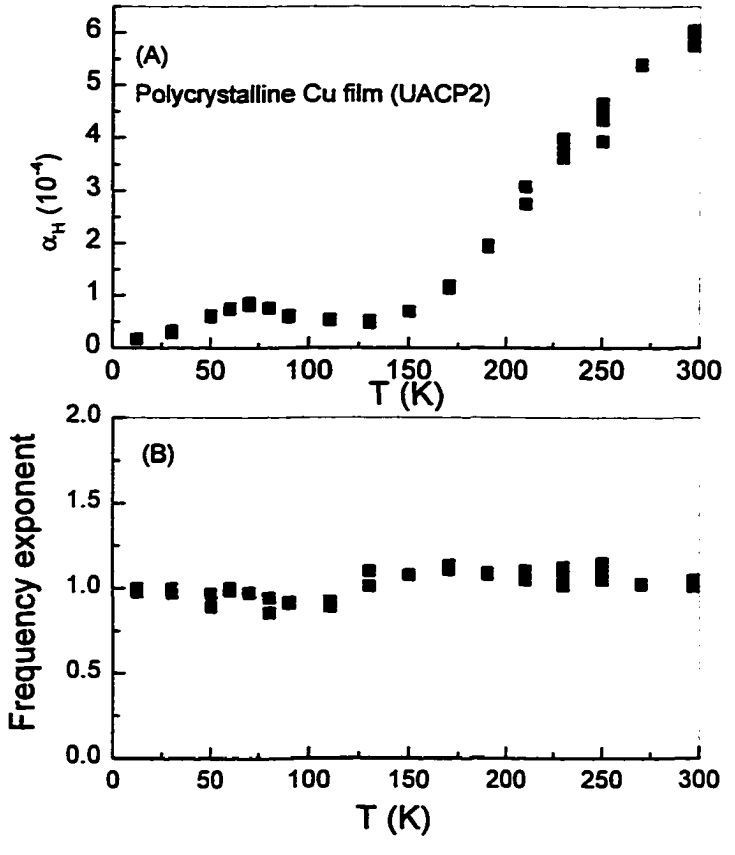

Fig. 4. 16: (A) The temperature dependence of α_H and (B) Frequency exponent in polycrystalline Cu film. (UACP2).

4.6.2 Discussion

T > 150 K, the increase of α_H was observed in all Al samples. The onset temperature of α_H gives an estimated energy ~ 0.36 eV. This suggests the threshold energy of GB electromigration is relatively lower than that energy in Al. Since the peak activation energy in Cu is higher than that in Al, these Cu samples have broader distributions of energies. This should be able to confirm in MTF study. T < 150 K, the peak emerged at 70 K in all samples. The energy estimation gives ~ 0.16 eV. Like Al results, this does not correspond to any energy of known points defects, i.e. a formation or a migration energy. Also no correlation between peak α_H and α_H at 294 K was found.

4.6.3 General discussion

Ralls and Buhman studied a 1/f noise in metallic nanoconstruction [86]. Al, Cu and Pd were studied. They found all noise power S_v decreased with decreasing temperatures. In Cu nanobridge, the temperature dependence of S_v was a quite similar to our polycrystalline Cu results. However, S_v decreased only a decade instead of 2.5 decades in our Cu films. At T < 150 K, some peaks emerged. Comparing the S_v at neighboring temperature around the peak, 60-70 % of increase of S_v was observed. This seems clearly beyond the errors. In our measurement, the error of spectrum at a temperature is about 10 % in Cu films. The α_H of Cu nanobridge is 1.6×10^{-3} at room temperature. Since resistance of nanobridge is constant at all temperatures, α_H is proportional to S_v. The minimum α_H is estimated ~ 1×10^{-4}. On the other hand, $\alpha_H \sim 1 \times 10^{-3}$ at room temperature and ~ 1.7×10^{-4} at 11 K were observed in polycrystalline Cu films. Somewhat Cu

nanobridge is noisier at less than 150 K. In Al, the temperature dependence of S_v is noticeably different from our results. S_v was rather flat down to 200 K then rapidly decreased down to 100 K. At less than 100 K, the fluctuation was unobservable.

Compared with an original assumption of UCF in thin films, why did no such peaks emerge unlike our samples? One reason may be "the typical nanobridge consists of a single-crystal dendrite" [86]. This may imply an inelastic scattering length L_{in} may not be as long as in clean bulk. Such L_{in} should be determined by a local microstructure, i.e. temperature independent. Another reason may be more important that an average number of multiple scattering may be much less within a nanobridge region. A volume of this region is very small which the total number of atoms 10^4-10^6. The bottleneck length of the bridge along net electron flow can be crudely estimated about less than 10 nm. Since the length is too short, the multiple scattering is less likely occurred in the bottleneck. In the concave region, a high amount of back scattering may be expected. However, the bottle part of the length may not be long enough to create multiple back scattering. Thus electrons can easily escape. Nonetheless, Cu nanobridge exhibited a substantial 1/f noise. The nanobridge region is not exactly a single crystal but dendrites. Therefore, there are many relatively easy paths for atomic or vacancy diffusion. Although it was mentioned no electromigration was observed when a current density was less than 10^8 A/cm^2, such a high current density is more likely to cause small amount of atomic diffusion. For example, if current density exceeds more than 4×10^6 A/cm^2 in a single crystal sample, the instability was observed, in

other words the total fluctuation quantity rapidly increased. Our single crystal samples have higher heat dissipation than ordinary thin film samples because the trench structure covers all sides of Al strip except a top surface. And single crystal itself has a high resistivity for electromigration. This result seemed a good agreement with electromigration regime due to pipe diffusion. Ralls and Buhrman argued particularly defects glass was formed in bridge. This may go under low activation energy dynamics through the defects complex. It is no surprise if the glass regions are existed in our single crystal samples. However, because of a low resistivity, it can not be a high fraction of the complexes and the noise results revealed no such broad distribution of the low energies was found. However, a fundamental difference lies between nanobridges and our samples, which is ballistic and non-ballistic regime. This is one of the difficulties of the naive comparisons.

4.7 Conclusion

We have measured the 1/f noise in a variety of thin metal films. The increase of α_H above 150 K is explained by GB electromigration in Al and Cu polycrystalline films. It was shown that addition to Cu atoms in Al suppressed the α_H compared with that in pure Al. This is a good agreement with other reports[12]. Single crystal samples were measured at low temperatures. The onset temperatures were somewhat similar to those polycrystalline Al and Al alloys. However, they showed obviously lower α_H than polycrystalline samples down to 150 K. The relationships between; (a) the ratio of α_H maximum (peak) to α_H minimum,

($\alpha_{H(max)}$ /$\alpha_{H(min)}$), and (b) the residual resistivity ratio at 294K and 15K, RRR, were investigated. Surprisingly, a trend appeared where $\alpha_{H(max)}$ /$\alpha_{H(min)}$ increased proportionally to RRR. This indicates that cleaner samples have larger low temperature noise peaks. Above 200 K, it is believed that defects or impurities contribute to 1/f noise simply through thermally activated kinetics. These peaks seen in this work can not be explained using simple thermally activated kinetics. Instead, a quantum interference effect, universal conductance fluctuation (UCF), may provide another explanation of our data. This result may lead to a better understanding of quantum coherent transport in clean metals. The Cu films also exhibited the α_H peaks. It is not clear whether the origin of the α_H peaks in Cu and Al is based on an equivalent physical process or not. The same UCF argument may be able to applied to Cu films. However, it may be suspected because the short phase coherent length may destroy a primary effect of a quantum interference. Rather, those peaks may be explained by a complicated dislocation dynamics. A double-kinks formation process or a kink diffusion process may be responsible to the peaks. However, why the impure samples showed no peak is not explained well.

Chapter 5

Summary

One of our original intentions was to develop the highest performance noise measurement system. We aimed to measure the slowly varying voltage fluctuation of about 10 pV without being disturbed by any external interference. To achieve tough requirements, we employed the AC cross-correlation technique. A strong advantage of this technique is the ability to reduce any random noise. Especially this has shown a remarkable performance to reduce a thermal noise from the sample, amplifier and any additional electronics. Our measurement system accomplished an extremely low background noise 3×10^{-22} V^2/Hz and an outstanding temperature stability ~10mK. Several pieces of testing equipment was also developed to observed the instabilities of the system, e.g. a high precision testing modulator with a white noise generation function or a specially designed Cu wire resistor to detect the temperature instability down to 1 mK. Based on a successful development, the 1/f noise study was accomplished in Al and Cu thin films from 11 to 300 K for the first time. One of the striking results was that the 1/f noise was observed even at the lowest temperature 11 K in all films. In the Al study, single crystal films showed substantially lower noise than polycrystalline. Thus investigations agree that a primary 1/f noise is generated by grain boundary electromigration in thin metal films at room temperature. When the sample temperature is less than 200 K, this argument is no longer valid. We found the increase of the noise at about 40 K which corresponds to the energy ~0.08eV in Al

films. This also has never been reported since no experiment had been ever done. Not many species can diffuse at such a low temperature. This suggests that none of the diffusion by point defects may be responsible to create this resistance fluctuation. Rather the thermally activated dislocations may be plausible. Among many kinds of dislocation dynamics, kink diffusion or double-kinks formation may be considerable since the expected activation energies can be quite low. Although indications were made by internal friction experiments, there has never been any direct evidence for the thermally activated kink kinetics at low temperatures. Our results suggest the thermal kink may be activated at about 40 K. In general, kink motions can be separated two types. One is that a kink moves by flow stress. The other is that a double-kinks is thermally formed and diffused. A single crystal sample was kept at a particular low temperature more than a week. It still exhibited a same amount of the resistance fluctuation. This reduces one possibility that an origin of the 1/f noise is the kink diffusion by stress. Rather thermally generated kinks, a double-kinks, may be responsible. If further evidence could be obtained, it may lead an exclusive experimental evidence of thermally generated kinks without applying any external forces. However, further investigation is necessary to remove other possibilities. For example, although our standard knowledge simply excludes any atomic diffusion at such low temperature ass we discussed, it still may be able to consider some atomic diffusion in special cases. A real single crystal contains always a number of dislocations. Dislocation core and the vicinity can be an easy path for diffusion. If some diffusion species are available, it may be conceivable that the noise is generated near the dislocation core. However, another

question arises. How can those defects be created? This is a difficult question. In single crystal metal films, there are not many chances for the formation process of interstitials. Only this may happen by the existence of a high stress. Thin metal films are highly stressed due to a thermal mismatch between metal, buffer layer and substrates. This may cause the formation of interstitials at low temperatures. The further investigation is required. The 1/f noise study in Cu film revealed another surprising result. The temperature dependence of the noise power, Hooge parameter and resistivity fluctuation, all of them, showed a peak at about 70 K. This result can not be explained by a simple defect motion. Rather a complicated defect-defect interaction or an enhancement effect of quantum interference may be involved. Further experiment, e.g. B field dependence, may reveal the details.

Finally, based on a successful development of a high performance noise measurement system, we measured the 1/f noise in Al and Cu films. No one ever demonstrated such detail and systematic study. Some new findings were made although a further investigation is necessary to understand the detailed mechanism. We hope this study may contribute a further understanding of condensed matter physics.

Appendix A: Wiener-Khinchin theorem.

Wiener-Kinchin theorem provides a powerful tool to evaluate a fluctuation quantity. As long as the physical object is stationary stochastic process and the auto correlation function is obtainable, it is quite straight forward to obtain the fluctuation spectrum by employing Wiener-Kinchin theorem. First, let's define Fourier integration.

$$x(t) = \int_{-\infty}^{\infty} df\, Y(f,T)\, e^{2\pi f t i} \qquad \text{(A. 1)}$$

$$Y(f,T) = \int_{0}^{T} dt\, x(t) e^{-2\pi f t i} \qquad \text{(A. 2)}$$

Average can be expressed as,

$$< x(t) >= \lim_{T\to\infty} \frac{1}{T} \int_{0}^{T} dt\, x(t) \qquad \text{(A. 3)}$$

We like to know a fluctuation. This can be written as,

$$(< (x(t) - < x(t) >)^2 = < x^2(t) > - < x(t) >^2 \qquad \text{(A. 4)}$$

For brevity, set $< x(t) >= 0$.

$$< (x(\quad < (x(t) - < x(t) >)^2 >= \lim_{T\to\infty} \frac{1}{T} \int_{0}^{T} dt\, x^2(t) \qquad \text{(A. 5)}$$

$$\overline{T\to\infty}\, T \quad 0$$

Applying Eq.(A.1),

$$<(x(t)-<x(t)>)^2>=\lim_{T\to\infty}\frac{1}{T}\int_0^T df\, Y(f,T)Y^*(f,T) \quad \textbf{(A. 6)}$$

Spectrum component may be described as,

$$\varphi(f)=\lim_{T\to\infty}\frac{1}{T}|Y(f,T)|^2 \quad \textbf{(A. 7)}$$

Now define autocorrelation function.

$$c(\tau)=\lim_{T\to\infty}\frac{1}{T}\int_0^T dt\, x(t)x(t+\tau)=\lim_{T\to\infty}\frac{1}{T}\int_{-\infty}^{\infty} df\,|Y(f,T)|^2 e^{-2\pi f\tau i}$$

(A. 8)

Multiply $e^{2\pi f'\tau i}$, then integrate.

$$\varphi(f)=\lim_{T\to\infty}\frac{1}{T}|Y(f,T)|^2=\int_{-\infty}^{\infty} d\tau\, c(\tau)e^{2\pi f\tau i}=2\int_0^{\infty} d\tau\, c(\tau)\cos(\omega\tau)$$

(A. 9)

This relation is called Wiener-Khinchin Theorem.

Appendex B : Two Level System.

In Fig.2.5, Two Level System (TLS) was described. Both wells are supposed to be quasi stable states. Let's say state A and B. Each state has decay time respectively, a and b [88]. The probability of making a transition from A to B is dt/a in a short time dt. At arbitrary time, the probability of state A is described as $\frac{a}{a+b}$ and the probability of state B is $\frac{b}{a+b}$. Now if variable x shows A state at t, a auto correlation function may be written.

$$\varphi(\tau) = < x(t)x(t+\tau) >$$
$$= a^2\left\{\frac{a}{a+b}\right\}_{at}\left\{\frac{a}{a+b}\right\}_{at+\tau} + ab\left\{\frac{a}{a+b}\right\}_{at}\left\{\frac{b}{a+b}\right\}_{at+\tau} + ba\left\{\frac{b}{a+b}\right\}_{at}\left\{\frac{a}{a+b}\right\}_{at+\tau}$$
$$+ b^2\left\{\frac{b}{a+b}\right\}_{at}\left\{\frac{b}{a+b}\right\}_{at+\tau} \qquad \textbf{(B. 1)}$$

$$= A^2\frac{a}{a+b}P_{AA}(\tau) + AB\frac{a}{a+b}P_{AB}(\tau) + BA\frac{b}{a+b}P_{BA}(\tau) + B^2\frac{b}{a+b}P_{BB}(\tau)$$

(B. 2)

$P_{AA}(\tau)$ is the probability from A to A and $P_{AB}(\tau)$ is the probability from A to B. Third and forth terms are zero since only A state is allowed at t.

$$P_{AA}(\tau) + P_{AB}(\tau) = 1 \qquad \textbf{(B. 3)}$$

$$P_{AA}(\tau+d\tau) = P_{AB}(\tau)\frac{d\tau}{b} + P_{AA}(\tau)\left(1-\frac{d\tau}{a}\right)$$
$$= P_{AA}(\tau) + \frac{dP_{AA}}{d\tau}d\tau \qquad \textbf{(B. 4)}$$

Finally,

$$\frac{dP_{AA}(\tau)}{d\tau} + \left(\frac{1}{a}+\frac{1}{b}\right)P_{AA}(\tau) = \frac{1}{b} \qquad \textbf{(B. 5)}$$

Since τ=0, $P_{AA}(\tau)$=1.

$$P_{AA} = \frac{1}{a+b}\left\{b e^{-\kappa\tau} + a\right\} \qquad \textbf{(B. 6)}$$

where, $\kappa = \left(\frac{1}{a}+\frac{1}{b}\right)$.

$$A(\tau) = A(A-B)\frac{ab}{(a+b)^2}e^{-\kappa\tau} + const. \qquad \textbf{(B. 7)}$$

Bibliography

1) W. H. Press, Comments Astrophys. Space Phys. 7, **103** (1978).

2) T. Musha and H. Higuchi, Proc. Symp. 1/f Fluctuations, Inst. Elect. Engineering, Tokyo, Japan (1977).

3) M. J. Backingham, in *Noise in Electronic Devices and System*, Ellis Harwood Series Electrical and Electric Engineering, John Wiley & Sons (1983).

4) F. N. Hooge, Phys. Lett. **29A**, 139 (1969).

5) J. Pelz and J. Clarke, Phys. Rev. B **38**, 10371 (1988).

6) J. H. Scofield, J. V. Mantese and W. W. Webb, Phys. Rev. B **34**, 723 (1986).

7) D. M. Fleetwood and N. Giordano, Phys. Rev. B **28**, 3625 (1983).

8) J. A. Schwarz, A. J. Patrinos, I. S. Bakshee, E. A. Salkov and B. I. Khizhnyak, J. Appl. Phys. **70**, 1561 (1991).

9) D. B. Knorr, D. P. Tracy and K. P. Rodbell, App. Phys. Lett. **59**, 3241 (1991).

10) C. D. Keener and M. B. Weissman, Phys. Rev. B **44**, 9178 (1991).

11) J. L. Vossen, Appl. Phys. Lett. **2**, 287 (1973).

12) R. H. Koch, J. R. Lloyd and J. Cronin, Phys. Rev. Lett. **55**, 2487 (1985).

13) A. H. Verbruggen, R. H. Koch and C. P. Umbach, Phys. Rev. B **35**, 5864 (1987).

14) M. J. C. van den Homberg, A. H. Verbruggen, P. F. A. Alkemade and S. Radelaar, p. 127, in *Materials Reliability in Microelectronics 6*, ed. W. F.

Filter, J. J. Clement, A. S. Oates, R. Rosenberg and P. M. Lenahan, MRS Pittsburgh (1996).

15) C. V. Tompson and J. R. Lloyd, MRS Bull. **12**, 19 (1993).

16) J. G. Cottle and T. M. Chen, J. Electron. Mater. **17**, 467 (1988)

17) S. Feng, P. A. Lee and A. D. Stone, Phys. Rev. Lett. **56**, 1960 (1986).

18) G. A. Garfunkel, G.B. Alers, M. B. Weissman, J. M. Mochel and D. J. Van Harlingen., Phys Rev. Lett. **60**, 2773 (1988).

19) C.V. Heer, in *Statistical Mechanics, Kinetic Theory, and Stochastic Processes*, Academic Press, New York (1972)

20) A. L. MacWhorter, in *Semiconductor Surface Physics*, ed. R. H. Kingston, University of Pennsylvania (1957)

21) M. B. Weissman, Rev. Mod. Phys. **60**, 537 (1988)

22) P. Dutta, P. Dimon and P. H. Horn, Phys. Rev. Lett **43**, 646 (1979).

23) R. D. Black, P. J. Restle, M. B. Weissman, Phys. Rev. B **28**, 1935 (1983)

24) D. M. Fleetwood, T. Postel and N. Giordano, J. Appl. Phys. **56**, 3256 (1984)

25) P. Dutta and P. M. Horn, Rev. Mod. Phys. **53**, 497 (1981)

26) J. Peltz and J. Clarke, Phys. Rev. B **36,** 4479 (1987).

27) J. W. Martin, J. Phys. F **2**, 842 (1972).

28) J. Peltz and J. Clarke, Phys. Rev. Lett. **55**, 738 (1985)

29) J. Briggmann et al., Phys. Stat. Sol (a) **146**, 325 (1994)

30) I. A. Blech, J. Appl. Phys. **47**, 1203 (1976)

31) F. M. d'Heule and I. Ames, Appl. Phys. Lett. **16**, 80 (1970).

32) T. M. Chen and A. M. Yassine, IEEE Trans. Electron Devices, **41**, 2165 (1994)

33) R. G. Smith, G. A. Biery and K. P. Rodbell, App. Phys. Lett. **65**, 315 (1994).

34) L. D. Landau and E. M. Lifshitz, pp 384-389, in *Statistical Physics, Course of Theoretical Physics* vol. 5, 3rd ed. Part 1, Pergamon Press (1980)

35) R. De Batist, in *Internal friction of structual defects in crystalline solids, Defects in crystalline solids* vol. 5, ed. S. Amelinckx, R. Gevers and J. Nihoul, North-Holland (1972).

36) Sh. M. Kogan and K. E. Nagaev, Sov. Phys. Solid State **24**, 466 (1985).

37) J. W. Eberhard and P.M. Horn, Phys. Rev. B **18**, 6681 (1978).

38) G. B. Alers, Ph. D. Thesis, University of Illinois at Urbana-Champaign (1991).

39) L. A. Girifalco, in *Atomic Migration in Crystals*, Blaisdell Publishing (1964).

40) T. Gárecki and Z. Michno, pp 369-373, in *Diffusion in Metals and Alloys, Diffusion and Defect Monograph Series* No. 7, Trans Tech Publications (1983).

41) N. V. Chi and D. Bergner, pp 334-337, in *Diffusion in Metals and Alloys, Diffusion and Defect Monograph Series* No. 7, Trans Tech Publications (1983).

42) N. L. Peterson and R. J. Rothman, Phys. Rev. B **17**, 4666 (1978).

43) G. Neumann, pp 3-18, in *Diffusion in Metals and Alloys, Diffusion and Defect Monograph Series* No. 7, Trans Tech Publications (1983).

44) W. K. Warbarton and D. Turnbull, pp 171-229, in *Diffusion in Solids*, ed. A. S. Nowick and J. J. Barton, Academic Press, New York (1975).

45) J. Völkl and G. Alefeld, pp 231-302, in *Diffusion in Solids*, ed. A. S. Nowick and J. J. Barton, Academic Press, New York (1975).

46) G. B. Alers, M. B. Weissman, R. S. Aerback and H. Syu, Phys. Rev. B **40**, 900 (1989).

47) N. M. Zimmerman and W. W. Webb, Phys. Rev. Lett. **61**, 889 (1988).

48) D. Bergner, pp 223-240, *in Diffusion in Metals and Alloys, Diffusion and Defect Monograph Series* No. 7, Trans Tech Publications (1983).

49) M. J. C. van den Homberg et al., Phys. Rev. B **57**, 53 (1998).

50) J. P. Hirth and J. Lothe in *Theory of Dislocations*, McGraw-Hill, New York (1968).

51) A. Seeger and P. Schiller, pp 361-495, in *Physical Acoustics* vol. 3, ed. M. P. Warren, Academic Press, New York (1966).

52) N. W. Ashcroft and N. D. Mermin, in *Solid State Physics*, Saunders College, Philadelphia (1976).

53) B. L. Al'tsuler, JETP Lett. **41**, 648 (1985).

54) P. A. Lee, A. D. Stone and H. Fukuyama, Phys. Rev. B **35**, 1039 (1987)

55) C. P. Umbach, S. Washburn, R. B. Laibowitz and R. A. Webb, Phys. Rev. B **30**, 4048 (1984).

56) A. H. Verbruggen, H. Vloeberghs, P. A. M. Holweg, C. van Haesendonck, S. Radelaar and Y. Bruynseraede, Phys. Rev. B **45**, 8779 (1992).

57) W. J. Skocpol, L. D. Jackel, R. E. Howard, H. G. Craighead, L. A. Fetter, P. M. Mankiewich, P. Grabbe and D. M. Tennant, Surf. Sci. **142**, 14 (1984).

58) S. Feng, C. Kane, P. A. Lee and A. D. Stone, Phys. Rev. Lett. **61**, 834 (1988).

59) C. L. Kane, R. A. Serota and P. A. Lee, Phys. Rev. B, **37**, 6701 (1988).

60) P. McConville and N. O. Birge, Phys. Rev. B **47**, 16667 (1993).

61) A. D. Stone, Phys. Rev. Lett. **54**, 2692 (1985).

62) G. A. Garfunkel, PhD.Thesis University of Illinois at Urbana-Champaign (1989).

63) J. H. Scofield, Rev. Sci. Instrum, **58**, 985 (1987).

64) A. H. Verbruggen, H.Stoll, K.Heeck and R.H.Koch, App. Phys. A **48**, 233 (1989).

65) M. J. C. van den Homberg and A. H. Verbruggen, Microelectron. Eng. **35**, 277, (1997)

66) K. P. Rodbell and R.H.Koch, Phys. Rev. B **44**, 1767 (1991).

67) F. M. d'Heurle and P.S.Ho, *Electromigration in Thin Films, in Thin Films: Interdiffusion and Reactions*, ed. J.Poate, K.N.Tu and J.Mayer, J.Willey & Sons, NewYork (1978).

68) G. A. Biery, R. G. Smith and P. J. Ficalora, unpublished.

69) C. Reale, Phys. Stat. Sol. (B) **58**, K5 (1973).

70) A. G. Guy and J. J. Hren, in *Elements of Physical Metallurgy*, Addison-Wesley Publishing, Massachusetts (1974).

71) R. W. Cahn, pp1129-1197, in *Physical Metallurgy*, ed. R. W. Cahn, North-Holland Publishing (1970).

72) R. W. Balluffi, J. Nucl. Mater. **69&70**, 240 (1978).

73) T. E. Volin, K. H. Lie and W. Balluffi, Acta Metal. **19**, 263 (1970).

74) I. A. Blech, pp 3-13, in *Stress Induced Phenomena in Metallization*, ed. H. Okabayashi, S. Shingubara and P. Ho, AIP Conf. Proc. 418, AIP New York (1998).

75) T. S. Kê, Phys. Rev. **72**, 41 (1947).

76) T. J. Coutis in *Electrical Conduction in Thin Metal Films*, ch. 6, Elsevier Scientific, Amsterdam (1974)

77) A. Seeger, D. Schumacher, W. Schilling and J.Diehl, Ed., *Vacancies and Interstitials in Metals* (North-Holland, Amsterdam (1970).

78) E. Ochs, PhD. Thesis, Universitaet Stuttgart (1998).

79) P. S. Ho, I. S. Yeo, S. G. H. Anderson and C. K. Hu, in *Stress induced phenomena in Metallization* (P. S. Ho, C-Y, Li, P.Totta, eds.), pp. 62-97, Am. Inst. Phys., New York, (1993)

80) R. A. Brown, J. Phys. F: Metal Phys. **7**, 1283 (1977).

81) S. Washburn, in *Quantum Coherence in Mesoscopic Systems* (B. Kramer eds.) pp. 341-367, Plenum Press New York, (1991).

82) K. S. Ralls and R. A Buhrman, Phys. Rev. Lett. **60**, 2434 (1988).

83) I. Nakamichi, J. Phys. Condens. Matter **6**, 9585 (1994).

84) L. J. Bruner, Phys. Rev. **118,** 399 (1960).

85) A. D. Stone, Phys. Rev. B **39**, 10736 (1989).

86) S. Hershfield, Phys. Rev. B **37**, 8557 (1988).

87) K. S. Ralls and R. A Buhrman, Phys. Rev. B **44**, 5800 (1991).

88) S. Machlup, J. Appl. Phys. **25**, 341 (1954).

IMAGE EVALUATION
TEST TARGET (QA-3)

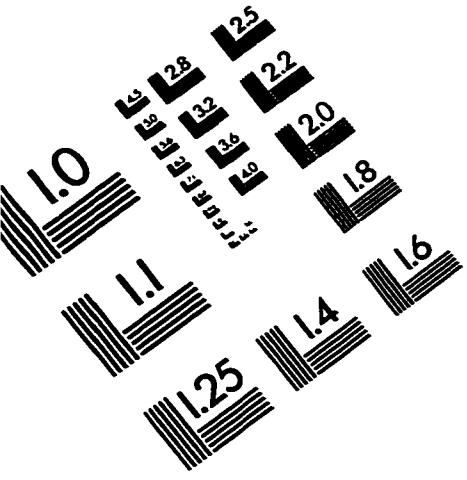

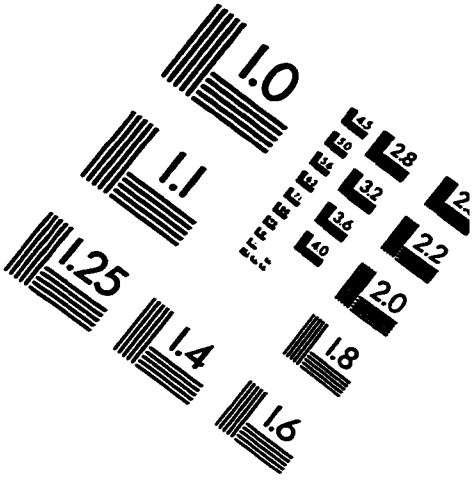

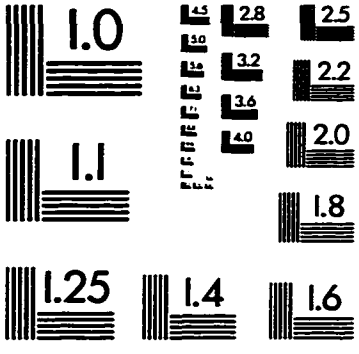

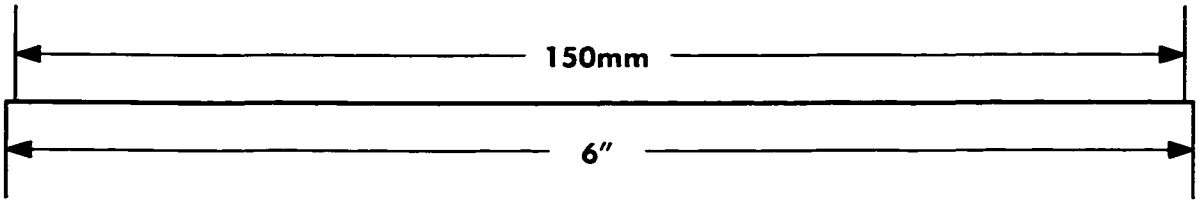

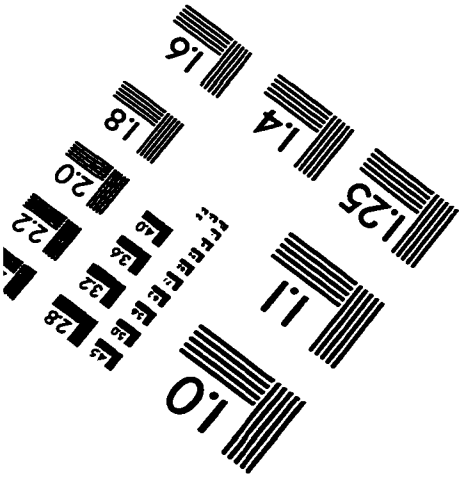

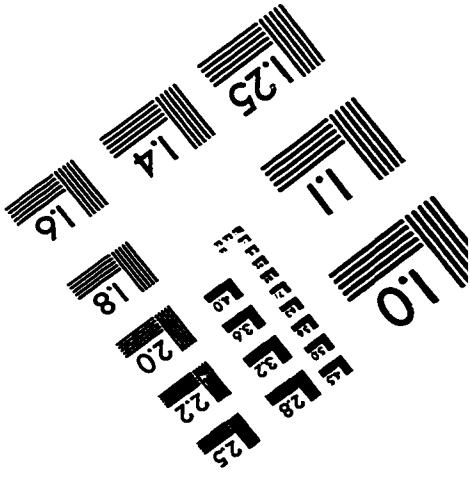

APPLIED IMAGE, Inc
1653 East Main Street
Rochester, NY 14609 USA
Phone: 716/482-0300
Fax: 716/288-5989